NASA SP-94

Significant Achievements in

Satellite Geodesy 1958-1964

Scientific and Technical Information Division 1966
NATIONAL AERONAUTICS AND SPACE ADMINISTRATION
Washington, D.C.

FOR SALE BY THE SUPERINTENDENT OF DOCUMENTS
U.S. GOVERNMENT PRINTING OFFICE, WASHINGTON, D.C., 20402 - PRICE $.70

Foreword

THIS VOLUME IS ONE OF A SERIES which summarize the progress made during the period 1958 through 1964 in discipline areas covered by the Space Science and Applications Program of the United States. In this way, the contribution made by the National Aeronautics and Space Administration is highlighted against the background of overall progress in each discipline. Succeeding issues will document the results from later years.

The initial issue of this series appears in 10 volumes (NASA Special Publications 91 to 100) which describe the achievements in the following areas: Astronomy, Bioscience, Communications and Navigation, Geodesy, Ionospheres and Radio Physics, Meteorology, Particles and Fields, Planetary Atmospheres, Planetology, and Solar Physics.

Although we do not here attempt to name those who have contributed to our program during these first 6 years, both in the experimental and theoretical research and in the analysis, compilation, and reporting of results, nevertheless we wish to acknowledge all the contributions to a very fruitful program in which this country may take justifiable pride.

HOMER E. NEWELL
Associate Administrator for
Space Science and Applications, NASA

Preface

GEODESY IS THE STUDY of the size and shape of the Earth and of locations on the Earth. In its crudest forms, it is, like astronomy, almost as old as history. The beginning of the era of space geodesy may be set in 1958 with the announcement, based on the analysis of observations of Vanguard I (1958β), that the flattening of the Earth's poles is significantly smaller than had been derived from terrestrial geodesy. This result implies the possible existence of considerable stress differences in the Earth's interior which may be supported by internal mechanical strength or by convection currents.

The first definite evidence that the Earth's gravitational field was irregular was derived from observations of several satellites early in 1959. These observations and analyses showed that the Northern Hemisphere of the Earth contains slightly more material than the Southern Hemisphere. Therefore the equipotential surface (i.e., the fictitious surface on which the pull of gravity is the same everywhere) is farther from the Equator at the North Pole than it is at the South Pole. Since water follows such an equipotential surface, the oceans define a pear-shaped Earth.

This result was quickly followed by further analyses of the Earth's gravitational field as it affects the orbits of satellites. Mathematicians find it convenient to describe this field in terms of components which vary with latitude and components which vary with longitude. The latter are somewhat harder to determine, since they affect satellite orbits in much the same way as atmospheric drag, light pressure, and other disturbing factors.

The increasingly accurate description of the Earth's gravitational field will eventually lead to a more precise understanding of the internal structure of the Earth. If, as has been proposed, the irregularities in the terrestrial gravity field are correlated with the rate of heat conduction from the interior of the Earth, we may have an important clue to physical conditions in various parts of the Earth's mantle. Moreover, a more detailed analysis of these results should enhance our understanding of seismic and volcanic activity. On a more direct and practical level, most oceanic navigation is based on a knowledge of local gravity and of the gravitational shape of the Earth. Thus, an improved knowledge of the terrestrial gravity field can lead to improved navigation accuracy in areas not reached by modern electronic navigation beacons.

Not only can a detailed knowledge of the Earth's gravitational field be derived from the analysis of orbits of satellites but the process can and must be reversed to provide us more accurate predictions for satellite- and space-probe trajectories. Such knowledge is vital, for example, for proper direction of manned satellites which will rendezvous with other satellites launched earlier.

Four satellites have been of outstanding importance for geodetic studies. The two Echo balloon satellites provided a readily visible target which could be photographed against a star background from widely separated sites on the surface of the Earth. By photographing the satellite simultaneously from several sites, the lengths and relative orientations of the baselines between the sites can be derived by standard triangulation techniques. The first satellite designed and launched specifically for geodetic purposes was the Anna satellite launched by DOD in 1962. This satellite carried a high-intensity xenon lamp which could be commanded to provide a sequence of five closely spaced flashes. These flashes provided starlike images which were observed against a background of stars. The images could be measured with precision, and the active nature of the satellite's flashes insured that observations were indeed simultaneous. The Anna satellite also carried a highly stable transmitter for Doppler studies of satellite motion. The SECOR electronic ranging system did not work satisfactorily on this satellite, but has since been successfully tested on other satellites. Anna provided a useful and encouraging test of both the flashing-light and Doppler-beacon systems, and many of the lessons learned from Anna have been used in the design of the Geos satellite, whose launch was planned for 1965.

Another satellite of special geodetic usefulness, Syncom, was, like the Echos, launched as a communication satellite. Because of its special orbit which keeps it essentially fixed with respect to a given longitude, it is particularly sensitive to certain terms in the Earth's gravitational field which are difficult to derive from an observation of satellites in lower orbits. It is encouraging to find that the analysis of the orbital motions of Syncom substantially confirmed analyses based on other satellites. Much progress has been made in satellite geodesy during the years 1958 to 1964, although it is likely that substantial improvements will follow the launch of the Geos and Pageos satellites.

The tracking of satellites, and particularly of space probes, has resulted in improvements in both terrestrial and other planetary constants sufficiently great that the International Astronomical Union (IAU) undertook a review of the constants used in the various national ephemerides as well as in computing the orbits of satellites and space probes. On the basis of the detailed analysis of all the evidence to date, the IAU adopted, at its meeting in Hamburg in August 1964, a new set of astronomical constants. This was the first major change in the astronomical constants in this century, and will significantly improve astronomical predictions in the future.

The use of Geos and further analysis of Syncom data should substantially improve our knowledge of the Earth's gravitational field, but the most outstanding accomplishments expected in satellite geodesy within the relatively near future are in geometrical geodesy (i.e., the accurate location of various sites on the same Earth-centered reference frame), a field which has barely been touched by satellite techniques. Observations of both Geos and Pageos will permit, for the first time, accurate mapping throughout the world on a single coordinate system, and a determination of the relative locations and orientations of the various geodetic datums which in the past have been derived separately for each country or region with little or no possibility of interconnection. This unification will, of course, lead to appreciably more accurate maps and better defined distances between points on different continents, and to accurate location of isolated islands. These improved maps will also permit more accurate tracking and guidance of interplanetary probes, since tracking stations will be better located with respect to the center of the Earth.

Although NASA has provided the majority of the satellites used for geodetic studies, and much of the tracking data on which the analyses have been based, there has been substantial participation by many groups throughout the world. Probably the work done directly by NASA or with NASA support represents only about one-quarter of the activity in the field.

So far, almost all the geodetic studies have referred to the Earth. However, the lunar-orbiter program will extend the techniques of satellite geodesy to the Moon. Mariner II already has provided an improved value for the mass of Venus. Improved techniques for observing the Martian satellites, stimulated by NASA interest in that planet, will improve our knowledge of the Martian gravity field. Geodetic studies of planets other than the Earth by measurement of and from planetary orbiters will be very important in the next decade.

Contents

CONTENTS

Introduction

FOR THE PURPOSE OF THE PRESENT REVIEW, satellite geodesy is defined as those areas of dynamical and geometrical geodesy to which satellite techniques have contributed extensively. This review indicates the contributions to our understanding of the Earth's gravitational field which have come from analyses of satellite motions, and also the contributions to the lesser but potentially more important use of satellites for geodetic triangulation. There are many related areas of geodesy and geophysics which have important interfaces with satellite geodesy; these have not been included in this review.

Many authors have reviewed various aspects of the progress in the field of satellite geodesy. Rather than rewrite their material, representative publications have been collected and combined to form this report. Except where otherwise noted, the editing has been limited to the occasional selection of appropriate portions from longer articles. It should be emphasized that while an attempt has been made to include appropriate articles, in many cases, other equally valid choices might have been included instead. Some articles are included not because they give significant results in themselves, but because they describe an important technique. Together, it is believed that these articles give a reasonably complete review of the progress and activity in the field of satellite geodesy during the period 1958 to 1964.

More specifically, the following material is covered in the report:

(1) The state of knowledge in geodesy at the time of NASA's creation.

(2) Early results in satellite geodesy.

(3) Dynamical geodesy based on optical observations. This is the first technique employed in satellite geodesy and has

produced the most extensive results to date. Three modern summaries include recent determinations of both zonal and tesseral harmonics.

(4) Dynamical geodesy based on nonoptical tracking. Doppler tracking was applied to determining the orbit of the first sputnik. It has recently proven an important geodetic tool. The SECOR ranging system and the various range-and-range-rate systems are beginning to provide geodetic data. A particularly important contribution has resulted from the use of a range-and-range-rate system to track Syncom.

(5) Astronomical constants: This important area is included because of the role of satellite geodesy in determining the terrestrial constants and because of the closely related techniques used for determining other constants.

(6) Geometrical geodesy using optical techniques.

(7) Geometrical geodesy using nonoptical techniques.

(8) Special satellites (Anna and Echo) for geodesy and tests of techniques for using these satellites.

No attempt has been made to include the theory used in deriving the terrestrial gravity field from observations of artificial satellite orbits. This has been extensively reviewed by Cook,[1] Kaula,[2] Mueller,[3] and others. The interested reader is referred to these authors both for the mathematical bases of the geodetic analyses and for more detailed background on the applications of the various mathematical techniques.

Late in 1958, a conference on "Contemporary Geodesy" was held in Cambridge, Mass., to review the rapid impact of electronic and satellite tracking techniques on this ancient field. To set the background for further discussion, Dr. Alwyn R. Robbins of Oxford University presented a review of the history and current status of geodesy. The following was originally published in

[1] Cook, A. H.: Space Science Reviews, vol. 2, Sept. 1953, pp. 355–437.

[2] Kaula, W. M.: Celestial Geodesy. *In:* Advances in Geophysics. Vol. 9, Academic Press, 1962, pp. 192–293.

[3] Mueller, Ivan I.: Introduction to Satellite Geodesy. Frederick Ungar Pub. Co. (New York), 1964.

Contemporary Geodesy, Geophysical Monograph No. 4, American Geophysical Union of the National Academy of Sciences-National Research Council Publication No. 708, 1959.

Evolution of the Geodetic Concept

ALWYN R. ROBBINS
Oxford University
Oxford, England

GEODESY IS A VERY OLD PROFESSION. If you look in the Bible, I think the Book of Numbers or Deuteronomy where there is a list of curses, you will find one which in effect says: "Cursed be he who moves his neighbor's boundary stone." So it goes back some way.

Next, the ancient Greeks thought the Earth was a plane supported by four elephants on the back of a turtle. Aristotle went a step further and said it was a sphere. Later Eratosthenes noticed that the Sun shone directly down a well at noon at the summer solstice; he observed the sun somewhere else at the same time, made a traverse by camel caravan, and computed the radius of the Earth.

Then things stood still for a few centuries. With the coming of the telescope and the use of logarithms, triangulation was originated. Finally the size and shape of the Earth was measured by triangulating along meridians to compute the semiaxis and the flattening of the ellipsoid. One measurement appeared to show that the Earth was a prolate spheroid; this was disputed by Newton and others and then we had the famous French arcs in 1735 and 1736 which proved it was an oblate spheroid.

In the nineteenth century, with the realization of the need for maps, many countries observed the national framework of triangulation and some of them determined their own spheroid, or figure of the Earth, that happened to fit their country best. That was all right but when communications improve, national barriers become meaningless and geodetic networks must be international. The spheroid that fits one country doesn't necessarily fit others.

During this century, the International Union of Geodesy and Geophysics has given geodesy international recognition. During the last thirty years, especially since the last world war, these national triangulations have been linked more and more and many datums have been tied together by triangulation.

When triangulation over large areas is computed on an ellipsoid or spheroid whose size and shape are known, position of the spheroid in relation to the geoid must also be determined. A datum contains seven constants: two, the semiaxis and the flattening of the spheroid, and two additional constants to make the minor axis parallel to the axis of rotation of the Earth. These last two you do not use per se but you use them, without noticing as it were, when computing geodetic azimuth from astronomical. As far as these four constants are concerned, you can compute on any spheroid you choose but you still will not necessarily be on the same datum. Finally, you define the latitude and longitude and geoid-spheroid separation at the origin. Now the datum is completely defined. Nothing else can be defined; everything else must be computed. So if you have two disconnected triangulation systems on the same spheroid, they are still on different datums in that they have different origins.

The definition of latitude and longitude and geoid-spheroid separation at the origin is completely arbitrary. You can assume that the separation is zero and that the geodetic latitude and longitude are the same as the astronomical. If you do that and if you happen to be in an unlucky spot where the geoid rises or falls slightly, then as the network extends hundreds of miles, this tilt will become more pronounced and the separation of the two surfaces will increase. Generally, you will reduce your bases to mean sea level but you should reduce them to the spheroid. If you have enough deviations of the vertical you can compute along section lines and calculate the separation and its effect on scale. But one seldom has enough information.

There is, however, one way of going about it: You can compute deviations of the vertical on one world datum if you have enough information on the intensity of gravity over the world. However, there is not enough gravity information so there will probably be some residual errors left in computation because of insufficient data. Perhaps some will disagree with that statement.

Be that as it may, it is important to recognize that deviations of the vertical from Stokes' theorem are on one datum, and any others computed on other datums are different. The two cannot agree except by chance. So we have a multiplicity of datums. The task of the geodesist is to reduce these and combine them into one world geodetic datum. You can do it by having more observations of gravity and so on, or you can make intercontinental ties between triangulation systems. Then you have the problem of computing the separation of the geoid and spheroid across the sea gaps. One way is to use gravity and interpolate. Ways of doing it are now being studied; some research is being done on that at the moment. So it does not really matter what datum you have, as long as you have one which fits reasonably well and as long as you have enough observations. It is the lack of sufficient observational information that is holding things up to some extent at the moment. The objective is to have a world datum and to portray the geoid on it.

We have come a long way since the introduction of the telescope. I do not recall the date of the early triangulation in Great Britain but I remember their geodetic theodolite had a sixty-inch circle and they had to put it on top of St. Paul's Cathedral on a scaffolding. Nowadays one can get better results with a five inch. Of course we also have shoran, and more recently still the satellite.

On the gravity side, for the pendulum we have come up with more accurate timing devices. The gravimeter is being improved and new types are being developed which can be used aboard surface ships as well as under water.

Finally we come to the Earth satellites which are, perhaps, controversial. How much can we get out of them? I would personally like to see it the other way around. How much information can we geodesists give to the physicists? If we know the gravity on the Earth and then tell the physicist what gravity is doing to the satellite, the physicist can determine what the effect of atmospheric drag is and so on. That, again, is the reverse of what many people are thinking. The other way around is to try to find out from the physicist what the drag is doing, whence to determine gravity all over the Earth. It all depends on the relative sizes of the effects we get from one source or the other.

Part 1

Early Results in Satellite Geodesy

The effect of the Earth's gravitational field on the motion of near-Earth satellites is so marked that even comparatively crude tracking techniques sufficed to produce the first results in satellite geodesy. An improved value for the flattening of the Earth and a lack of symmetry between Northern and Southern Hemispheres were reported in 1958 and early in 1959, respectively. The following are early papers in this field.

Page intentionally left blank

The following paper was originally published in Nature, *vol. 182, 1958, pp. 198–199.*

Motion of the Nodal Line of the Second Russian Earth Satellite (1957β) and Flattening of the Earth

E. Buchar
Observatory of the Technical University
Karlovo nám. 13, Prague II

Despite the fact that the observation of an artificial satellite can be carried out only on a small region of the Earth's surface, we can use these measurements for determining the geocentrical co-ordinates of the satellite, if we know the approximate value of its distance from the Earth's centre. The most suitable observations are those in the neighbourhood of the zenith. If we know the inclination of the orbit, we can then determine also the position of the orbital node.

In order to determine the motion of the orbital node, we used 33 visual observations, made between December 7, 1957, and March 21, 1958, at various places in Czechoslovakia. By adjustment of the positions of the node grouped about five normal positions, the following expression for the right ascension of the ascending node was derived:

$$\Omega = 256.59° \pm 0.20° - (2.9007° \pm 0.0046°)(t - t_0) - (0.00234° \pm 0.00012°)(t - t_0)^2$$

Epoch t_0 = January 22.0, 1958, U.T. Time t is expressed in days. The mean errors were computed from the deviations of the normal places. The daily motion of the node is then given by:

$$\frac{d\Omega}{dt} = -2.9007 \pm 0.0046° - (0.00468° \pm 0.00024°)(t - t_0)$$

It is well known that the theoretical value of this motion is given by the approximate equation:

$$\frac{d\Omega}{dt} = -\frac{3k(C-A)}{2ma^2}(1 + 2e^2)\cos i$$

where $C-A$ is the difference between the moments of inertia of the terrestrial spheroid, m the mass of the Earth and k the gravitational constant. The symbol a stands for the major semi-axis of the orbit, expressed in units of the equatorial radius of the Earth, e and i being the eccentricity and inclination of the orbit, respectively.

It is obvious that, by using this equation, we can derive from the observed motion of the node the quantity $K=(C-A)/m$. If, for the time $t=t_0$, we assume $a=1.1127\pm 0.0003$ and for e and i the values published by D. G. King-Hele,[1] namely, $e=0.0731\pm 0.0005$, $i=65.29°\pm 0.03°$, we then arrive at:

$$K=0.0010856\pm 0.0000024$$

The mean error was computed as the total effect of the errors of the basic data. The oblateness of the Earth, α, can be computed from the expression:

$$\alpha=\frac{3}{2}K+\frac{h}{2}+\frac{3}{4}(3K^2+Kh-h^2)$$

where h is the ratio of the centrifugal force to the value of gravity at the equator.

The reciprocal value of the Earth's flattening is then:

$$\frac{1}{\alpha}=297.7\pm 0.3$$

If we use four more values for a and e determined[2] between February 10 and March 3, 1958, we arrive finally at the result:

$$K=\frac{C-A}{m}=0.0010883\pm 0.0000014$$

$$\frac{1}{\alpha}=297.4\pm 0.2$$

In these numerical results approximate account was taken of the second term of the disturbing function.

These preliminary results show that satellite observations of greater precision will give us the possibility of determining correctly the oblateness of the Earth.

---

[1] King-Hele, D. G., *Nature*, 181, 738 (1958).

[2] Smithsonian Astrophys. Obs. Circulars (Cambridge, U.S.A.).

The following paper was originally published in Science, *vol. 129, No. 3348, Feb. 27, 1959, p. 565.*

Vanguard Measurements Give Pear-Shaped Component of Earth's Figure

J. A. O'Keefe, Ann Eckels, and R. K. Squires
Theoretical Division
National Aeronautics and Space Administration
Washington, D.C.

The determination of the orbit of the Vanguard satellite, 1958β_2, has revealed the existence of periodic variations in the eccentricity of that satellite (*1*). Our calculations indicate that the periodic changes in eccentricity can be explained by the presence of a third zonal harmonic in the earth's gravitational field. The third zonal harmonic modifies the geoid toward the shape of a pear. In the present case, the stem of the pear is up—that is, at the North Pole. According to our analysis, the amplitude of the third zonal harmonic is 0.0047 cm/sec^2 in the surface acceleration of gravity, or 15 meters of undulation in the geoid.

Figure 1 shows the observed variation in eccentricity. The period of the variation in eccentricity is 80 days, approximately equal to the period of revolution of the lines of apsides. The eccentricity is a maximum when the perigee is in the Northern Hemisphere. The amplitude

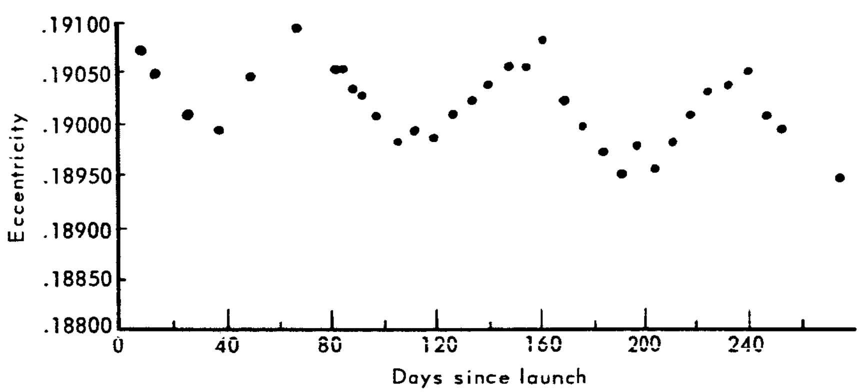

Figure 1.—Eccentricity of satellite 1958β_2 (Vanguard).

of the variation is 0.00042 ± 0.00003. Similar perturbations may exist in the angle of inclination of the orbit, although the data for them are much less accurate. No perturbations of this magnitude appear to exist in the semimajor axis.

In principle, the perturbation might be caused by both odd and even harmonics. However, the even harmonics can be excluded because the observed effect has opposite signs in the Northern and Southern hemispheres. Furthermore, we can also exclude tesseral harmonics (those which depend on longitude as well as latitude) because these also are the same in the Northern and Southern hemispheres, apart from a shift in longitude. We are left with the zonal harmonics (those which depend only on latitude) of odd degree.

Of the odd zonal harmonics, the first degree is forbidden; and those of higher degree are unlikely to have a large effect because they die out inversely as the $(n+1)$ power of the distance. The effect is therefore due mostly to the third zonal harmonic, with a possible contribution from the fifth.

Accordingly, a calculation was made of the effect of the third zonal harmonic on the orbit elements of $1958\beta_2$, by methods developed by O'Keefe and Batchlor (*2*). In the resultant expression for the eccentricity, the dominant terms were those whose argument was the mean motion of perigee. These were larger than the others by a factor of 10^3. Keeping only the large terms, we find

$$e = e_0 + \frac{3}{2} A_{3,0} \frac{(1-e^2)^{1/2}}{na^6} \frac{1}{n'} \times \sin i \left(1 - \frac{5}{4}\sin^2 i\right) \sin \omega \tag{1}$$

where $A_{3,0}$ represents the coefficient of the third zonal harmonic in the notation of Jeffreys (*3*), n is the orbital mean motion and n' is the mean motion of the perigee, e is the eccentricity and e_0 the mean eccentricity, i is the angle of inclination, ω is the argument of perigee, and a is the semimajor axis.

Setting in the constants of the orbit and the observed amplitude of e, we find

$$A_{3,0} = (2.5 \pm 0.2) \times 10^{29} \tag{2a}$$

in meter-second units. Utilizing the relation given by Jeffreys,

$$A_{n,s} = \frac{c^{n+2}}{n-1} g_{n,s}$$

(where $A_{n,s}$ is the coefficient of the disturbing potential, $g_{n,s}$ is the acceleration of gravity at the surface of the earth, and c is the earth's equatorial radius), we find that the third zonal harmonic of gravity at the earth's surface, in milligals, is

$$g_{3,0}=4.7\pm0.4 \tag{2b}$$

Equation 2 is relevant to what Vening Meinesz (*4*) and Heiskanen call the "basic hypothesis of geodesy." These authors assume that the earth's gravitational field is very nearly that of a fluid in equilibrium. They consider that the deviations from such an ellipsoid, in any given area, do not exceed about 30 milligal-megameter units—that is, they assume that one will not find deviations of more than 30 milligals over an area of 1000 kilometers on a side, or deviations of more than 3 milligals in an area 3000 kilometers on a side.

Our determination of the third-degree zonal harmonic shows that the hypothesis of Vening Meinesz and Heiskanen is not justified; for example, each of the polar areas has a value of about 120 milligal-megameters, and each of the equatorial belts a value more than twice as great.

The presence of a third harmonic of the amplitude (*2*) indicates a very substantial load on the surface of the earth. Following the arguments of Jeffreys, we may calculate the values of this load and the minimum stress required in the interior to support it. We find a crustal load of 2×10^7 dy/cm^2. We can choose between assuming that stresses of approximately this order of magnitude exist down to the core of the earth, or that stresses of about 4 times that amount exist in the uppermost 700 kilometers only (*3*, p. 199). These stresses must be supported either by a mechanical strength larger than that usually assumed for the interior of the earth or by large-scale convection currents in the mantle (*5*).

REFERENCES AND NOTES

1. Siry, J. W.: Distribution to orbit-computing centers, 1958.
2. O'Keefe, J. A.; and Batchlor, C. D.: *Astron. J.* 62, 183 (1957).
3. Jeffreys, H.: *The Earth* (Cambridge Univ. Press, Cambridge, 1952).
4. Heiskanen, W. A.; and Vening Meinesz, F. A.: *The Earth and Its Gravity Field* (McGraw-Hill, New York, 1958), pp. 72, 73.

5. We would like to thank the Vanguard Minitrack Branch, the IBM Vanguard Computing Center, and Dr. Paul Herget, whose work in obtaining and processing the data made this study possible.

Part 2

Derivation of the Earth's Gravity Field From Optical Photographs of Satellites

The network of Baker-Nunn wide-angle cameras which was established during the International Geophysical Year has been tracking American and Russian satellites by photographing them at dawn and at dusk against a star background. Drive motors permit the camera to compensate for the motion of the satellite, thus allowing the photography of very faint satellites. In this mode, stellar images are short trails. So that they can be measured at a given instant of time, these trails are chopped by an accurately timed shutter. Although various techniques can be and have been used to track satellites and geodetic information has been derived from most of these techniques, the Baker-Nunn cameras have undoubtedly produced the most important body of data on which such analyses have been based. The following are the results of three recent analyses of these optical data. The section by Kaula is a coalition of two of his papers which appeared in the Journal of Geophysical Research in 1963.

Page intentionally left blank

Page intentionally left blank

The following paper is a compilation and coalition of two papers originally published in Journal of Geophysical Research, *vol. 68, 1963, pp. 473–484 and 5183–5190.*

Current Knowledge of the Earth's Gravitational Field From Optical Observations

W. M. Kaula
Goddard Space Flight Center, NASA

This paper describes the analysis of Baker-Nunn camera observations listed by Veis et al. [1962] and Haramundanis [1962] by the methods described by Kaula [1961a, b; 1962a, b]. An IBM 7090 computer was used. Solutions were made for all geodetic and gravitational parameters estimated to have effects of more than ± 20 meters on satellite orbits. The intent of the analysis was to apply all devices short of allowing for covariance of observations at different times. This intent resulted in programs so complicated that most of the time spent on the work was consumed by purely computational difficulties.

OBSERVATIONS

The Baker-Nunn camera system, its accuracy, and experience in its operation by the Smithsonian Institution Astrophysical Observatory are described by Henize [1960], Lassovszky [1961], Weston [1960], and Veis and Whipple [1961]. That the random error of the plate measurements is of the order of $\pm 2''$ has been confirmed in this analysis by the accuracy with which a line can be fitted to plotted residuals with respect to an orbit of observations close together in the same pass. Since the significant timing error is virtually constant throughout a pass, no such test of timing error is possible because of the dominant effect of drag error in the orbit.

The precisely reduced Baker-Nunn camera observations of 1959α, 1959η, and 1960ι_2 from launch until the end of 1961, of 1961δ, from launch until the middle of 1961, and of 1961$\alpha\delta$, in the spring of 1962 were analyzed. The observations through mid-1961 have been published in the catalogs compiled by Veis et al. [1961–1962] and are referred to in the 1950 mean positions of the stellar catalog. For this analysis, the epoch of the right ascension and declination was updated to the epoch of the orbital arc fitted to the observations, taking into account precession plus nutational terms of more than $0.25''$ amplitude—i.e., the

18.6 year and semiannual terms. All times are given for the observations, which are treated as equivalent to ephemeris time. A small correction was applied in calculating Greenwich sidereal times to allow for the precession and nutation between the epoch of the orbital arc and the instant of observation.

The above-mentioned $\pm 2''$ accuracy of fitting of a line to residuals is appreciably smaller than the residuals themselves, which indicates that extra observations within a pass did not add extra weight to the analysis of the orbit. Hence, to conserve computer time and to avoid overweighting certain passes, observations were omitted which were neither terminal observations of a pass nor observations interior to a pass at intervals of 2 minutes or more.

The final rejection criterion applied was to omit observations on days of appreciable atmospheric disturbance, as measured by the geomagnetic index A_p. For the 1960ι_2 analysis observations were omitted on days for which A_p exceeded 50; for 1959α_1 and 1959η, when A_p exceeded 70. In some cases additional observations on adjacent days were omitted in order that an orbital arc would not bridge across days of high A_p index.

The principal defect in the observations is, of course, their poor distribution—due to the dependence on reflected sunlight, and to the limited number of tracking stations (twelve). The number of observations of each satellite used is given in Table 1.

Table 1.—*Satellite Orbit Specifications*

	Satellite				
	1959α_1	1959η	1960ι_2	1961δ_1	1961$\alpha\delta_1$
Epoch	1959 Feb. 28.5	1959 Sept. 28.5	1960 Sept. 22.0	1961 Feb. 20.0	1962 Mar. 8.5
Semimajor axis	1.304585	1.334500	1.250057	1.252779	1.568136
Eccentricity	0.16582	0.19008	0.01146	0.12135	0.01197
Inclination	0.57381	0.58212	0.82434	0.67835	1.67316
Argument of perigee	3.36062	3.20403	2.26377	2.02733	4.28853
Longitude of node	2.52442	3.48304	2.28139	2.76786	5.71336
Mean anomaly	6.00463	3.82408	2.72868	5.96587	1.51124
Perigee motion/day	+0.09181	+0.08501	+0.05186	+0.08315	−0.01733
Node motion/day	−0.06108	−0.05712	−0.05413	−0.06347	+0.00367
Max. A/m, cm²/g	0.21	0.27	0.27	15.9	0.08
Min. A/m, cm²/g	0.21	0.04	0.08	15.9	0.02
Perigee height, km	560	510	1500	640	3500
Number of days	1032	792	480	150	54
Number of observations	3513	3034	2502	1395	552

Geometry.—The observation equation used was expressed in terms of the meridian and prime vertical components of the plate measurement, assuming that the satellite was on the camera axis [Kaula, 1961a, 1962c]. It consists of the first two rows of the matrix equation

$$\begin{Bmatrix} d\delta \\ d\alpha \cos \delta \\ dr/r \end{Bmatrix} = \begin{Bmatrix} \frac{d\mathbf{b}}{r} \end{Bmatrix}_{\text{obs}} = -\begin{Bmatrix} \frac{\mathbf{b}}{r} \end{Bmatrix}_{\text{obs}} + \mathbf{R}_{\text{bx}}\{\mathbf{R}_{\text{xq}}\mathbf{q}$$

$$+\mathbf{C}_{\text{xe}}de + \mathbf{C}_{\text{x}M}n\ dt - \mathbf{R}_3(-\theta)d\mathbf{u}_0\}/r \quad (1)$$

In (1), δ is the declination, α the right ascension, r the camera-satellite range. The first two rows of $(\mathbf{b}/r)_{\text{obs}}$ are zero if the observed δ, α are used in $\mathbf{R}_{\text{bx}}$, the matrix which rotates the inertial coordinate system to a rectangular system with the 3-axis coinciding with the camera-satellite line and the 1-axis coinciding with the meridian. $\mathbf{q}$ is the satellite position in orbit-referred coordinates, with the 1-axis toward osculating perigee and the 3-axis normal to the osculating orbit; $\mathbf{R}_{\text{xq}}$ is the rotation from orbit-referred to inertial coordinates; $\mathbf{C}_{\text{xe}}$ is a 3×6 matrix of partial derivatives of the inertial rectangular coordinates with respect to the osculating Keplerian elements, corrections to which are symbolized by de; $\mathbf{C}_{\text{x}M}$ is the row of $\mathbf{C}_{\text{xe}}$ corresponding to the mean anomaly; n is the mean motion; dt is a correction to the time of observation; $\mathbf{R}_3\ (-\theta)$ is the geodetic to inertial rotation matrix, with the Greenwich sidereal time, θ, as argument; and $d\mathbf{u}_0$ is a vector of corrections to station position. (Derivations of all these variables are given in equations (46), (47), and (52) to (60) of Kaula [1961a], or equations (3.1) to (3.8) and (3.11) to (3.15) of Kaula [1962c].)

The partial derivatives in (1),

$$\mathbf{C}_1 = \begin{Bmatrix} \partial\delta/\partial t \\ \partial(\alpha \cos \delta)/\partial t \end{Bmatrix} = \begin{Bmatrix} 1, 0, 0 \\ 0, 1, 0 \end{Bmatrix} \mathbf{R}_{\text{bx}}\mathbf{C}_{\text{x}M}n/r \quad (2)$$

were not actually used to determine timing corrections, but rather in three other ways: first, to apply a correction $r\mathbf{C}_t/c$ for the time of travel of the signal, where c is the velocity of the light; second, to give lower weight to the along-track component than to the across-track component of the observation, by giving each observation a 2×2 covariance matrix:

$$V_{\text{obs}} = \begin{Bmatrix} \sigma_d^2 & 0 \\ 0 & \sigma_d^2 \end{Bmatrix} + \mathbf{C}_t\sigma_t^2\mathbf{C}_t^T \quad (3)$$

where σ_d^2 is the variance of the direction measurement, σ_t^2 is the variance of the timing, and the superscript T denotes transpose; and, third, to compute residuals in along-track and across-track components by applying to (δ, $\alpha \cos \delta$) residuals the rotation

$$\mathbf{R}_{tt} = \begin{cases} C_1/\sqrt{C_1^2+C_2^2}, & C_2/\sqrt{C_1^2+C_2^2} \\ -C_2/\sqrt{C_1^2+C_2^2}, & C_1/\sqrt{C_1^2+C_2^2} \end{cases} \tag{4}$$

where $\mathbf{C}_1$, $\mathbf{C}_2$ are the two elements of $\mathbf{C}_t$.

Table 2.—*Tracking Station Data*

[In length units of 6.378165 meters]

Station	Lat. and Long., deg	Datum	Starting coordinates	Pre-assigned σ	Prelimi-nary solution	Final solution
Organ Pass	32.4	Am.	−240778.9	±3.0	−14.8	−02.8±0.9
	253.4		−810109.7	±3.9	−05.6	−03.8±1.8
			533234.2	±3.1	+03.3	−00.2±1.0
Arequipa	−16.5		304591.7			
	288.5		−909989.8			
			−281725.5			
Curacao	12.1		353050.9			
	291.2		−912004.8			
			+208082.5			
Jupiter	27.0		+153068.1			
	279.8		−878214.3			
			+451581.1			
Olifantsfontein	−26.0	EASI	792726.2	±3.4	+16.3	+05.4±1.3
	28.3		425915.7	±2.9	−17.8	−08.0±1.4
			−435196.6	±2.9	+00.1	+02.6±2.5
San Fernando	36.5		800487.5			
	353.8		− 87038.6			
			591033.8			
Naini Tal	29.4		159630.5			
	79.5		857808.2			
			487532.6			
Shiraz	29.6		529444.8			
	52.5		690490.0			
			491723.2			
Woomera	−31.1	Au.	−624562.7	±11.3	+06.4	−15.0±4.0
	136.8		586884.9	±14.5	+14.5	+04.4±8.3
			−513573.3	±13.2	+02.8	+08.7±6.5
Tokyo	35.7	JKM	−618774.5	±5.2	+00.0	−08.5±2.7
	139.5		527787.3	±6.9	+15.2	+06.8±3.4
			579917.5	±5.2	+01.9	+00.9±2.4
Villa Dolores	−31.9	Ar.	357509.6	±28.4	+27.1	+36.9±3.9
	294.9		−770550.4	±22.8	−02.2	+03.4±5.0
			−526083.5	±26.2	+01.2	+03.3±6.6
Maui	20.7	H	−857008.8	±21.7	+01.8	+01.5±6.1
	203.7		−376954.1	±35.8	+28.5	+14.1±7.9
			351587.3	±37.1	−53.3	−50.1±4.7

Since effects were investigated that were expected to be as small as ± 20 meters, all stations were assumed to have position error, but those stations connected to the same geodetic system were assumed to shift together. Hence the twelve cameras were referred to six datums: four to the Americas (Am.) system; four to the Europe-Africa-Siberia-India (EASI) system; and one each to the Australia (Au), Japan-Korea-Manchuria (JKM), Argentina (Ar) and Hawaii (H) systems. The initial station positions used are the solutions given in Table 2. Corrections for errors in the computed positions of three stations relative to the principal datums were provided by I. G. Izsak of the Smithsonian Institution Astrophysical Observatory. Corrections to coordinates u_1, u_2, and u_3 in earth radii are listed in sequence (all values times 10^{-6}):

San Fernando	+5.6	−5.0	−8.5
Naini Tal	+2.7	−5.0	+4.9
Curacao	−1.0	0.0	+2.8

For the Am., EASI, and JKM systems, the starting station positions were those obtained in the solution for a world geodetic system by Kaula [1961c]. For the Au, Ar, and H systems the positions calculated by Veis [1961b] were taken and shifted by placing tangent to the datum origin an ellipsoid of flattening 1/298.3 and an equatorial radius of 6,378,165+N_0 meters, where N_0 is the geoid height in the vicinity of the datum origin as given by Kaula [1961c]. The initial station positions are given in Table 1 in length units of 6.378165 meters referred to the **u** coordinate system, with axes toward 0°, 0°; 0°, 90° E; and 90° N, respectively.

The datum shifts listed in Table 3 apply to the starting coordinates in column 4 of Table 2.

Dynamics.—Variables in the observation equation (1) that are dependent on the dynamics of the satellite orbit are

$$\mathbf{R}_{xq} = \mathbf{R}_3(-\Omega)\mathbf{R}_1(-i)\mathbf{R}_3(-\omega) \tag{5}$$

$$\mathbf{q} = \begin{Bmatrix} a(\cos E - e) \\ a\sqrt{1-e^2}\sin E \\ 0 \end{Bmatrix} \tag{6}$$

where E, a, e, i, ω, and Ω are the osculating eccentric anomaly, semimajor axis, eccentricity, inclination, argument of perigee, and longitude of the ascending node, respectively; and

$$d\mathbf{e} = \mathbf{J}\, d\mathbf{e}_0' + \mathbf{C}_{eg}d\mathbf{p}_g + \mathbf{C}_{et}d\mathbf{p}_t + \mathbf{C}_{ed}d\mathbf{p}_d + \mathbf{C}_{ep}d\mathbf{p}_p \tag{7}$$

where $\mathbf{e}_0'$ denotes the elements of an intermediate orbit at epoch; $\mathbf{p}_0$ are

Table 3.—*Datum Shifts*

[In length units of 6.378165 meters]

Datum	Coordinate	$1959\alpha_1$	1959η	$1960\iota_2$	$1961\delta_1$	$1961\alpha\delta_1$	Weighted mean
Americas	Δu_1	−02.5	−02.6	−03.7	−03.8	−06.4	−03.8 ± 1.0
	Δu_2	−04.7	−05.2	−09.6	−11.3	−04.2	−05.1 ± 0.8
	Δu_3	−00.9	−00.5	+00.6	−01.9	−00.3	−00.4 ± 0.2
Europe-Africa-Siberia-India	Δu_1	+06.5	+07.3	+06.6	+11.6	+04.6	+05.8 ± 0.7
	Δu_2	−07.8	−07.8	−09.3	−04.1	−10.2	−08.9 ± 0.5
	Δu_3	+02.0	+01.3	+02.2	−01.4	+02.1	+01.9 ± 0.2
Australia	Δu_1	−16.3	−19.6	−19.6	−11.2	−26.6	−17.3 ± 1.5
	Δu_2	+09.6	+06.0	+06.7	+07.5	+03.0	+05.2 ± 1.7
	Δu_3	+10.8	+14.6	+10.0	+14.7	+09.4	+10.5 ± 0.4
Japan-Korea-Manchuria	Δu_1	−08.9	−11.5	−08.3	−08.5	−06.5	−08.9 ± 0.5
	Δu_2	+04.1	+05.2	+13.0	+08.7	+09.3	+09.4 ± 0.7
	Δu_3	+01.4	+00.1	+01.8	−00.1	+04.4	+01.5 ± 0.8
Argentina	Δu_1	+35.6	+37.9	+39.9	+50.7	+34.4	+38.3 ± 1.6
	Δu_2	−03.7	+03.8	−02.4	−02.1	+00.0	−02.3 ± 0.6
	Δu_3	+10.0	+07.5	+09.9	+04.2	−06.3	+05.7 ± 3.5
Hawaii	Δu_1	+03.3	+01.3	−05.2	+00.4	−00.3	−04.0 ± 1.6
	Δu_2	+06.1	+04.5	+16.0	+01.2	+15.2	+09.2 ± 2.8
	Δu_3	−45.4	−48.6	−47.7	−67.9	−25.0	−45.5 ± 3.6

parameters expressing variations in the earth's gravitational field (i.e., spherical harmonic coefficients); $\mathbf{p}_t$ are arbitrary polynomials of the Keplerian elements; $\mathbf{p}_d$ are parameters of an atmospheric model and the interaction of the satellite therewith; and $\mathbf{p}_p$ are parameters expressing radiation pressure effects.

The procedure used to compute the osculating elements M, a, e, i, ω, and Ω, and the partial derivatives matrices $\mathbf{J}$, $\mathbf{C}_{eg}$, $\mathbf{C}_{et}$, $\mathbf{C}_{ed}$, $\mathbf{C}_{ep}$, was as follows.

Preliminary orbits were determined by iterated differential correction fitted to the observations based on the following parameters: (a) the constants of integration of the orbital theory of Brouwer [1959]; (b) the gravitational field parameters kM and the zonal harmonics J_2, J_3, J_4; and (c) arbitrary polynomials in terms of the Keplerian elements. The principal purpose of this preliminary orbit determination was to obtain osculating elements at the instant of each observation close enough to the true values so that the corrections could be considered linear.

The intermediate orbit elements defining the preliminary orbit were used to generate Fourier series to express the effects of the several perturbations and the partial derivatives of the osculating elements with respect to the parameters of the perturbations described below.

For $\mathbf{C}_{e_\theta}$, the effect of spherical harmonics of the earth's gravitational field, the disturbing function developed by Kaula [1961a] was used:

$$R_{nm}=\frac{a_e^n\mu}{a^{n+1}}\sqrt{\frac{(n-m)!(2n+1)\kappa_m}{(n+m)!}}\sum_{p=0}^{n}F_{nmp}(i)\sum_{q=-\infty}^{\infty}G_{npq}(e)$$
$$\times\left[\begin{Bmatrix}\bar{C}_{nm}\\-\bar{S}_{nm}\end{Bmatrix}_{(n-m)\text{odd}}^{(n-m)\text{even}}\cos\{(n-2p)\omega+(n-2p+q)M\right.$$
$$+m(\Omega-\theta)\}+\begin{Bmatrix}\bar{S}_{nm}\\\bar{C}_{nm}\end{Bmatrix}_{(n-m)\text{odd}}^{(n-m)\text{even}}\sin\{(n-2p)\omega$$
$$\left.+(n-2p+q)M+m(\Omega-\theta)\}\right]\tag{8}$$

where $\kappa_0=1$; $\kappa_m=2$, $m\neq 0$. This disturbing function was used in the Lagrangian equations of motion [Brouwer and Clemence, 1961, p. 289] and integrated under the assumption that a, e, and i remained constant and that M, ω, and Ω changed secularly. The program automatically determined for each spherical harmonic all terms above a specified minimum in absolute magnitude and stored the results as subscripted numerical arrays to be multiplied by the sines and cosines evaluated at the instant of each observation. An example of one of the 210 such partial derivatives formed for satellite 1960ι_2 follows:

$$\begin{aligned}\partial e/\partial\bar{C}_{31}=&1.850\cos(\omega+\Omega-\theta)\\&-0.001\cos(\omega+M+\Omega-\theta)\\&+5.058\cos(-\omega+\Omega-\theta)\\&+0.002\cos(-\omega-M+\Omega-\theta)\\&-0.609\cos(-\omega-2M+\Omega-\theta)\end{aligned}\tag{9}$$

Using a rejection criterion of $0.1n^{1.2}$ applied to partial derivatives of the elements $M+\omega+\Omega\cos i$, $e^2(\omega+\Omega\cos i)$, $\Omega\sin i$, e, i, and a between one and six significant periodicities were found for each term.

The harmonics listed in Table 4 were selected as having an rms anticipated effect on the satellite orbit of ± 20 meters or more, using the degree variances given by Kaula [1959].

As expected, the partial derivatives indicated poor separation of even-degree harmonics of the same order m, causing principally along-track perturbations of frequency $m(\dot{\Omega}-\dot{\theta})$. However, the effect of odd-degree harmonics, especially third, was unexpectedly distinct, differing not only in frequency but also in perturbing mainly the eccentricity (or perigee height) of a nearly circular orbit.

Table 4.—*Gravitational Coefficient Data*

[Multiply all numbers by a scaling factor of 10^{-6}]

Coefficient	Starting value	Preassigned σ	Preliminary solution	Final solution
$\Delta\bar{C}_{00}$	0.00	±10.00	4.52	1.23±3.29
$\Delta\bar{C}_{20}$	−0.054	±0.07	0.01	−0.06±0.01
$\bar{C}_{21}$	0.00	±2.00	−0.04	Fixed
$\bar{S}_{21}$	0.00	±2.00	−0.07	Fixed
$\bar{C}_{22}$	0.00	±2.00	2.96	1.84±0.19
$\bar{S}_{22}$	0.00	±2.00	−1.71	−1.71±0.28
$\bar{C}_{30}$	0.970	±0.02	1.07	0.98±0.01
$\bar{C}_{31}$	0.00	±1.26	1.89	1.77±0.21
$\bar{S}_{31}$	0.00	±1.26	0.28	−0.11±0.20
$\bar{C}_{32}$	0.00	±1.26	−0.37	0.34±0.26
$\bar{S}_{32}$	0.00	±1.26	0.30	0.08±0.35
$\bar{C}_{33}$	0.00	±1.26	−0.32	−0.31±0.46
$\bar{S}_{33}$	0.00	±1.26	0.61	0.74±0.46
$\bar{C}_{40}$	0.613	±0.12	0.79	0.55±0.10
$\bar{C}_{41}$	0.00	±0.63	−0.10	−0.21±0.16
$\bar{S}_{41}$	0.00	±0.63	0.60	0.46±0.15
$\bar{C}_{42}$	0.00	±0.63	0.66	−0.03±0.19
$\bar{S}_{42}$	0.00	±0.63	0.25	0.32±0.19
$\bar{C}_{43}$	0.00	±0.63	1.23	0.50±0.21
$\bar{S}_{43}$	0.00	±0.63	0.10	0.16±0.19
$\bar{C}_{44}$	0.00	±0.63	−0.48	−0.24±0.27
$\bar{S}_{44}$	0.00	±0.63	1.12	0.55±0.29
$\bar{C}_{50}$	0.019	±0.02	−0.30	0.03±0.01
$\bar{C}_{51}$	0.00	±0.39	0.35	0.08±0.14
$\bar{S}_{51}$	0.00	±0.39	0.70	0.26±0.15
$\bar{C}_{60}$	−0.110	±0.10	0.00	−0.10±0.02
$\bar{C}_{61}$	0.00	±0.28	0.06	0.02±0.08
$\bar{S}_{61}$	0.00	±0.28	−0.05	−0.18±0.07
$\bar{C}_{62}$	0.00	±0.28	0.21	0.00±0.06
$\bar{S}_{62}$	0.00	±0.28	0.07	0.06±0.07
$\bar{C}_{63}$	0.00	±0.28	1.11	0.13±0.08
$\bar{S}_{63}$	0.00	±0.28	0.31	0.21±0.16
$\bar{C}_{64}$	0.00	±0.28	0.00	0.13±0.11
$\bar{S}_{64}$	0.00	±0.28	−0.28	−0.24±0.10
$\bar{C}_{70}$	0.121	±0.02	−0.13	0.10±0.01

NOTES.—$\bar{C}_{nm}$, $\bar{S}_{nm}$ are coefficients of spherical harmonic terms $kM/r(a/r)^n H_{nm}$ such that $\int H_{nm}^2\, d\sigma = 4\pi$ for integration over the sphere [Kaula, 1959, equations (16) to (18)].

$\Delta\bar{C}_{00}$, $\Delta\bar{C}_{20}$ are corrections to 0.3986032×10^{21} $(1.0 - 0.00108236 P_2)$ cgs.

For tesseral harmonic coefficients, initial values of zero were assumed; for zonal harmonic coefficients, the values of Kozai [1962a] were used.

For the gravitational effects of the sun and moon, a similar disturbing function was used [Kaula, 1962d]. All secular terms were retained, plus periodic terms of more than 2×10^{-5} amplitude, of which two to nine were found for each orbit.

For the radiation pressure effect of the sun, the disturbing function given by Kaula [1962d], was used. Because of the irregular effect of the earth's shadow, the perturbations were not integrated analytically, and a numerical harmonic analysis was applied instead. A harmonic analysis interval of 15 days (or a minimum period of 30 days) was found sufficient to reflect all variations in amplitude of more than 2×10^{-5}. Partial derivatives were formed only for one parameter: the mean reflectivity times the cross-sectional area.

For drag, the effect of an empirical atmospheric model was applied, with density in the form [Jacchia, 1960]:

$$\rho=\rho_0\left(\frac{S}{100}\right)^m \exp\left\{\frac{h-h_0}{H}+ce^{-dh}\right\}\cdot\left\{1+b(e^{ah}-k)\cos^n\frac{\psi}{2}\right\} \tag{10}$$

In (10), S is the solar flux of 10.7- or 20-cm wavelength, h is the height above the earth's surface, and ψ is the angle from the center of the diurnal bulge, determined by

$$\cos\psi=\{1,0,0\}\mathbf{R}_3(\lambda^*)\mathbf{R}_1(\epsilon)\mathbf{R}_3(\chi)\mathbf{R}_{xq}\mathbf{q}/r \tag{11}$$

where λ^* is the sun's longitude, ϵ is the inclination of the ecliptic, and χ is the lag of the atmospheric bulge behind the sun.

The atmosphere was assumed to rotate with the solid earth and to have the oblateness of a fluid. The customary assumption of the drag force being proportional to the square of the velocity was made. The force components that are radial, transverse, and normal to the satellite and its orbital plane were used in the Gaussian equations of motion [Brouwer and Clemence, 1961, p. 301], and numerical Fourier series were developed for the effects on the Keplerian elements. In generating these series, second-order effects on the angular elements that are dependent on the secular motions due to the oblateness were included. With an analysis interval of 3 days, variations in amplitude as small as 3×10^{-6} were obtained in M.

For satellites 1959α_1 and 1959η the values of the parameters in (9) that were determined by Jacchia [1960] were used. For satellite 1960ι_2, c, a, and k were set equal to zero, and ρ_0, m. H, b, n, and χ were determined so as to fit the atmospheric models of Harris and Priester [1962]. For 1959α_1 and 1959η, the Jacchia model absorbed most of the long-period drag variations but did not fit variations characterized by periods of less than 10 days. For 1960ι_2, the Harris and Priester model did not reduce residuals significantly and had a negligible effect on the values determined for the geodetic parameters, and hence it was omitted.

In computing the effects of arbitrary polynomials or the partial derivatives with respect thereto, the second-order effects of the acceleration based on the assumption of constant perigee height [equations (5) to (14), O'Keefe et al., 1959; equation 2.100, Kaula, 1962c] were applied.

In the partial derivatives J with respect to the intermediate orbit elements at epoch (equation 7), the effects of secular motions due to oblateness were included [Kaula, 1961a, equation 49]. To ensure that the ± 20-meter specification was met, the extension of Brouwer's theory to periodic terms of order $J_2{}^2$ by Kozai [1962b] was examined but was found not to be needed.

In the final analysis of the orbit all the perturbations were added to the osculating elements as determined from the preliminary orbit at each observation. The long-period and secular perturbations that are due to luni-solar attraction, radiation pressure, and drag by a specified atmospheric model were omitted. For the orbital arc lengths of 10 to 20 days, it was found that these effects were adequately absorbed by an arbitrary acceleration in the mean anomaly. Their inclusion made little difference in the solutions obtained for tesseral harmonics or station shifts—if anything, they may have distorted the results by shifting computed satellite directions farther from those observed.

Data analysis.—As discussed in earlier papers [Kaula, 1961b, 1962a, b], difficulties are created by (1) the nonuniform distribution of observations; (2) the similarity of effects on the observations of different gravitational coefficients and station-position errors; (3) the inadequacy of the atmospheric model; and (4) the prohibitive amount of computing time which would be required by a solution that takes into account serial correlation between different times. Three methods were used to overcome these difficulties:

(1) Preassigning variance and covariance V for the starting values of parameters to which corrections z are being determined so that the solution becomes [Kaula, 1961a]

$$z = (\mathbf{M}^T\mathbf{W}^{-1}\mathbf{M} + V^{-1})^{-1}\mathbf{M}^T\mathbf{W}_0{}^{-1}\mathbf{f} \tag{12}$$

where $\mathbf{W}$ is the covariance matrix of the observations, $\mathbf{M}$ is the matrix of partial derivatives in the observation equations, and $\mathbf{f}$ is the vector of residuals.

(2) Assigning higher weight to the across-track than to the along-track component of an observation, as described by equation 3.

(3) Using arbitrary polynomials.

It was found that inclusion or omission of effects which were secular or of periods of more than a few days had very little influence on the values determined for the station shifts or tesseral harmonics. The most troublesome inadequacy was the inability of the empirical atmospheric models to explain orbital variations in the 1.0 to 0.1 cycle per day part of the spectrum. The principal improvement which might be made would be to utilize the correlation of corpuscularly caused density variations with the A_p index [Jacchia, 1962].

It was found necessary to apply the device, specifying variance and covariance for the starting values of the parameters, in order to avoid absurdly distorted results due to the ill-conditioning caused by the non-uniform distribution of observations and the inadequate accounting for drag effects. For the stations on the Am., EASI, and JKM geodetic systems, the 9×9 covariance matrix generated in the solution of Kaula [1961c] was used. For the three isolated datums, the assigned covariance matrices were based on assumed error ellipsoids of ±35-meter vertical semiaxes in all three cases, and horizontal semiaxes of ±100 meters for Au., ±200 meters for Ar., and ±250 meters for H. The smaller uncertainty for the Australian system is based on the improvement of its position by adjusting deflections of the vertical [Veis, 1961]. For the zonal spherical harmonic coefficients of the gravitational field, the preassigned variances were based on the uncertainties given by Kozai [1962a], multiplied by 4. For the tesseral harmonics $n, m=2,1$ and $2,2$, the preassigned variance of $(2.0\times10^{-6})^2$ was based on the order of magnitude of earlier determinations of J_{22} by Kozai [1961], Kaula [1961b], and Newton [1962], except that $\bar{C}_{21}$ and $\bar{S}_{21}$ were held fixed. For the tesseral harmonic coefficients of the third and higher degrees, the preassigned σ's in Table 4 were computed from the degree variances $\sigma_n^2\{\Delta g\}$ [Kaula, 1959]:

$$\sigma^2\{\bar{C}_{nm} \text{ or } \bar{S}_{nm}\}=\frac{\sigma_n^2\{\Delta g\}}{(n-1)^2g^2(2n+1)} \tag{13}$$

The observational variance employed was $(0.026 \text{ sec})^2$ time and $(9.2 \text{ sec})^2$ direction for 12-day arcs of $1959\alpha_1$ and 1959η, $(0.047 \text{ sec})^2$ time and $(13.4 \text{ sec})^2$ direction for 20-day arcs of $1960\iota_2$; $(0.146 \text{ sec})^2$ time and $(43.8 \text{ sec})^2$ direction for 10-day arcs of $1961\delta_1$; and $(0.047 \text{ sec})^2$ time and $(13.4 \text{ sec})^2$ direction for 18-day arcs of $1961\alpha\delta_1$. The principal criterion used in determining the observational variances was the χ^2 test; i.e., the quantity

$$s = (\mathbf{f}^T\mathbf{W}^{-1}\mathbf{f} - \mathbf{z}^T\mathbf{M}^T\mathbf{W}^{-1}\mathbf{f}/n - p) \tag{14}$$

should average 1 for several orbital arcs, where **f** is the vector of observation equation residuals; **W** is the covariance matrix of observations; **z** is the vector of corrections to parameters; **M** is the matrix parameter coefficients in the observation equations; n is the number of observations; and p is the number of free parameters. In forming the covariance matrix **W**, observations in the same pass were treated as having the same timing error.

The arc lengths used were chosen after some experimentation as giving a reasonable compromise between magnitude of residuals and number of observations.

The use of arbitrary polynomials was held to a minimum; i.e., the only one used was a t^2 variation in the mean anomaly.

In determining the estimated mean value and its standard deviation from several orbital arcs of the same satellite, the weighting of a particular arc was considered to be proportionate to its degrees of freedom. The computer program limited to fifteen the number of arcs that could be combined at a time. In combining the results of several sets of fifteen (or fewer) arcs, the weight ascribed to the mean of each set was considered to be the inverse of its variance, or standard deviation squared.

In order that the final mean and standard deviation reflect as much as possible any systematic differences which were functions of orbital specifications, all sets were combined, with inverse-variance weighting, into four groups: 1959α_1 and 1959η, twelve sets; 1960ι_2, two sets; 1961δ_1, one set; and 1961$\alpha\delta_1$, one set. The final means and standard deviations given in Table 5 are the result of an inverse-variance weighted combination of these four group solutions. However, for most of the variables, the standard deviations from combining the four groups were smaller than the standard deviations combining all sixteen sets at once, primarily because the differences between the 1960ι_2 mean and the 1959α_1 and 1959η mean were smaller than the scatter of 1959α_1 and 1959η solutions about their own mean.

To avoid the tendency to prejudge the order of magnitude of the solution, which is the main defect of the preassigned-variance technique, some computer experimentation was tried in determining the amplitudes of specified periodic variations, in place of harmonic coefficients, in holding the reference orbit fixed, and in analyzing residuals. Applying these methods to one satellite at a time did not give as good results as the preassigned-variance method, to judge by the scatter of solutions. To apply them to data from more than one satellite simultaneously required considerable program revision which did not seem worthwhile

Table 5.—*Gravitational Coefficient Solutions*

[Multiply all numbers by a scaling factor of 10^{-6}]

Coefficient[a]	$1959\alpha_1$	1959η	$1960\iota_2$	$1961\delta_1$	$1961\alpha\delta_1$	Weighted mean
$\Delta\bar{C}_{00}$	4.96	−8.88	−0.75	−18.50	−9.85	-2.46 ± 2.36
$\Delta\bar{C}_{20}$	−0.06	−0.06	−0.05	−0.29	0.00	-0.03 ± 0.02
$\bar{C}_{22}$	1.30	1.36	1.99	1.80	2.52	1.88 ± 0.29
$\bar{S}_{22}$	−1.74	−0.76	−1.63	−0.32	−0.89	-1.38 ± 0.17
$\bar{C}_{30}$	0.97	0.96	0.98	1.01	0.97	0.97 ± 0.01
$\bar{C}_{31}$	1.30	1.62	1.53	−0.96	1.18	1.52 ± 0.03
$\bar{S}_{31}$	0.29	0.99	−0.10	−0.34	0.46	0.14 ± 0.16
$\bar{C}_{32}$	−0.14	−0.13	0.29	2.35	−0.84	-0.02 ± 0.26
$\bar{S}_{32}$	0.49	0.29	0.38	−0.16	0.98	0.42 ± 0.06
$\bar{C}_{33}$	0.36	1.11	0.42	2.36	1.70	0.70 ± 0.26
$\bar{S}_{33}$	0.83	1.11	0.89	0.43	−1.33	0.76 ± 0.29
$\bar{C}_{40}$	0.68	0.67	0.61	−0.35	0.62	0.67 ± 0.02
$\bar{C}_{41}$	−0.38	−0.38	−0.33	−0.48	−1.00	-0.33 ± 0.01
$\bar{S}_{41}$	0.43	0.53	0.45	0.39	0.45	0.37 ± 0.15
$\bar{C}_{42}$	−0.10	−0.10	0.02	0.03	0.47	0.01 ± 0.02
$\bar{S}_{42}$	0.52	0.68	0.36	−0.43	0.06	0.35 ± 0.15
$\bar{C}_{43}$	0.18	0.35	0.50	0.44	0.17	0.17 ± 0.02
$\bar{S}_{43}$	0.29	0.11	−0.00	0.16	0.42	0.41 ± 0.03
$\bar{C}_{44}$	0.12	0.01	−0.20	0.20	−0.24	-0.01 ± 0.08
$\bar{S}_{44}$	0.11	0.22	0.36	0.29	0.32	0.18 ± 0.05
$\bar{C}_{50}$	0.02	0.03	0.03	0.01	0.02	0.02 ± 0.01
$\bar{C}_{51}$	−0.14	−0.02	−0.01	−0.63	(b)	-0.13 ± 0.02
$\bar{S}_{51}$	−0.06	−0.03	−0.01	0.23	(b)	-0.01 ± 0.01
$\bar{C}_{60}$	−0.09	−0.08	−0.04	1.10	−0.10	-0.09 ± 0.02
$\bar{C}_{61}$	−0.01	−0.03	0.00	−0.26	−0.09	-0.05 ± 0.03
$\bar{S}_{61}$	−0.09	−0.02	−0.07	−0.49	−0.06	-0.06 ± 0.01
$\bar{C}_{62}$	−0.04	0.05	−0.01	−0.07	0.05	0.01 ± 0.01
$\bar{S}_{62}$	−0.09	−0.18	−0.01	−0.07	0.01	-0.02 ± 0.03
$\bar{C}_{63}$	−0.02	−0.10	0.15	−0.02	(b)	0.15 ± 0.01
$\bar{S}_{63}$	−0.12	−0.01	−0.08	−0.06	(b)	-0.08 ± 0.01
$\bar{C}_{64}$	−0.00	0.06	0.06	−0.19	−0.01	-0.01 ± 0.01
$\bar{S}_{64}$	−0.06	−0.09	−0.42	−0.30	0.03	-0.03 ± 0.07
$\bar{C}_{70}$	0.12	0.12	0.07	0.09	0.12	0.12 ± 0.01

[a] $\bar{C}_{nm}$ and $\bar{S}_{nm}$ are coefficients of spherical harmonic terms $kM/r/a/r)^n\ H_{nm}$ such that $\int H_{nm}^2\,d\sigma=4\pi$ for integration over the sphere. $\Delta\bar{C}_{00}$ and $\Delta\bar{C}_{20}$ are corrections to 0.3986032×10^{21} $(1.0-0.00108236P_2)$ cgs.

[b] No determinations of $\bar{C}_{51}$, $\bar{S}_{51}$, $\bar{C}_{63}$, $\bar{S}_{63}$ were made from $1961\alpha\delta_1$ because the partial derivatives of the orbit with respect to these coefficients were all smaller than the criterion $0.1n^{1.2}$ [Kaula, 1963a].

because this method has been applied extensively by Izsak [1963]. Other changes tried and dropped as unnecessary were deleting orbital segments for which observations are scanty and holding fixed the station shifts obtained from the previous analysis of 1960ι_2 observations. The device of weighting observations inversely as their density with respect to the phase angle (node-GST) was tried and dropped.

Results.—The analysis described above took much time to apply to the large quantity of 1959α_1 and 1959η data. The attempt to combine solutions from different sets of arcs was not made until this analysis had been completed. Consequently, the good agreement shown by Table 5 between the results from 1960ι_2 on the one hand and from 1959α_1 and 1959η on the other came as a pleasant surprise. The combination of results is not as good, of course, as is suggested by the formal standard deviations given in the table; in particular, the errors in difference of position between stations in North and South America—or between stations in Europe, Africa, and India—which were held fixed with respect to each other, are probably several times as great as some of the stated uncertainties. The good agreement is even more marked for the spatial representations given in Figures 1 and 2; e.g., for the seven

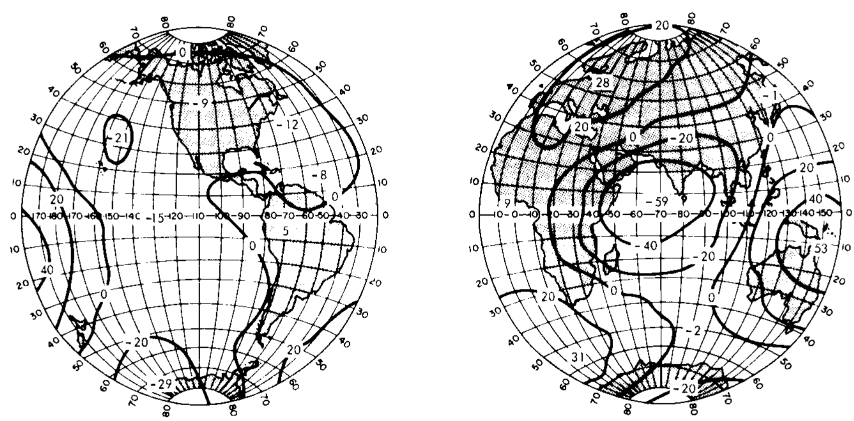

Figure 1.—**Vanguard geoid. Geoid heights, in meters, referred to an ellipsoid of flattening 1/298.24, determined from observations of satellites 1959α_1 and 1959η.**

most extreme maximums and minimums in the Vanguard geoid of Figure 1, there are maximums and minimums in the Echo rocket geoid of Figure 2 agreeing within 10° in location and within 11 meters in magnitude. The degree of independence in these solutions is fairly satisfying. The orbits differ by 0.23 in inclination, and 0.16 in eccentricity; the arc lengths used differed in a ratio of 5 to 3, and the observational weighting differed in a ratio of 3 to 2. It would be very desirable, however, to obtain comparable series of observations of a satellite of much higher inclination.

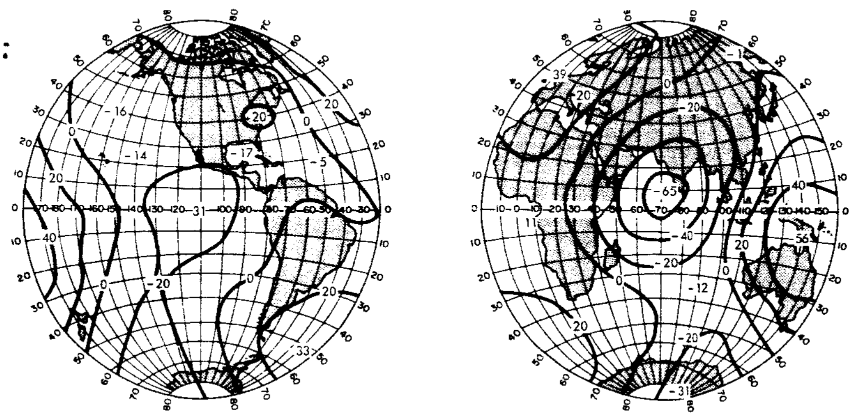

Figure 2.—Echo rocket geoid. Geoid heights, in meters, referred to an ellipsoid of flattening 1/298.24, determined from observations of satellite $1960\iota_2$.

The principal sources of systematic error likely to be common to satellites $1959\alpha_1$, 1959η, and $1960\iota_2$ seem to be (1) that the magnitudes of the results will be influenced by the preassigned variances and (2) that the relative positions of tracking stations on the same geodetic datum may be appreciably in error.

For a parameter whose effects are fairly distinct in periodicities, etc., from those of other parameters, it is implausible that its preassigned variance could cause a correction that is too large or of wrong sign, but it might cause a correction that is too small. However, the variance actually used in the analyses is not the estimated squared magnitude of the correction $\sigma^2(c)$, but rather $N\sigma^2(c)$, where N is the number of orbital arcs in a set. Since N was always between 10 and 15, this seems to be no more than a mild restraint preventing occasional ill-conditioned arcs from obtaining absurdly large corrections beyond the range of linearity.

Distortion caused by the preassigned variances seems most likely to occur in separating gravitational coefficients whose principal effects are of the same period; i.e., coefficients J_{nm} and J_{k1}, such that $m=1$ and $n-k$ is even. The most prominent set of such coefficients is J_{22}, J_{42}, and J_{62}, all of which cause semidaily variations of argument $2(\Omega-\theta)$. A way of removing some (but not all) of the influence of the preassigned covariances would be to assume that what we have determined is not the coefficients themselves but the amplitudes of semidaily variations in the orbital elements; e.g., for the cos $2(\Omega-\theta)$ term in the variation of the inclination

$$\Delta i=\frac{\partial i}{\partial \bar{C}_{22}}\bar{C}_{22}+\frac{\partial i}{\partial \bar{C}_{42}}\bar{C}_{42}+\frac{\partial i}{\partial \bar{C}_{62}}\bar{C}_{62} \tag{15}$$

The semimajor axis and the eccentricity have no semidaily variation. If we omit the 1961δ_1 and the 1961$\alpha\delta_1$ results and assume that the similar 1959α_1 and 1959η orbits should be combined, we have two sets of eight equations for three unknowns. Using values $\bar{C}_{22}=1.315\times10^{-6}$, $\bar{S}_{22}=-1.473\times10^{-6}$, $\bar{C}_{42}=0.101\times10^{-6}$, $\bar{S}_{42}=0.567\times10^{-6}$, $\bar{C}_{62}=-0.009\times10^{-6}$, $\bar{S}_{62}=-0.104\times10^{-6}$ for the combined 1959α_1 and 1959η solution (corresponding to Figure 1) and using values from Table 5 for 1960ι_2 we get the computed amplitudes of periodic perturbations in columns 6 and

Table 6.—*Semidaily Perturbations of Satellite Orbits*

Satellite (1)	Element (El) (2)	$\frac{\partial \mathrm{El}}{\partial \bar{C}_{22}}$ (3)	$\frac{\partial \mathrm{El}}{\partial \bar{C}_{42}}$ (4)	$\frac{\partial \mathrm{El}}{\partial \bar{C}_{62}}$ (5)	$10^6\times$ Comp $\Delta\mathrm{El}_c$ (6)	$\frac{\partial \mathrm{El}}{\partial \bar{S}_{22}}$ (7)	$\frac{\partial \mathrm{El}}{\partial \bar{S}_{42}}$ (8)	$\frac{\partial \mathrm{El}}{\partial \bar{S}_{62}}$ (9)	$10^6\times$ Comp $\Delta\mathrm{El}_s$ (10)
1959α_1 and	M	−2.92	0.36	5.74	− 3.93	2.92	− 0.36	− 5.74	− 3.91
1959η	i	3.62	− 5.89	3.83	5.33	3.62	− 5.89	3.83	− 9.12
combined.	ω	1.68	12.21	−24.58	1.20	−1.68	−12.21	24.58	− 7.09
	Ω	−5.54	4.22	4.88	− 7.76	5.54	− 4.22	− 4.88	−11.10
1960ι_2-----	M	−6.04	0.00	− 0.86	−12.05	6.04	0.00	0.86	− 9.86
	i	5.48	− 5.08	− 0.34	10.81	5.48	− 5.08	− 0.34	−10.76
	ω	−2.59	20.86	− 2.61	− 4.76	2.59	−20.86	2.61	−11.70
	Ω	−5.07	− 3.26	7.66	−10.12	5.07	3.26	− 7.66	− 7.07

10 of Table 6. Using these amplitudes as the observation equation constants and solving by the rule of minimizing $\Sigma(d\Delta\mathrm{El})^2$ yields

$$\bar{C}_{22}=1.85\times10^{-6} \qquad \bar{S}_{22}=-1.75\times10^{-6}$$

$$\bar{C}_{42}=0.05\times10^{-6} \qquad \bar{S}_{42}=0.34\times10^{-6}$$

$$\bar{C}_{62}=0.10\times10^{-6} \qquad \bar{S}_{62}=-0.22\times10^{-6}$$

All the coefficients are increased over the mean in Table 5 except $\bar{S}_{42}$, which hints of ill conditioning. However, it looks as though only $\bar{C}_{62}$ and $\bar{S}_{62}$ might have been significantly reduced by the preassigned-variance method.

The assumption that the relative positions of tracking stations on the same datum should be known through triangulation networks with a rms error of ±20 meters or less was based on standard methods of estimating triangulation accuracy [Bomford, 1962, pp. 143–159], as is confirmed by the misclosures of large loops of triangulation: (1) 15 meters in the 4000-km loop around the western Mediterranean [Whitten, 1952];

(2) less than 25 meters in the 10,000-km loop around the Caribbean [Fischer, 1959]; and (3) within 15 meters for the 10,000-km loop around the Black Sea and Caspian Sea, through Turkestan, and connecting in northwest India [Fischer, 1961].

The connections between the three northern hemisphere stations of the EASI system are closely associated with loops 1 and 3, and the connections between the three northern hemisphere stations of the Am. system are closely associated with loop 2. More in doubt are the positions of the stations in the southern hemisphere in Peru and South Africa, which depend on long single arcs of triangulation. A test run was therefore made on all the $1960\iota_2$ data, in which the stations Arequipa (in Peru) and Olifantsfontein (in South Africa) were assumed to be on separate datums. The results of this test corroborated the assumption as to triangulation accuracy; the station in Peru moved 24 meters with respect to those in North America, while the station in South Africa moved 14 meters with respect to those in Eurasia. The changes in the gravitational coefficients were insignificant—$\bar{C}_{22}$, from 1.99 to 2.11×10^{-6}; $\bar{S}_{22}$, from -1.63 to -1.60×10^{-6}; $\bar{C}_{31}$, from 1.53 to 1.49×10^{-6}; $\bar{C}_{41}$, from -0.33 to -0.28×10^{-6}; etc.—and the maximum effect on any geoid height in Figure 2 was 4 meters.

There still exists the possibility of errors in the local connection of tracking stations to the triangulation systems, a matter in which better standardization of procedures is needed [Kaula, 1963b]. To check this type of error for stations on the major datums we calculate the geometric geoid heights corresponding to the final positions in rectangular coor-

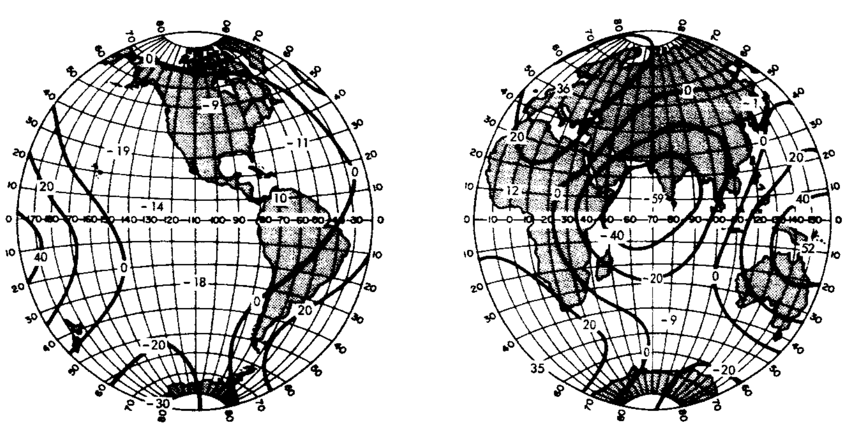

Figure 3.—**Combined geoid. Geoid heights, in meters, referred to an ellipsoid of flattening 1/298.24, determined from observation of satellites $1959\alpha_1$, 1959η, $1960\iota_2$, $1961\delta_1$, and $1961\alpha\delta_1$.**

dinates and then compare these heights with the gravitational geoid heights in Figure 3. To estimate the size of discrepancies to be expected, we have the geoid height variance of 1076 m^2 from autocovariance analysis of gravimetry [Kaula, 1959] and a mean square height of the satellite geoid of 466 m^2, obtained from the sum of the squares of the coefficients in Table 5. If the station positions and the equatorial radius were correct, the rms expected discrepancy between the geometric and gravitational geoid heights due to the inability of the satellite orbits to pick up the shorter-wave variations would be $(1076-466)^{1/2} = \pm 25$ meters.

The results of the comparison are shown in Table 7. Applying the mean correction of +31 meters yields a mean equatorial radius of 6,378,196±11 meters and a rms discrepancy of ±38 meters, which implies a rms radial position error of $(382-252)^{1/2} = \pm 29$ meters. Of the stations on the major datums, the 60-meter discrepancy for San

Table 7.—*Comparison of Geometric and Gravitational Geoid Heights*

Station	Datum	Geometric geoid height, m	Gravitational geoid height, m	Discrepancy for 6,378,196 m radius, m	Discrepancy for 6,378,196 m radius, m
Organ Pass	Am.	−4	−10	+6	−25
Arequipa		−16	−8	−8	−39
Curaçao		−25	−10	−15	−46
Jupiter		−18	−9	−9	−40
Olifantsfontein	EASI	+22	+5	+17	−14
San Fernando		+117	+26	+91	+60
Naini Tal		−17	−41	+24	−7
Shiraz		+14	−18	+32	+1
Woomera	Au.	+47	+24	+23	−8
Tokyo	JKM	+54	+4	+50	+19
Villa Dolores	Ar.	+104	+4	+100	+69
Maui	H	+54	−12	+66	+35

NOTE.—Geoid heights referred to ellipsoid of equatorial radius 6,378,165 meters, flattening 1/298.24.

Fernando causes suspicion of local connection error; however, there is also a 69-meter discrepancy for Villa Dolores, which was free to move to its correct position.

The solution in Figure 3 agrees with astrogeodetic [Fischer, 1961] and gravimetric [Uotila, 1962] solutions, particularly in showing a more pronounced negative in the western Atlantic. The discrepancies which exist may in part be ascribed to the method of analysis of the terrestrial data, since the agreement is appreciably better with the combination of astrogeodetic, gravimetric, and satellite zonal harmonic data of Kaula [1961c], especially for western Europe.

The reference flattening of 1/298.24 is used in Figures 1, 2, and 3 to facilitate comparison with the results of Kaula [1961c, 1963a]. The flattening equivalent to the solution obtained for $\Delta\bar{C}_{20}$ is 1/298.28. The J_2 equivalent is 1082.48×10^{-6}.

In conclusion it can be said that better explanations are needed for the systematic discrepancies indicated by Tables 5 and 7. However, considering that the observations used herein depended on reflected sunlight; that they were all made more than 3 years before the minimum of solar activity; and that the orbital specifications are far from ideal, the prospects are bright for extracting more information on the gravitational field from more recent and anticipated satellites. It will be of particular interest to push the analysis to a good determination of some sixth- or eighth-degree harmonics to see whether or not they corroborate other indicators of a weak upper mantle.

REFERENCES

Bomford, G.: Geodesy, 2nd ed., 561 pp., Oxford University Press, London, 1962.

Brouwer, Dirk: Solution of the problem of artificial satellite theory without drag, Astron. J., 64, 378–396, 1959.

Brouwer, Dirk; and G. M. Clemence: Methods of Celestial Mechanics, Academic Press, New York, 1961.

Fischer, I.: A tentative world datum for geoidal heights based on the Hough ellipsoid and the Columbus geoid, J. Geophys. Res., 64, 73–84, 1959.

Fischer, I.: The present extent of the astro-geodetic geoid and the geodetic world datum derived from it, Bull. Geod., 61, 245–264, 1961.

Haramundanis, K.: Catalogue of precisely reduced observations, no. P–4, Smithsonian Inst. Astrophys. Obs. Res. in Space Sci., Spec. Rept. 95, 1962.

Harris, I.; and W. Priester: Theoretical models for the solar-cycle variation of the upper atmosphere, NASA Tech. Note D–1444, 261 pp., 1962.

Henize, K. G.: Tracking artificial satellites and space vehicles, Advan. Space Sci., 2, 117–142, 1960.

Izsak, I. G.: Tesseral harmonics of the geopotential, Nature, 199, 137–139, 1963.

Jacchia, L. G.: A variable atmospheric density model from satellite accelerations, J. Geophys. Res., 65, 2775–2782, 1960.

Jacchia, L. G.: Electromagnetic and corpuscular heating of the upper atmosphere, Space Research, 3: Proc. Intern. Space Sci. Symp., 3rd, Washington, North-Holland Publishing Co., Amsterdam, in press, 1962.

Kaula, W. M.: Statistical and harmonic analysis of gravity, J. Geophys. Res., 64, 2401–2421, 1959.

Kaula, W. M.: Analysis of gravitational and geometric aspects of geodetic utilization of satellites, Geophys. J., 5, 104–133, 1961a.

Kaula, W. M.: Analysis of satellite observations for longitudinal variations of the gravitational field, Space Research, 2: Proc. Intern. Space Sci. Symp., 2nd, Florence, pp. 360–372, North-Holland Publishing Co., Amsterdam, 1961b.

KAULA, W. M.: A geoid and world geodetic system based on a combination of gravimetric, astrogeodetic, and satellite data, J. Geophys. Res., 66, 1799–1812, 1961c.

KAULA, W. M.: Satellite orbit analysis for geodetic purposes (in Russian), Bull. Inst. Theoret. Astron: Proc. Conf. on General and Practical Problems of Theoretical Astronomy, Moscow, in press, 1962a.

KAULA, W. M.: Satellite orbit analyses for geodetic purposes, Proc. I.U.T.A.M. Symp. Dynamics of Satellites, Paris, Springer-Verlag, Berlin, in press, 1962b.

KAULA, W. M.: Celestial geodesy, Advan. Geophys., 9, 191–293, 1962c.

KAULA, W. M.: Development of the lunar and solar disturbing functions for a close satellite, Astron. J., 67, 300–303, 1962d.

KAULA, W. M.: Tesseral harmonics of the gravitational field and geodetic datum shifts derived from camera observations of satellites, J. Geophys. Res., 68, 473–484, 1963a.

KAULA, W. M.: A review of geodetic parameters; Paper presented at the Intern. Astron. Union Symp., no. 21, The System of Astronomical Constants; to appear in Bull. Astron., 1963b.

KOZAI, Y.: Tesseral harmonics of the potential of the earth as derived from satellite motions, Astron. J., 66, 355–358, 1961.

KOZAI, Y.: The potential of the earth derived from satellite motions, Proc. I.U.T.A.M. Symp. Dynamics of Satellites, Paris, Springer-Verlag, Berlin, in press, 1962a.

KOZAI, Y.: Second-order solution of artificial satellite theory without air-drag, Astron. J., 67, 446–461, 1962b.

LASSOVSKY, K.: On the accuracy of measurements made upon films photographed by Baker-Nunn satellite tracking cameras, Smithsonian Inst. Astrophys. Obs. Res. in Space Sci., Spec. Rept. 74, 1961.

NEWTON, R. R.: Ellipticity of the equator deduced from the motion of Transit 4A, J. Geophys. Res., 67, 415–416, 1962.

O'KEEFE, J. A.; ECKELS, ANN; AND SQUIRES, R. K.: The gravitational field of the earth, Astron. J., 64, 245–253, 1959.

UOTILA, U. A.: Harmonic analysis of world-wide gravity material, Publ. Isostatic Inst. Intern. Assoc. Geodesy, 39, 18 pp., 1962.

VEIS, GEORGE: The positions of the Baker-Nunn camera stations, Smithsonian Inst. Astrophys. Obs. Res. in Space Sci., Spec. Rept. 59, 1961.

VEIS, G.; HARAMUNDANIS, K.; SIMONS, L.; STERN, P.; AND MACDONALD, J. E.: Catalogues of precisely reduced observations, nos. P–1 through P–7, Smithsonian Inst. Astrophys. Obs. Res. in Space Sci., Spec. Repts. 82, 1961; 85, 91, 95, 102, 104, 106, 1962.

VEIS, G.; AND WHIPPLE, F. L.: Experience in precision optical tracking of satellites for geodesy, Space Research, 2: Proc. Intern. Space Sci. Symp., 2nd, Florence, pp. 17–33, North-Holland Publishing Co., Amsterdam, 1961.

WESTON, E.: Preliminary time reduction for the determination of precise satellite positions, Smithsonian Inst. Astrophys. Obs. Res. in Space Sci., Rept. 41, 11–13, 1960.

WHITTEN, C. A.: Adjustment of European triangulation, Bull. Geod., 24, 187–206, 1952.

The following paper was originally published in Journal of Geophysical Research, *vol. 69, no. 12, June 15, 1964, pp. 2621–2630.*

Tesseral Harmonics of the Geopotential and Corrections to Station Coordinates

IMRE G. IZSAK
Smithsonian Astrophysical Observatory and Harvard College Observatory, Cambridge, Massachusetts

INTRODUCTION

IN THE PAST THREE YEARS numerous attempts have been made to determine the small, large-scale, longitude-dependent irregularities in the gravitational field of the earth from their effects on the motion of artificial satellites. As often happens with methods still under development, the first investigations on this subject were handicapped by an oversimplified analysis of insufficient observational material; they led to contradictory results and are already obsolete. It was only recently that determinations based on optical data [Kaula, 1963*a*, *b*; Izsak, 1963] and Doppler data [Anderle and Oesterwinter, 1963; Guier, 1963] have shown encouraging agreement in the main features of the geopotential as independently obtained by these authors. At the same time their results compare favorably with those derived from an analysis of surface-gravity data [Kaula, 1961*b*; Uotila, 1962]. Despite the reported progress, much work must be done before we can reach definite conclusions about the longitudinal dependence of the earth's gravitational field. The purpose of this paper is to present new evidence concerning the subject. No attempt will be made to evaluate critically the methods and results of the authors mentioned above, for this would seem premature at this time.

The basic philosophy adopted in the present investigation is that a statistical problem of such complexity should be considered from an experimental rather than from a theoretical point of view. Instead of trying to anticipate what might happen in the process of a very intricate least-squares fitting, I think it preferable to carry out many different solutions under conditions as different as possible and then to choose the best solution by comparing residuals, standard deviations, correlation coefficients, etc. Questions regarding the convergence of the geopotential's development into an infinite series of spherical harmonics seem irrelevant to me. A least-squares fitting of a finite number of terms can merely give an approximation in the mean, which, in practical applications, is what we really are concerned with.

Our main interest is in the external gravitational field of the earth. However, since the interpretation of satellite observations is affected by the errors in the assumed coordinates of the Baker-Nunn camera stations, it is imperative to improve the latter. Experimental evidence shows that the correlations among harmonic coefficients and station coordinates are generally weak, and those among corrections to the coordinates of different stations are entirely negligible. Since the original connection of the stations to major geodetic systems proved to be unreliable in several instances, I decided to treat the 12 tracking stations individually.

COMPUTATIONAL PROCESS

The analysis of the observations begins with a painstaking computation of satellite orbits.

DOI 3, our differential orbit improvement program [Gaposchkin, 1964], accounts analytically for the first-order short-period perturbations resulting from the oblateness and for the long-period perturbations caused by the equatorial unsymmetry of the earth, as well as for lunar perturbations with biweekly periods. Secular perturbations of gravitational origin, the effect of atmospheric drag and solar radiation pressure, however, are as a rule determined empirically in the process of least-squares fitting. The length of an orbital arc represented by a single set of mean orbital elements varies between one and four weeks, depending on the particular object; in such a time interval there are 60 to 500 observations. On completing the computations, DOI 3 produces for each observation a binary card that contains among other useful information the sidereal time at Greenwich θ_i, the along-track and across-track residuals dU_i and dW_i of the observation, as well as the instantaneous values M_i, a_i, e_i, I_i, ω_i, and Ω_i of the mean orbital elements. The binary cards pertaining to several satellites in several time intervals are collected, and their content is put on a magnetic tape, which will serve as input in the subsequent analysis.

The residuals dU_i and dW_i comprise, besides components not sufficiently accountable, the positional and timing errors of the Baker-Nunn observations, the effect of the tesseral harmonics in the geopotential, and the effect of small errors in the adopted station coordinates. By analyzing many thousand observations one can arrive at reasonable least-squares estimates of the tesseral harmonics' numerical coefficients and of the corrections to the station coordinates. This is the purpose of the tesseral harmonics and station coordinates program, a brief description of which follows:

Let the geocentric position vector of a satellite as computed by DOI 3 be denoted by $\mathbf{r}_c$, and a station vector as used in the computations be $\mathbf{R}_c$; the corresponding topocentric position vector of the satellite is $\boldsymbol{\varrho}_c = \mathbf{r}_c - \mathbf{R}_c$. If the correction to be applied to the station vector is $d\mathbf{R} = \mathbf{R} - \mathbf{R}_c$, and the perturbations caused by the hitherto neglected tesseral harmonics are given by $d\mathbf{r} = \mathbf{r} - \mathbf{r}_c$, the corresponding change in the topocentric position vector will be $d\boldsymbol{\varrho} = d\mathbf{r} - d\mathbf{R}$. Having only angular residuals at our disposal, we disregard the line-of-sight component of this vector by projecting it onto the directions of the along-track and across-track unit vectors $\mathbf{e}_U$ and $\mathbf{e}_W$. For the angular corrections in these directions we have then

$$du = du^h - du^s \qquad dw = dw^h - dw^s \tag{1}$$

where

$$du^s = \rho^{-1}\mathbf{e}_U \cdot d\mathbf{R} \qquad dw^s = \rho^{-1}\mathbf{e}_W \cdot d\mathbf{R} \tag{2}$$

and

$$du^h = \rho^{-1}\mathbf{e}_U \cdot d\mathbf{r} \qquad dw^h = \rho^{-1}\mathbf{e}_W \cdot d\mathbf{r} \tag{3}$$

The positions of the Baker-Nunn stations [Veis, 1961, 1963*a*] being given in an earth-fixed rectangular coordinate system X, Y, Z, we put

$$d\mathbf{R} = \mathbf{e}_X\, dX + \mathbf{e}_Y\, dY + \mathbf{e}_Z\, dZ \tag{4}$$

Here the unit vector $\mathbf{e}_X$ lies in the intersection of the equator with the meridian of Greenwich; $\mathbf{e}_Z$ points toward the north pole; and $\mathbf{e}_Y$ is perpendicular to both of them.

The explicit representation of the vector $d\mathbf{r}$ is much more involved, of course. It requires the elaboration of a perturbation theory for the tesseral harmonics in the geopotential, a topic that will be touched upon below. At present it suffices to say that any perturbations of the orbital elements result in a vectorial displacement,

$$d\mathbf{r} = \frac{\partial \mathbf{r}}{\partial M}\, dM + \frac{\partial \mathbf{r}}{\sigma a}\, da + \frac{\partial \mathbf{r}}{\partial_e}\, de + \frac{\partial \mathbf{r}}{\partial I}\, dI + \frac{\partial \mathbf{r}}{\partial \omega}\, d\omega + \frac{\partial \mathbf{r}}{\partial \Omega}\, d\Omega \tag{5}$$

and that the perturbations in question are linear in the numerical coefficients of the tesseral harmonics. Full details concerning equations 1 through 5 were given in an earlier paper [Izsak, 1962].

In this way we obtain the observation equations

$$du_i = du_i^h - du_i^s = dU_i$$

and

$$dw_i = dw_i^h - dw_i^s = dW_i \tag{6}$$

To be minimized is

$$\sum_i \left[(dU_i - du_i)^2 + (dW_i - dw_i)^2\right]$$

where the summation is extended over the available observations of a number of satellites at all participating stations. An earlier version of the program had the facility of applying different weights to the along-track and across-track residuals, but the advantages of such an approach seemed rather dubious in practice.

Concerning the perturbation theory for tesseral (and sectorial) harmonics I confine myself to a few remarks. The disturbing function, which determines Lagrange's equations for the variation of orbital elements and thus the perturbations of the latter, is written in the form

$$R=\mu\sum_{n}\left\{(a_E{}^n/r^{n+1})\cdot\sum_{m=1}^{n}(C_{nm}\cos m\lambda+S_{nm}\sin m\lambda)P_{nm}(\sin\varphi)\right\}$$

the adopted definition of the Legendre associated functions being

$$P_{nm}(x)=(1-x^2)^{m/2}\,d^mP_n(x)/dx^m$$

To utilize Lagrange's equation, we must develop the disturbing function in terms of the orbital elements. This is conveniently done in two steps.

We note first that any rotation of the X, Y, Z coordinate system induces a linear transformation of the nth-degree spherical harmonics [Wigner, 1959], while the elements of the transformation matrix are easily calculated as functions of the Eulerian angles of rotation by means of the corresponding Cayley-Klein parameters. Let the X' and Z' axis of a new coordinate system point toward the perigee and pole of the satellite's orbit, so that the Eulerian angles coincide with $\Omega-\theta$, I, and ω. In this system the polar coordinates of the satellite are $\lambda'=v$ and $\varphi'=0$; therefore the spherical surface harmonics degenerate into trigonometric functions. Implementing these considerations we arrive at the expansion

$$P_{nm}(\sin\varphi)\exp(im\lambda)=\sum_{j=0}^{n}K_{nm}{}^{j}i^{n-m}\cdot\exp\{i[(n-2j)(v+\omega)+m(\Omega-\theta)]\}$$

where

$$K_{nm}{}^{j}=\frac{(n+m)!}{2^nj!(n-j)!}\cdot\sum_{k}(-1)^k\begin{bmatrix}2n-2j\\ k\end{bmatrix}\begin{bmatrix}2j\\ n-m-k\end{bmatrix}\gamma^{2n-\nu}\sigma^{\nu}\qquad(7)$$

$\gamma=\cos(I/2)$, $\sigma=\sin(I/2)$, $\nu=m-n+2j+2k$, and the range of the k summation is

$$\max\{0,\,n-m-2j\}\le k\le\min\{2n-2j,\,n-m\}$$

The polynomials (7) have the symmetry

$$K_{nm}{}^{j}(\gamma|\sigma)=(-1)^{n-m}K_{nm}{}^{n-j}(\sigma|\gamma)$$

In the second step, the functions

$$r^{-n-1} \exp [i(n-2j)v]$$

are to be developed into a Laurent series of exp (iM), a process that invokes the well-known Hansen coefficients from celestial mechanics. This and related subjects were dealt with recently [Izsak et al., 1964].

For the actual computation of the effect of tesseral harmonics on the orbital elements, we used a program that William M. Kaula of the Goddard Space Flight Center kindly made available to us; its mathematical formulation has already been described by Kaula [1961*a*]. Once given the orbital elements a, e, and I, this program yields for the several harmonics—apart from the at-this-stage-unknown numerical coefficients C_{nm} and S_{nm}—the perturbations $dM, \cdots, d\Omega$ in the form of trigonometric polynomials. Three terms are used if n is even, and four if n is odd. Thus, for instance, the effect of the second-, third-, and fourth-degree harmonics upon each orbital element is represented by a total of 54 trigonometric terms. The complete expressions for the perturbations are

$$\begin{aligned} dM &= \sum_{n,m} (C_{nm} p_M{}^{nm} + S_{nm} q_M{}^{nm}) \\ &\vdots \\ d\Omega &= \sum_{n,m} (C_{nm} p_\Omega{}^{nm} + S_{nm} q_\Omega{}^{nm}) \end{aligned} \tag{8}$$

the symbols $p_M{}^{nm}$, $q_M{}^{nm}$, $\cdots$, $p_\Omega{}^{nm}$, $q_\Omega{}^{nm}$ standing for the trigonometric polynomials given by Kaula's program. As examples, pertaining to the mean orbital elements $a = 8306.8$ km, $e = 0.16446$, and $I = 32.883°$ of the satellite $1959\alpha_1$ (Vanguard 2), we choose

$$\begin{aligned} p_M{}^{22} = 4.008 &\sin [2\omega + 2M + 2(\Omega - \theta)] \\ -2.979 &\sin [2(\Omega - \theta)] \\ -0.025 &\sin [-2\omega - 2M + 2(\Omega - \theta)] \end{aligned}$$

and

$$\begin{aligned} q_\Omega{}^{31} = -2.255 &\cos [-\omega + (\Omega - \theta)] \\ +5.481 &\cos [\omega + (\Omega - \theta)] \\ -1.113 &\cos [-\omega - M + (\Omega - \theta)] \\ -3.135 &\cos [\omega + M + (\Omega - \theta)] \end{aligned}$$

As a matter of fact, Kaula's program was adapted to fully normalized spherical harmonics, the integral of whose square over the unit sphere is

4π. The relation between the coefficients C_{nm}, S_{nm} of the ordinary, and $\bar{C}_{nm}$, $\bar{S}_{nm}$ of the fully normalized, spherical harmonics is

$$C_{nm} = N_{nm}\bar{C}_{nm} \qquad S_{nm} = N_{nm}\bar{S}_{nm}$$

where

$$N_{no} = (2n+1)^{1/2}$$

$$N_{nm} = \left[\frac{2(2n+1)(n-m)!}{(n+m)!}\right]^{1/2} \qquad (m \neq 0)$$

Let us now return to the observation equations 6. They are set up as follows. Comparison of (3) and (4) gives for the station that secured the observation

$$du^s = u^X\, dX + u^Y\, dY + u^Z\, dZ$$

$$dw^s = w^X\, dX + w^Y\, dY + w^Z\, dZ$$

where

$$u^X = \rho^{-1}(\mathbf{e}_U \cdot \mathbf{e}_X), \ \cdots, \ w^Z = \rho^{-1}(\mathbf{e}_W \cdot \mathbf{e}_Z)$$

As to the harmonics, from (2) and (5) we have

$$du^h = u^M\, dM + u^a\, da + u^e\, de + u^I\, dI + u^\omega\, d\omega + u^\Omega\, d\Omega$$

$$dw^h = 0.dM + w^a\, da + w^e\, de + w^I\, dI + w^\omega\, d\omega + w^\Omega\, d\Omega$$

with the abbreviations

$$u^M = \rho^{-1}(\mathbf{e}_U \cdot \partial r/\partial M), \cdots, \ w^\Omega = \rho^{-1}(\mathbf{e}_W \cdot \partial r/\partial \Omega)$$

Then, using (8) and collecting terms that belong to the same harmonic, we get

$$du^h = \sum_{n,m} (u_C{}^{nm} C_{nm} + u_S{}^{nm} S_{nm})$$

$$dw^h = \sum_{n,m} (w_C{}^{nm} C_{nm} + w_S{}^{nm} S_{nm})$$

where

$$u_C{}^{nm} = u^M p_M{}^{nm} + \cdots + u^\Omega p_\Omega{}^{nm} \quad u_S{}^{nm} = u^M q_M{}^{nm} + \cdots + u^\Omega q_\Omega{}^{nm}$$

$$w_C{}^{nm} = w^a p_a{}^{nm} + \cdots + w^\Omega p_\Omega{}^{nm} \quad w_S{}^{nm} = w^a q_a{}^{nm} + \cdots + w^\Omega q_\Omega{}^{nm}$$

Once the observation equations are set up, they are solved by the computer using standard least-squares techniques. In its present version our program can simultaneously handle up to 150 orbital arcs of 10 different satellites; this corresponds to about 20,000 individual observations. The selection of the unknowns to be solved for is arbitrary. Their number, however, is limited to 44. Of these unknowns not more than 38 may be tesseral-harmonics coefficients, and not more than 36 may be corrections to station coordinates. The printout of the program has been devised to give detailed information concerning the intricate least-squares process under discussion. Its main features are:

(1) A list of the original (DOI 3); the stations—improved (if any); the harmonics—improved (if any); and the improved residuals

$$dU_i \qquad dW_i$$

$$\delta U_i^s = dU_i + du_i^s \qquad \delta W_i^s = dW_i + dw_i^s$$

$$\delta U_i^h = dU_i - du_i^h \qquad \delta W_i^h = dW_i - dw_i^h$$

and

$$\delta U_i = dU_i - du_i \qquad \delta W_i = dW_i - dw_i$$

(2) The mean values

$$\left\{(2N)^{-1}\sum_{i=1}^{N}[(dU_i)^2+(dW_i)^2]\right\}^{1/2}$$

and

$$\left\{(2N)^{-1}\sum_{i=1}^{N}[(\delta U_i)^2+(\delta W_i)^2]\right\}^{1/2}$$

of the original and of the improved residuals per orbital arc, as well as for all the observations. We call their ratios the respective improvement factors of a solution.

(3) The least-squares estimates of the fully normalized tesseral and sectorial harmonics coefficients and of the corrections to station coordinates together with their standard deviations.

(4) The matrix of the correlation coefficients, that is, the normalized inverse matrix of the normal equations.

DATA ANALYSIS

As indicated by the foregoing description of the computational process, the mathematics involved is rather straightforward; the difficulty of the problem lies in the analysis of real data. First of all, the information contained in the original residuals is contaminated by unaccountable effects with a total that is significantly larger than the well-established accuracy of the observations: 2 seconds in the across-track and 3 seconds in the along-track direction. Second, while the perturbations caused by the presence of the various spherical harmonics are continuous functions of time, optical observations necessarily result in discrete data of a distribution that, for a single orbital arc, is often anything but uniform. This situation, though especially troublesome in case of perturbations with high frequencies, is comparatively harmless so far as station coordinates are concerned. Third, the effect of the different harmonics is not very much different in size and, for some terms, not even in shape. Therefore the perturbations caused by the various harmonics are hard to separate, a fact borne out by eventually considerable correlations among the computed values of the unknowns. About the only thing one can do to minimize the influence of these disadvantageous circumstances is to use a huge number of observations of several satellites with a variety of orbital elements, particularly with different inclinations. The self-explanatory Table 1 constitutes a breakdown of the 15,191 observations on which this analysis is based.

Table 1.—*Observational Material*

Satellite	I, deg	e	a, km	Arcs	Number of observations
1959α_1, Vanguard 2	32.9	0.165	8301	15	2091
1959α_2, Rocket of	32.9	0.183	8492	2	229
1959η, Vanguard 3	33.4	0.189	8496	12	1824
1961δ_1, Explorer 9	38.9	0.115	7985	16	2446
1962$\alpha\epsilon_1$, Telstar 1	44.8	0.242	9672	3	269
1960ι_2, Echo 1, rocket	47.2	0.012	7972	34	4324
1962$\beta\mu_1$, Anna 1B	50.1	0.007	7508	3	296
1961o_1, Transit 4A	66.8	0.008	7318	13	971
1961o_2, Injun 1—Greb 3	66.8	0.008	7319	7	494
1961$\alpha\delta_1$, Midas 4	95.9	0.011	10005	6	2247

In the present computational approach, we need the coordinates of the Baker-Nunn camera stations in some uniform rectangular system. The method of reducing the fundamental geodetic coordinates of the stations, based on field surveys and referred to five different geodetic datums to such a system, has been given by *Veis* [1961]. The actual values used in our computations, however, come from later, yet unpublished, work of his. They were determined on the basis of improved geodetic information available June 15, 1962, and (instead of the international ellipsoid) reduced to the ellipsoid (recommended by Kaula) with the characteristics $a_E = 6378.165$ km and $f = 1/298.3$. For the sake of easy reference, we list in Table 2 the initial coordinates of our tracking stations as derived by Veis.

Table 2.—*Observing Stations*

	X, km	Y, km	Z, km	Datum	Number of observations
1. Organ Pass	−1535.702	−5167.026	3401.108	Am.	1826
2. Olifantsfontein	5056.123	2716.523	−2775.799	Eu.	1742
3. Woomera	−3983.602	3743.226	−3275.656	Aus.	2023
4. San Fernando	5105.623	−555.194	3769.670	Eu.	1315
5. Tokyo	−3946.522	3366.453	3698.855	Jap.	965
6. Naini Tal	1018.135	5471.207	3109.519	Eu.	161
7. Arequipa	1942.762	−5804.082	−1796.838	Am.	931
8. Shiraz	3376.872	4404.022	3136.250	Eu.	1123
9. Curaçao	2251.841	−5816.928	1327.236	Am.	831
10. Jupiter	976.319	−5601.410	2880.311	Am.	1458
11. Villa Dolores	2280.645	−4914.512	−3355.441	Arg.	1276
12. Maui	−5466.118	−2404.068	2242.437	Am.	1540

The satellite observations set forth in Table 1 have been used recently in a great variety of computer runs. In some cases the required machine time was well over an hour. There is little point in giving a full account of the numerical results obtained. Instead, we select samples of them in the form of tables that we think are pertinent to the problems under discussion. All (fully normalized) harmonics coefficients will be expressed in units of 10^{-6}, and the station corrections will be given in meters. Throughout the computations we used the value $\mu = GM = 3.986032 \times 10^{20}$ cm^3 sec^{-2} recommended by Kaula.

Table 3 shows how futile it is to use a single satellite even for the determination of one pair of coefficients. The results per satellite are incompatible, probably because the effect of the several harmonics

Table 3.—*Second-Degree Solutions per Satellite*

(Scaled by 10^6)

Satellite	$\bar{C}_{22}$	$\bar{S}_{22}$	Residuals, sec	
			Original	Improved
$1959\alpha_1$	$0.97 \pm .08$	$-2.17 \pm .08$	14.27″	12.95″
1959η	$1.22 \pm .10$	$-2.32 \pm .10$	13.53	12.49
$1961\delta_1$	$1.50 \pm .06$	$-1.64 \pm .06$	15.56	13.63
$1960\iota_2$	$1.51 \pm .03$	$-1.37 \pm .03$	16.02	12.67
$1961o_1$	$0.81 \pm .04$	$-0.52 \pm .04$	23.61	20.43
$1961o_2$	$0.85 \pm .06$	$-0.26 \pm .06$	24.36	21.50
$1961\alpha\delta_1$	$2.29 \pm .05$	$-0.52 \pm .05$	9.84	7.99
All ten	$1.08 \pm .02$	$-0.89 \pm .02$	15.67″	13.86″

averages out differently according to the inclination of the objects. The considerable differences in the mean angular residuals result primarily from the variety in the mean topocentric distances of the objects.

Table 4 illustrates the interaction of harmonic coefficients and station corrections in a least-squares adjustment. In the first run only the harmonics up to the third degree were considered unknown; in the second only the stations were varied. In the third and definitive run these two problems were solved simultaneously. Clearly, the presence of tesseral harmonics influences the computed station coordinates much more than small errors in the latter affect the computed harmonic coefficients. The most conspicuous correlation coefficients among harmonics and

Table 4.—*Third-Degree Solutions for Harmonics (Scaled by 10^6) and Corrections to Station Coordinates (in meters)*

$\bar{C}_{22}\ \bar{S}_{22}$	1.03	−1.14				1.02±.02	−1.13±.02	
$\bar{C}_{31}\ \bar{S}_{31}$	1.02	−0.32				1.35±.02	−0.18±.02	
$\bar{C}_{32}\ \bar{S}_{32}$	0.30	−0.45				0.35±.03	−0.73±.03	
$\bar{C}_{33}\ \bar{S}_{33}$	−0.31	0.99				−0.37±.04	1.01±.04	
$dX^1\ dY_1\ dZ_1$			−10	19	51	−40± 5	34± 5	−20± 5
$dX_2\ dY_2\ dZ_2$			31	64	−10	11± 5	−26± 5	−32± 6
$dX_3\ dY_3\ dZ_3$			2	−20	13	−67± 4	−16± 4	10± 4
$dX_4\ dY_4\ dZ_4$			42	−72	10	−24±11	−34± 8	68± 8
$dX_5\ dY_5\ dZ_5$			−47	−89	−41	−101± 7	−80± 7	12± 8
$dX_6\ dY_6\ dZ_6$			49	−64	84	44±16	−76±26	75±20
$dX_7\ dY_7\ dZ_7$			−59	−44	−65	42± 7	−1± 8	−103± 8
$dX_8\ dY_8\ dZ_8$			77	−39	115	33± 7	−40± 7	59± 7
$dX_9\ dY_9\ dZ_9$			−102	−55	−39	−10± 7	6± 9	−64± 8
$dX_{10}\ dY_{10}\ dZ_{10}$			−21	5	0	−41± 5	5± 6	−36± 6
$dX_{11}\ dY_{11}\ dZ_{11}$			−23	−43	9	−19± 6	−53± 7	−21± 7
$dX_{12}\ dY_{12}\ dZ_{12}$			53	−152	−138	37± 6	−152± 5	−163± 6
Improved residuals	13.03″			14.85″			12.11″	

stations are $\langle \bar{S}_{32}, dY_4 \rangle = -0.25$ and $\langle \bar{S}_{32}, dX_{10} \rangle = 0.25$ and those among the coordinates of different stations turn out to be $\langle dX_1, dY_4 \rangle = -0.07$ and $\langle dX_{10}, dY_{12} \rangle = 0.07$. These data refer, of course, to the third run, whose results concerning the station coordinates we regard as the best the present version of our computer program can yield in conjunction with the observational material used in this work. A generalization of the program now under development will be indicated below.

At this point it is interesting to compare the results of the third run with those obtained by *Kaula* [1963*b*] and *Veis* [1963*c*], who were both using dynamical methods. In addition, we consider the purely geometrical method of simultaneous observations, initiated and pursued at the Smithsonian Astrophysical Observatory by Veis [1963*b*]. This technique permits the determination of two components g^1 and g^2 of relative displacement of the participating stations, perpendicular to the direction of one station as seen from the other. Simultaneous observations have already been successful in the instance of four pairs of neighboring stations, thus providing a valuable check on results arrived at by dynamical

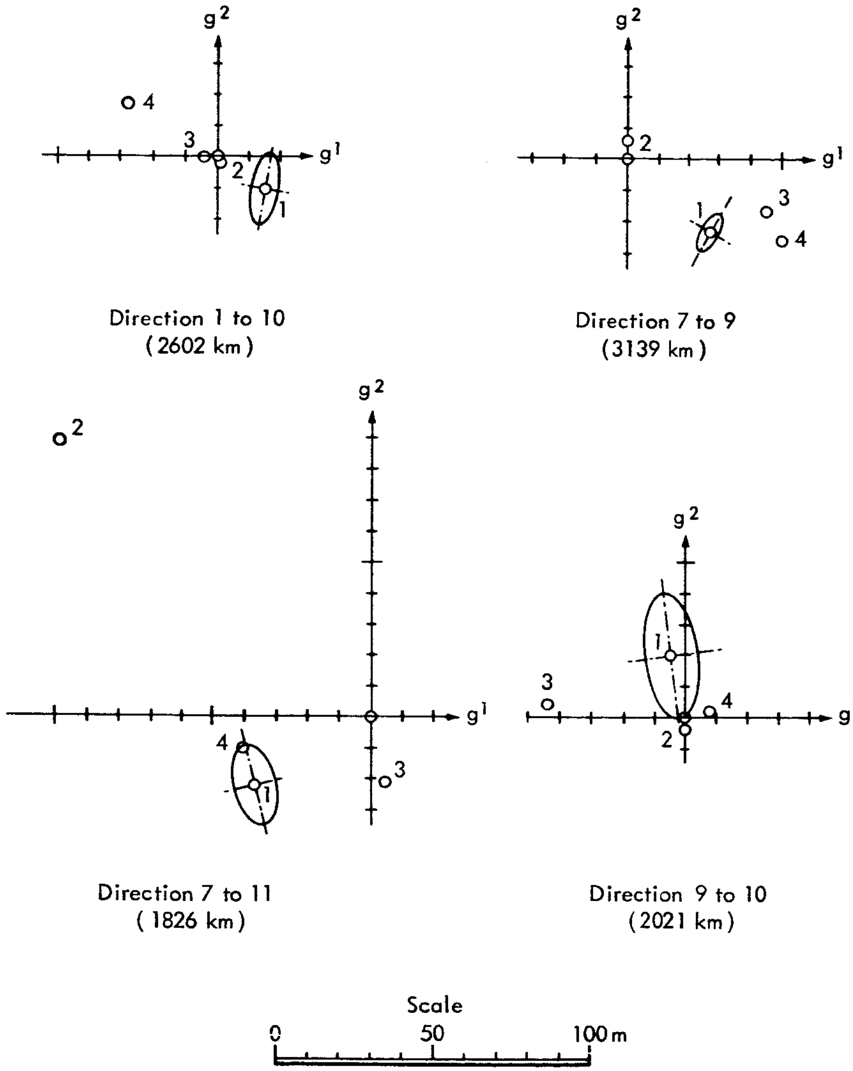

Figure 1.—Comparison of satellite results for the relative direction of Baker-Nunn camera stations 1° [Veis, 1963*b*]; 2° [Kaula, 1963*c*]; 3° [Veis, 1963*c*]; 4°, Izsak, Table 4.

methods. Figure 1 compares these results. The origin of the individual diagrams corresponds to the assumed direction of the respective stations. Small circles represent relative displacements according to 1° [Veis, 1963*b*], where error ellipses are also given; 2° [Kaula, 1963*b*]; 3° [Veis, 1963*c*]; and 4°, our Table 4.

The average agreement of the geometric results, 1°, seems to be best with the dynamical results, 4°. In case of the direction of Arequipa-Villa Dolores (7–11), the discrepancy between the determinations 2° and 1° is so striking as to call for a careful investigation.

During the experimental phase of this work the harmonic coefficients were computed in a variety of combinations. The purpose of such numerical experiments was merely to establish the capabilities of our program. We soon concluded that although the individual coefficients $\bar{C}_{nm}$ and $\bar{S}_{nm}$ may vary significantly from run to run, the combined contribution of the several harmonics to the gravitational field of the earth is

Table 5.—*Fourth-, Fifth-, and Sixth-Degree Solutions for Harmonics*
(Scaled by 10^6)

$\bar{C}_{22}$ $\bar{S}_{22}$	1.06	−0.73	1.08	−0.70	1.17 ± .02	−0.95 ± .03
$\bar{C}_{31}$ $\bar{S}_{31}$	0.88	−0.26	0.84	−0.21	0.81 ± .02	−0.25 ± .02
$\bar{C}_{32}$ $\bar{S}_{32}$	0.22	−0.36	0.30	−0.31	0.24 ± .03	−0.25 ± .03
$\bar{C}_{33}$ $\bar{S}_{33}$	−0.30	0.79	−0.53	0.87	−0.50 ± .04	0.93 ± .04
$\bar{C}_{41}$ $\bar{S}_{41}$	−0.18	−0.24	−0.19	−0.20	−0.18 ± .01	−0.25 ± .01
$\bar{C}_{42}$ $\bar{S}_{42}$	−0.16	0.52	−0.19	0.46	−0.11 ± .02	0.23 ± .02
$\bar{C}_{43}$ $\bar{S}_{43}$	0.34	−0.08	0.32	−0.08	0.28 ± .02	−0.08 ± .02
$\bar{C}_{44}$ $\bar{S}_{44}$	0.06	0.59	0.20	0.57	−0.08 ± .05	0.29 ± .06
$\bar{C}_{51}$ $\bar{S}_{51}$			−0.12	0.20	−0.09 ± .01	0.19 ± .01
$\bar{C}_{52}$ $\bar{S}_{52}$			0.30	−0.49	0.31 ± .03	−0.50 ± .03
$\bar{C}_{53}$ $\bar{S}_{53}$			−0.91	0.17	−0.72 ± .05	0.11 ± .05
$\bar{C}_{54}$ $\bar{S}_{54}$			−0.21	0.53	−0.18 ± .06	0.51 ± .06
$\bar{C}_{55}$ $\bar{S}_{55}$			0.17	−0.35	0.18 ± .10	−0.42 ± .10
$\bar{C}_{61}$ $\bar{S}_{61}$					−0.01 ± .01	0.13 ± .01
$\bar{C}_{62}$ $\bar{S}_{62}$					0.16 ± .02	−0.37 ± .02
$\bar{C}_{63}$ $\bar{S}_{63}$					0.14 ± .02	−0.17 ± .02
$\bar{C}_{64}$ $\bar{S}_{64}$					−0.20 ± .04	−0.41 ± .05
$\bar{C}_{65}$ $\bar{S}_{65}$					−0.40 ± .04	−0.28 ± .04
$\bar{C}_{66}$ $\bar{S}_{66}$					−0.53 ± .08	−0.41 ± .08
Improved residuals	12.50″		12.27″		12.10″	

rather well determined by sufficiently rich observational material. Table 5 is a compilation of recently obtained fourth-, fifth-, and sixth-degree solutions for harmonics, the last of which we regard as the definitive one. There seems little justification at present for going beyond sixth-degree terms. The standard deviations of the computed coefficients, whatever their significance, increase systematically with the index m, so that they are largest for the sectorial terms. We enumerate here only the most notable correlation coefficients:

$$\langle \bar{C}_{22}, \bar{C}_{42} \rangle = 0.72 \qquad \langle \bar{C}_{22}, \bar{C}_{62} \rangle = 0.55$$
$$\langle \bar{S}_{22}, \bar{S}_{42} \rangle = 0.78 \qquad \langle \bar{S}_{22}, \bar{S}_{62} \rangle = 0.56$$
$$\langle \bar{C}_{33}, \bar{C}_{53} \rangle = 0.36 \qquad \langle \bar{S}_{33}, \bar{S}_{53} \rangle = 0.36$$
$$\langle \bar{C}_{41}, \bar{C}_{61} \rangle = -0.38 \qquad \langle \bar{S}_{41}, \bar{S}_{61} \rangle = -0.36$$
$$\langle \bar{C}_{42}, \bar{C}_{62} \rangle = 0.61 \qquad \langle \bar{S}_{42}, \bar{S}_{62} \rangle = 0.63$$
$$\langle \bar{C}_{44}, \bar{C}_{64} \rangle = 0.65 \qquad \langle \bar{S}_{44}, \bar{S}_{64} \rangle = 0.67$$

To facilitate the visualization of numerical results, level curves of geoid heights pertaining to our sixth-degree solution are plotted in Figure 2. The reference ellipsoid of oblateness 1/298.28 and the purely latitudinal deviations from it are defined by the zonal harmonics coefficients of Kozai [1962]. The most interesting deviations of this figure from that in Izsak [1963] and Kaula [1963*b*] occur over the Atlantic and North Africa; their reality, however, cannot be ascertained without further evidence.

Extensions of the present computer program are feasible in a number of ways. First of all, one could increase the number of unknowns to 52, so that a simultaneous solution for the 12 stations of our network and second-, third-, and fourth-degree harmonics would become possible. Or, wishing to bring about a better separation of the geometric and dynamical part of the problem, one might be inclined to iterate previously obtained solutions. For instance, one could start with the results of the third run in Table 4, take its improved residuals and use these in a solution for higher-degree harmonics. The effect of the harmonics thus derived, in turn, would be subtracted from the original residuals when starting a new solution for the stations.

Appendix.—*Normalization Coefficients*

nm	N_{nm}	nm	N_{nm}
22	0.64550	51	0.85635
		52	0.16183
31	1.0801	53	0.033034
32	0.34157	54	0.0077863
33	0.13944	55	0.0024622
41	0.94868	61	0.78680
42	0.22361	62	0.12440
43	0.059761	63	0.020734
44	0.021129	64	0.0037855
		65	0.00080707
		66	0.00023298

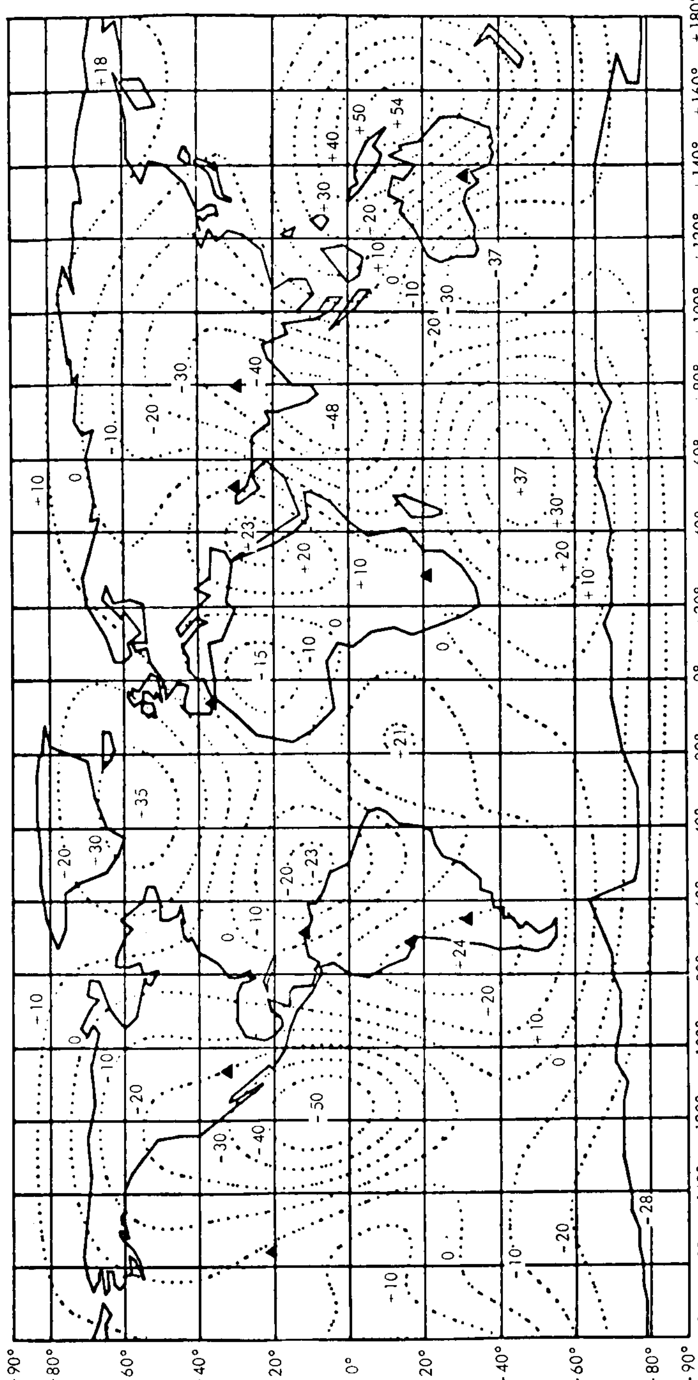

Figure 2.—Level curves of geoid heights at 10-m intervals. The small triangles indicate the positions of the 12 Baker-Nunn camera stations.

Acknowledgments.—This work was supported in part by grant NsG 87–60 from the National Aeronautics and Space Administration. I am much indebted to W. M. Kaula for helpful discussions on the subjects, as well as for his furnishing me with one of the basic subroutines. The complex computer programs used in this investigation are the skillful work of Mrs. Gladys Johnson, E. M. Gaposchkin, and W. L. Joughin. Figure 1 is based on the computations of A. Girnius.

REFERENCES

ANDERLE, R. J.; AND C. OESTERWINTER: A preliminary potential for the earth from Doppler observations on satellites, paper presented to Cospar, Warsaw, 1963.

GAPOSCHKIN, E. M.: A differential orbit improvement program, *Smithsonian Astrophys. Obs. Spec. Rept.*, in press, 1964.

GUIER, W. H.: Determination of the non-zonal harmonics of the geopotential from satellite Doppler data, personal communication, July, 1963, also *Nature, 200*(4902), 124–125, 1963.

IZSAK, I. G.: Differential orbit improvement with the use of rotated residuals, *Space Age Astronomy*, edited by A. J. Deutsch and W. B. Klemperer, Academic Press, New York and London, 1962.

IZSAK, I. G.: Tesseral harmonics in the geopotential, *Nature, 199*, 137–139, 1963.

IZSAK, I. G.; J. M. GERARD; R. EFIMBA; AND M. P. BARNETT: Construction of Newcomb operators on a digital computer, *Smithsonian Astrophys. Obs. Spec. Rept. 140*, 1964.

KAULA, W. M.: Analysis of gravitational and geometric aspects of geodetic utilization of satellites, *Geophys. J.*, *5*, 104–133, 1961*a*.

KAULA, W. M.: A geoid and world geodetic system based on a combination of gravimetric, astrogeodetic, and satellite data, *J. Geophys. Res.*, *66*, 1799–1811, 1961*b*.

KAULA, W. M.: Tesseral harmonics of the gravitational field and geodetic datum shifts derived from camera observations of satellites, *J. Geophys. Res.*, *68*, 473–484, 1963*a*.

KAULA, W. M.: Improved geodetic results from camera observations of satellites, *J. Geophys. Res.*, *68*, 5183–5190, 1963*b*.

KOZAI, Y.: Numerical results from orbits, *Smithsonian Astrophys. Obs. Spec. Rept. 101*, 1962.

UOTILA, U. A.: Harmonic analysis of world-wide gravity material, *Ann. Acad. Sci. Fenn., ser. A*, *3*(67), 1962.

VEIS, G.: The positions of the Baker-Nunn camera stations, *Smithsonian Astrophys. Obs. Spec. Rept. 59*, 1961.

VEIS, G.: Precise aspects of terrestrial and celestial reference frames, *Smithsonian Astrophys. Obs. Spec. Rept. 123*, 1963*a*.

VEIS, G.: The determination of absolute directions in space with artificial satellites, *Smithsonian Astrophys. Obs. Spec. Rept. 133*, 1963*b*.

VEIS, G.: The position of the B–N cameras obtained from analysis of 33087 P–R observations, personal communication, December, 1963*c*.

WIGNER, E. P.: The three-dimensional pure rotation group, in *Group Theory*, chap. 15, Academic Press, New York and London, 1959.

(Manuscript received January 31, 1964.)

PRECEDING PAGE BLANK NOT FILMED.

This work has been supported in part by the National Aeronautics and Space Administration through grant No. NsG 87/60. The following paper was originally published as Special Report No. 165, Smithsonian Astrophysical Observatory.

New Determination of Zonal Harmonics Coefficients of the Earth's Gravitational Potential

YOSHIHIDE KOZAI
Smithsonian Astrophysical Observatory
Tokyo Astronomical Observatory

Abstract.—From Baker-Nunn observations of nine satellites, whose inclinations cover a region between 28° and 95°, the following values were derived for the zonal harmonics coefficients of the earth's gravitational field:

$$
\begin{array}{ll}
J_2 = 1082.645\times10^{-6}, & J_3 = -2.546\times10^{-6},\\
\pm 6 & \pm 20\\
J_4 = -1.649\times10^{-6}, & J_5 = -0.210\times10^{-6},\\
\pm 16 & \pm 25\\
J_6 = 0.646\times10^{-6}, & J_7 = -0.333\times10^{-6},\\
\pm 30 & \pm 39\\
J_8 = -0.270\times10^{-6}, & J_9 = -0.053\times10^{-6},\\
\pm 50 & \pm 60\\
J_{10} = -0.054\times10^{-6}, & J_{11} = 0.302\times10^{-6},\\
\pm 50 & \pm 35\\
J_{12} = -0.357\times10^{-6}, & J_{13} = -0.114\times10^{-6},\\
\pm 47 & \pm 84\\
J_{14} = 0.179\times10^{-6}, & \\
\pm 63 &
\end{array}
$$

1. INTRODUCTION

IN A PREVIOUS PAPER (Kozai, 1963) I derived a set of values for the coefficients of zonal spherical harmonics in the earth's grativational potential from the available observations of artificial satellites. However, at that time I did not give much weight to observations of high-inclination satellites simply because accurate observations for such satellites were not available.

We now have precisely reduced Baker-Nunn observations for some of the high-inclination satellites, and I have found that secular motions of ascending nodes of these satellites cannot be accurately expressed by my previous values of zonal harmonics. Therefore, I had to improve my previous values by adding observations of the high-inclination satellites and higher-order harmonics to the expression of the earth's potential.

In this paper I have tried to eliminate any accidental errors in observational data, by using many more observations of a given satellite than in my previous paper. I have used fourteen sets of observations for 1959 α1 and ten sets for 1959η, in contrast to the single set of data used for each satellite previously. Consequently, I believe that the data reported here are more reliable than those in the previous paper even for low-inclination satellites. Although we still lack sufficient observations for satellites with inclinations of between fifty and eighty degrees, this gap in the data will probably be filled in the near future.

2. METHOD OF REDUCTION

The observations used in this determination were made by Baker-Nunn cameras, and the first steps in the reductions were made by Phyllis Stern by the Differential Orbit Improvement program, in which first-order short-periodic perturbations due to the oblateness of the earth are taken out. The mean orbital elements of each satellite for every two days or four days were obtained from observations covering four or eight days. Luni-solar periodic and solar radiation perturbations in the orbital elements were then computed and subtracted from the mean orbital elements.

To derive secular motions of the ascending node and the perigee and amplitudes of long-periodic terms from these orbital elements, I use data covering about one period of revolution of argument of perigee, that is, about 80 days for Vanguard satellites, for example.

Secular accelerations in the mean anomaly or the mean longitude, and secular decreases in the semimajor axis due to air-drag, are then evaluated roughly; they can be used to compute theoretically secular variation in the longitude of the ascending node, the argument of perigee; and the eccentricity due to the air drag with sufficient accuracy, by assuming the rate of secular decrease of the perigee height. The computed secular variations in the three orbital elements are subtracted from the mean elements.

After the corrections with long-periodic perturbations due to even zonal harmonic terms are made, the argument of perigee ω, the longitude of the ascending node, Ω, the inclination i, and the eccentricity e are expressed by the following simple forms:

$$
\begin{aligned}
\omega &= \omega_0 + \dot{\omega} t + A_\omega \cos \omega, \\
\Omega &= \Omega_0 + \dot{\Omega} t + A_\Omega \cos \omega, \\
i &= i_0 + A_i \sin \omega, \\
e &= e_0 + A_e \sin \omega.
\end{aligned}
\tag{1}
$$

By the method of least squares we can determine the constants appearing in the formulas (1) from a set of the corrected orbital elements. However, when the eccentricity is very small, say less than 0.02, the corrected eccentricity and the argument of perigee are more accurately expressed by the following formulas:

$$
\left.
\begin{aligned}
e \sin \omega &= e_0 \,(1-\alpha) \sin (\omega_0 + \dot{\omega} t) + A_e, \\
e \cos \omega &= e_0 \,(1+\alpha) \cos (\omega_0 + \dot{\omega} t),
\end{aligned}
\right\}
\tag{2}
$$

where α, which is due to even-order harmonics, can be computed with approximate values of J_n as

$$
\begin{aligned}
\alpha = \sin^2 i \{ & J_2^2 \,(14-15 \sin^2 i) + 5\, J_4 \,(6-7 \sin^2 i) \\
& -10.9375\, J_6 (16-48 \sin^2 i + 33 \sin^4 i)/a^2 \} / \{ 16 a^2\, J_2 (4-5 \sin^2 i) \}.
\end{aligned}
\tag{3}
$$

By using the formulas (2) we can determine $e_0 \sin \omega_0$, $e_0 \cos \omega_0$, A_e and a correction to an assumed value of $\dot{\omega}$ from observations by the method of least squares.

The relation between the anomalistic mean motion n and our semimajor axis a is given as

$$
n^2 a^3 = GM \left\{ 1 + \frac{3J_2}{4p^2} (1-e^2)^{\frac{1}{2}} (1-3 \cos^2 i) \right\},
\tag{4}
$$

where

$$
\begin{aligned}
GM &= 3.986032 \times 10^{20} \text{ cm}^3/\text{sec}^2, \\
p &= a(1-e^2).
\end{aligned}
\tag{5}
$$

Expressing the mean motion in revolutions per day and the semimajor axis in earth's equatorial radii, we can use the following number for GM:

$$
\sqrt{GM} = 17.043570,
\tag{6}
$$

where I adopt the following value of the equatorial radius:

$$
a_e = 6378.165 \text{ km}.
\tag{7}
$$

Table 1.—*Orbital Data for 1959 Alpha 1*

	Epoch	n	i_0	e_0	$\dot{\omega}$	$\dot{\Omega}$	A_e	A_i	A_ω	A_Ω
1	Apr. 2, 1959	4120°.861	32°.879 60	0.165 654	5°.262 32	−3°.500 307	0.469×10⁻³	−0°.677×10⁻²	0°.1600	0°.69×10⁻²
			±10	±4	±17	±18	±7	±17	±40	±5
2	June 21, 1959	4123 .878	.879 71	358	5 .270 05	−3 .505 504	0.474	−0 .715	0 .1516	0. 96
			±14	±3	±8	±21	±5	±18	±23	±7
3	Sept. 17, 1959	4125 .316	.880 02	283	5 .274 05	−3 .508 239	0.475	−0 .701	0 .1548	0 .40
			±16	±3	±8	±21	±6	±33	±36	±9
4	Dec. 6, 1959	4125 .995	.879 94	162	5 .275 48	−3 .509 301	0.459	−0 .647	0 .1618	0 .54
			±12	±5	±11	±16	±6	±16	±29	±4
5	Mar. 7, 1960	4126 .610	.879 28	0.164 958	5 .276 87	−3 .510 082	0.464	−0 .690	0 .1559	0 .76
			±5	±3	±6	±11	±4	±7	±17	±3
6	May 24, 1960	4127 .508	.878 44	763	5 .278 93	−3 .511 425	0.457	−0 .717	0 .1533	0 .87
			±10	±2	±3	±7	±4	±14	±12	±3
7	Aug. 22, 1960	4128 .877	.878 98	642	5 .282 59	−3 .513 799	0.464	−0 .642	0 .1534	0 .88
			±10	±2	±2	±13	±5	±13	±10	±6
8	Nov. 26, 1960	4130 .345	.879 47	577	5 .286 55	−3 .516 572	0.464	−0 .662	0 .1621	0 .57
			±15	±2	±6	±15	±3	±21	±18	±5
9	Feb. 18, 1961	4130 .675	.879 32	567	5 .287 59	−3 .517 208	0.453	−0 .680	0 .1560	0 .63
			±18	±3	±4	±12	±5	±30	±13	±4
10	May 13, 1961	4130 .769	.879 25	447	5 .287 40	−3 .517 094	0.460	−0 .667	0 .1564	0 .78
			±9	±2	±2	±12	±2	±11	±8	±5
11	Aug. 13, 1961	4130 .948	.878 48	330	5 .287 68	−3 .517 199	0.455	−0 .705	0 .1557	0 .85
			±5	±1	±2	±7	±2	±7	±10	±2
12	Nov. 17, 1961	4131 .525	.878 98	292	5 .289 317	−3 .518 265	0.465	−0 .702	0 .1577	0 .75
			±4	±1	±13	±6	±3	±7	±8	±4
13	Feb. 13, 1962	4131 .834	.878 94	378	5 .290 46	−3 .519 099	0.462	−0 .698	0 .1565	0 .41
			±11	±2	±2	±2	±3	±14	±14	±4
14	June 3, 1962	4132 .021	.879 44	396	5 .291 059	−3 .519 495	0.463	−0 .647	0 .1600	0 .56
			±8	±1	±19	±6	±2	±12	±9	±3

The earth's gravitational potential is expressed with Legendre polynomials as

$$U=\frac{GM}{r}\left\{1-\sum_{n=2}^{\infty} J_n(a_e/r)^n P_n(\sin\beta)\right\} \tag{8}$$

The secular motions of the node and the perigee and the amplitudes of long-periodic terms with argument ω derived from observations are compared with those computed from my previous value of J_n (Kozai, 1963),

$$\begin{aligned} J_2 &= 1082.48\times10^{-6}, & J_3 &= -2.562\times10^{-6}, \\ J_4 &= -1.84\times10^{-6}, & J_5 &= -0.064\times10^{-6}, \\ J_6 &= 0.39\times10^{-6}, & J_7 &= -0.470\times10^{-6}, \\ J_8 &= -0.02\times10^{-6}, & J_9 &= 0.117\times10^{-6}. \end{aligned} \tag{9}$$

Of course we must include luni-solar secular terms and a J_2^2 term, which can be computed with an approximate value of J_2 to compute secular motions. Therefore, each secular motion and amplitude provides us with (O–C), which will make it possible to improve values of J_n.

3. DATA

(a) 1959 Alpha 1—Table 1 lists fourteen sets of data for this satellite, and table 2 gives (O–C)'s referred to my previous values for J_n.

The standard deviations for the daily secular motions $\dot{\omega}$ and $\dot{\Omega}$ given in table 1 are determined from observations; those in table 2 are computed by adding uncertainties which come from those in e_0 and i_0. Weighted mean values for the fourteen sets are given at the bottom of the table. As can be seen, the scattering of (O–C)'s is much larger than that expected from the standard deviations assigned to the observed values. However, the standard deviations assigned to the mean values in table 2 should be more reliable, and will be used in the determinations of J_n.

(b) 1959 Eta—Ten sets of data are given in tables 3 and 4 for this Vanguard satellite. However, its orbital elements are not essentially different from those of 1959 α1 and the mean values of (O–C) in table 4 are almost identical with those in table 2, as expected. For the two Vanguard satellites (O–C) in $\dot{\Omega}$ and A_ω are significantly large.

(c) 1960 Iota 2—Since the eccentricity is very small for this rocket of Echo I, the formulas (2) are used in the reduction. Since $\dot{\omega}+\dot{\Omega}$ are very small for this satellite, it is necessary to take special care to compute terms with arguments $2(\omega+\Omega-\Omega_\odot)$ and $2(\omega+\Omega-\Omega_☾)$ in the luni-solar perturbations.

Five sets of data are given in tables 5 and 6. For this satellite the scattering of (O–C) for secular motions is very large. The large scatter-

Table 2.—(O–C) *Referred to Kozai's Previous Constants for 1959 Alpha 1*

	$\dot{\omega}\times10^6$	$\dot{\Omega}\times10^6$	$A_e\times10^6$	$A_i\times10^5$	$A_\omega\times10^4$	$A_\Omega\times10^4$
1......	19° ± 17°	−31° ± 18°	12 ± 7	13° ± 17°	90° ± 40°	−9° ± 5°
2......	0 ± 8	49 ± 23	17 ± 5	−26 ± 18	2 ± 23	19 ± 7
3......	3 ± 8	−23 ± 23	18 ± 6	−13 ± 33	33 ± 36	−37 ± 9
4......	−15 ± 11	−22 ± 21	2 ± 6	41 ± 16	102 ± 29	−23 ± 4
5......	3 ± 6	−42 ± 13	7 ± 4	−3 ± 7	41 ± 17	−1 ± 3
6......	−3 ± 4	−33 ± 10	0 ± 4	−31 ± 14	12 ± 12	10 ± 3
7......	6 ± 3	3 ± 14	7 ± 5	44 ± 13	12 ± 10	11 ± 6
8......	−5 ± 7	−27 ± 17	7 ± 3	24 ± 21	98 ± 18	−20 ± 5
9......	1 ± 5	−24 ± 16	−4 ± 5	6 ± 30	37 ± 13	−14 ± 4
10.....	−4 ± 3	−8 ± 15	3 ± 2	18 ± 11	40 ± 8	1 ± 5
11.....	0 ± 3	−4 ± 8	−2 ± 2	−20 ± 7	31 ± 10	8 ± 2
12.....	13 ± 3	−33 ± 7	8 ± 3	−17 ± 7	51 ± 8	−2 ± 4
13.....	3 ± 3	−46 ± 14	5 ± 3	−13 ± 14	40 ± 14	−36 ± 4
14.....	9 ± 2	−48 ± 8	6 ± 2	38 ± 12	75 ± 9	−21 ± 3
Mean..	4 ± 2	−26 ± 6	4 ± 2	−2 ± 8	42 ± 8	−5 ± 5

ing for $\dot{\omega}$ may be partly due to the fact that the radiation pressure effects in the argument of perigee are too large to handle accurately. Also, I suspect that the anomalistic mean motion cannot be determined with sufficient accuracy for a satellite of such small eccentricity. This might be one reason why we have large discrepancies in the secular motions of the node.

However, (O–C)'s in $\dot{\omega}$, $\dot{\Omega}$ and A_e are still significant.

(d) 1961 Nu—For this satellite precisely reduced Baker-Nunn observations are not available and observations must be used that are not precisely reduced. However, since the satellite is close to the earth and the inclination is the smallest used in this paper, the node and the perigee move rapidly and the relative accuracies in the determination of the secular motions are fair.

Four sets of data are given in tables 7 and 8, which show a wide scatter in the values of (O–C) in A_e and A_i. The residuals in the two secular motions take large values. This satellite was not used in the earlier determination of J_n; at that time the smallest inclination was 32°.9, for 1959 α1.

(e) 1961 Omicron—There are two separate satellites for 1961 o. However, since they have almost identical orbital elements, they are treated as one satellite here. The eccentricity is very small. Since the inclination is rather close to the critical inclination, the argument of perigee moves very slowly. Therefore, one set of observations must cover more than 500 days. However, as the mean motion changes rather rapidly due to air drag, I have used one set of 400-day observations.

Table 3.—*Orbital Data for 1959 Eta*

	Epoch	n	i_0	e_0	$\dot{\omega}$	$\dot{\Omega}$	A_e	A_i	A_ω	A_Ω
1	Nov. 4, 1959	3982°.496	33°.355 10	0.190 019	4°.872 23	−3°.272 67	0.442×10^{-3}	$-0°.820\times10^{-2}$	0°.1330	$0°.90\times10^{-2}$
			±15	±2	±7	±3	±5	±30	±25	±8
2	Feb. 4, 1960	3983 .406	.354 70	0.189 782	4 .874 03	−3 .273 818	0.451	−0 .760	0 .1299	0 .81
			±12	±3	±9	±9	±4	±20	±10	±2
3	May 4, 1960	3984 .637	.354 01	519	4 .876 67	−3 .275 477	0.441	−0 .759	0 .1327	0 .90
			±11	±2	±3	±6	±4	±16	±12	±2
4	Aug. 2, 1960	3986 .079	.353 34	326	4 .880 08	−3 .277 815	0.450	−0 .793	0 .1323	0 .93
			±10	±2	±3	±9	±3	±15	±11	±4
5	Nov. 10, 1960	3988 .708	.353 82	075	4 .886 54	−3 .282 159	0.451	−0 .817	0 .1358	0 .82
			±12	±3	±3	±10	±3	±18	±18	±6
6	Feb. 22, 1961	3989 .670	.354 72	059	4 .889 27	−3 .284 07	0.462	−0 .700	0 .1320	0 .86
			±20	±2	±4	±3	±5	±40	±15	±8
7	June 18, 1961	3989 .952	.354 36	001	4 .889 75	−3 .284 384	0.461	−0 .687	0 .1319	0 .83
			±13	±2	±2	±12	±2	±19	±11	±6
8	Oct. 16, 1961	3990 .168	.353 44	0.188 824	4 .889 70	−3 .284 302	0.455	−0 .770	0 .1335	0 .75
			±7	±2	±2	±11	±4	±9	±7	±3
9	Jan. 14, 1962	3990 .437	.354 42	742	4 .890 35	−3 .284 641	0.447	−0 .839	0 .1350	0 .87
			±8	±2	±2	±23	±2	±11	±11	±2
10	Apr. 22, 1962	3991 .063	.353 25	696	4 .891 779	−3 .285 739	0.467	−0 .806	0 .1353	0 .76
			±8	±2	±11	±3	±3	±13	±4	±2

Table 4.—(O–C) *for 1959 Eta*

	$\dot{\omega}\times10^5$	$\dot{\Omega}\times10^6$	$A_e\times10^6$	$A_i\times10^5$	$A_\omega\times10^4$	$A_\Omega\times10^4$
1	9° ± 8°	−70° ±31°	−9 ±5	−50° ±30°	50° ±25°	0° ±8°
2	14 ± 4	−70 ±13	0 ±4	10 ±20	17 ±10	−9 ±2
3	17 ± 4	−20 ± 9	−9 ±4	14 ±16	43 ±12	0 ±2
4	9 ± 4	−62 ±11	−2 ±3	−21 ±15	37 ±11	3 ±4
5	8 ± 4	−23 ±14	−1 ±3	−46 ±14	70 ±18	−8 ±6
6	26 ± 5	−160 ±40	10 ±5	7 ± 4	32 ±15	−4 ±8
7	10 ± 3	−70 ±14	9 ±2	84 ±19	30 ±11	−7 ±6
8	−4 ± 3	7 ±13	3 ±4	0 ± 9	45 ± 7	−15 ±3
9	32 ±20	−66 ±24	−5 ±2	−69 ±11	59 ±11	−3 ±2
10	−5 ± 3	−34 ± 7	15 ±3	−37 ±13	62 ± 4	−14 ±2
Mean	7 ± 3	−40 ± 9	2 ±2	−4 ± 9	50 ± 5	−7 ±2

Table 5.—*Orbital Data for 1960 Iota 2*

	Epoch	n	i_0	e_0	$\dot{\omega}$	$\dot{\Omega}$	A_ω	A_i	A_Ω
1	Nov. 12, 1960	4390°.918	47°.231 76	0.011 475	2°.977 64	−3°.101 208	0.6572×10^{-3}	$-0°.32\times10^{-3}$	$0°.18\times10^{-2}$
			±7	±1	±17	±3	±14	±11	±3
2	Mar. 12, 1961	4390°.915	.231 63	265	2 .978 32	−3 .101 186	0.6616	−0 .46	0 .03
			±8	±1	±21	±4	±14	±11	±3
3	July 10, 1961	4390 .893	.231 31	412	2 .977 76	−3 .101 200	0.6651	−0 .48	0 .00
			±7	±1	±18	±3	±14	±10	±3
4	Nov. 7, 1961	4390 .898	.231 92	490	2 .977 13	−3 .101 239	0.6600	−0 .40	0 .19
			±6	±1	±24	±3	±20	±10	±3
5	Mar. 7, 1962	4390 .923	.232 49	373	2 .978 82	−3 .101 192	0.6629	−0 .77	0 .13
			±5	±1	±14	±2	±11	±7	±2

Table 6.—*(O–C) for 1960 Iota 2*

	$\dot{\omega}\times10^5$	$\dot{\Omega}\times10^6$	$A_e\times10^7$	$A_i\times10^5$	$A_\Omega\times10^4$
1	67° ±17°	−31° ± 5°	44 ±14	8° ±11°	8° ±3°
2	134 ±21	−16 ± 6	88 ±14	−7 ±11	−2 ±3
3	75 ±18	−46 ± 5	123 ±14	−9 ±10	−10 ±3
4	22 ±24	−101 ± 5	72 ±20	0 ±10	10 ±3
5	200 ±24	−64 ± 4	101 ±11	−38 ± 7	4 ±3
Mean	90 ±30	−52 ±15	86 ±13	−9 ± 8	2 ±4

Table 7.—*Orbital Data for 1960 Nu*

	Epoch	n	i_0	e_0	$\dot{\omega}$	$\dot{\Omega}$	A_e	A_i	A_ω	A_Ω
1	May 12, 1961	4798°.022	28°.803 9	0.086 211	8°.102 98	−5°.003 817	0.452×10^{-3}	$-5°.98\times10^{-3}$	0°.3054	$0°.50\times10^{-3}$
			±3	±2	±13	±27	±3	±44	±25	±5
2	June 18, 1961	4798 .224	.803 9	197	8 .103 59	−5 .004 400	0.455	−5 .60	0 .3050	0 .49
			±2	±2	±10	±20	±3	±30	±40	±6
3	July 12, 1961	4798 .355	.804 1	195	8 .104 28	−5 .004 728	0.452	−5 .30	0 .3075	0 .54
			±3	±3	±15	±75	±5	±35	±34	±11
4	Sept. 6, 1961	4798 .561	.804 6	159	8 .104 20	−5 .005 105	0.480	−4 .43	0 .3166	0 .32
			±2	±7	±22	±41	±8	±24	±61	±12

For this satellite, the mean height is rather low, about 900 km, and the inclination is high. Therefore, the object is rather difficult to observe from the Baker-Nunn stations due to visibility conditions, and there are many gaps in the observations, periods for which accurate orbital elements are not available. As the Baker-Nunn stations are between $+35°$ and $-35°$ in latitude, the inclination of this satellite is poorly determined although the longitude of the node can be well determined. This situation is contrary to that of Vanguard satellites.

Table 8.—*(O–C) for 1960 Nu*

	$\dot{\omega}\times10^5$	$\Omega\times10^6$	$A_e\times10^6$	$A_i\times10^5$	$A_\omega\times10^4$	$A_\Omega\times10^4$
1	$-59°\pm15°$	$211°\pm30°$	-17 ± 3	$-173°\pm44°$	$-45°\pm20°$	$17°\pm5°$
2	$-74\ \pm10$	$90\ \pm20$	-14 ± 3	$-140\ \pm30$	$-50\ \pm40$	$16\ \pm6$
3	$-51\ \pm15$	$71\ \pm80$	-17 ± 3	$-105\ \pm35$	$-25\ \pm34$	$21\ \pm11$
4	$-10\ \pm22$	$111\ \pm45$	11 ± 8	$-20\ \pm24$	$64\ \pm61$	$0\ \pm12$
Mean	$-48\ \pm20$	$131\ \pm40$	-9 ± 14	$-110\ \pm70$	$-14\ \pm50$	$14\ \pm10$

The secular motion of the node is determined quite accurately, as we can see in table 9. However, we cannot compute theoretical values of the secular motions so accurately as the observed ones, because of uncertainties in the inclination. Therefore, the standard deviations in (O–C) of $\dot{\Omega}$ in table 10 are large. But (O–C)'s in $\dot{\Omega}$ themselves are quite large, as we can see in table 10. In the previous determination of J_n, accurate orbital elements from Baker-Nunn observations were not available.

The value of (O–C) in $\dot{\Omega}$ for the epoch 4 is quite different from the others, and I suspect this scattering is due to some accidental errors in i_0 for the epoch 4, and give small weight to this value in taking the mean.

For this satellite the radiation pressure effect in the argument of perigee is too large for my program to compute it with enough accuracy. This is also true for other satellites of small eccentricity.

(f) 1961 Alpha Delta 1—This satellite has a polar orbit. However, as the mean height is quite high, we can determine the orbit very accurately from Baker-Nunn observations.

This satellite, and the three listed in tables 13–17, which were launched in 1962, were not used in my previous determination.

The first set of data is determined from 300-day observations, and the second set is from 400-day observations, which cover one revolution of argument of perigee.

To compute the solar-perturbations there arise three small divisors, namely, $2(n_\odot-\dot{\omega})$, $2(\dot{\omega}-\dot{\Omega}+n_\odot)$, and $2(n_\odot-2\dot{\omega}-\dot{\Omega})$.

Tables 11 and 12 show that the eccentricity is very small and that (C–C) in $\dot{\Omega}$ is very significant.

Table 9.—*Orbital Data for 1960 Omicron*

	Epoch	n	i_0	e_0	$\dot{\omega}$	$\dot{\Omega}$	A_e	A_i	A_Ω
	Omicron 1:								
1	Mar. 5, 1962	4993°.199	66°.815 73	0.008 022	−0°.695 76	−2°.424 778	0.250×10^{-3}	$-0°.04\times10^{-3}$	$0°.72\times10^{-2}$
			±12	±2	±23	±1	±3	±19	±3
2	Nov. 16, 1962	4993 .276	.815 28	0.007 981	−0 .695 20	−2 .424 864	0.266	−0 .77	0 .60
			±13	±2	±8	±1	±2	±16	±3
	Omicron 2:								
3	Mar. 1, 1962	4992 .762	.815 40	0.008 055	−0 .695 62	−2 .424 295	0.256	−0 .22	0 .75
			±10	±2	±18	±1	±3	±19	±4
4	Nov. 16, 1962	4992 .817	.815 50	026	−0 .695 63	−2 .424 349	0.264	0 .02	0 .66
			±15	±2	±11	±1	±2	±21	±2

Table 10.—*(O–C) for 1960 Omicron*

	$\dot{\omega}\times10^{-5}$	$\dot{\Omega}\times10^{-6}$	$A_e\times10^{6}$	$A_i\times10^{5}$	$A_\Omega\times10^{4}$
1	50° ±23°	−1291° ±12°	−51 ±3	2° ±19°	7° ±3°
2	54 ± 9	−1238 ±13	−35 ±2	−18 ±16	−5 ±2
3	−2 ± 8	−1257 ±10	−46 ±3	−16 ±19	10 ±4
4	−20 ±11	−1162 ±15	−37 ±2	8 ±21	2 ±2
Mean	20 ±30	−1262 ±25	−42 ±6	−6 ±13	4 ±8

Table 11.—*Orbital Data for 1961 Alpha Delta 1*

	Epoch	n	i_0	e_0	$\dot{\omega}$	$\dot{\Omega}$	A_e	A_i	A_Ω
1	Aug. 4, 1962	3123°.598	95°.856 47	0.012 092	−0°.976 93	0°.210 391	0.787×10⁻³ → 0.787×10^{-3}	$0°.51\times10^{-3}$	$-1°.25\times10^{-3}$
			±5	±1	±11	±1	±2	±7	±25
2	Sept. 21, 1962	3123 .598	.856 69	0.012 073	−0 .977 97	0 .210 393	0.804×10^{-3}	0 .24	$0 .54\times10^{-3}$
			±6	±2	±10	±1	±3	±8	±20

Table 12.—*(O–C) for 1961 Alpha Delta 1*

	$\dot{\omega}\times10^5$	$\dot{\Omega}\times10^6$	$A_e\times10^6$	$A_i\times10^5$	$A_\Omega\times10^4$
1	33° ±11°	68° ±2°	4 ±2	−5 ± 7	−7 ±2
2	−72 ±10	63 ±2	21 ±3	18 ± 8	7 ±3
Mean	−20 ±50	65 ±2	8 ±4	7 ±10	7 ±7

Table 13.—*Orbital Data for 1962 Alpha Epsilon*

	Epoch	n	i_0	e_0	$\dot{\omega}$	$\dot{\Omega}$	A_e	A_i	A_ω	A_Ω
1	Oct. 7, 1962	3285°.400	44°.799 53	0.242 241	1°.986 171	−1°.858 849	0.5461×10^{-3}	$-0°.761\times10^{-2}$	0°.1117	0°.0176
			±6	±1	±8	±4	±16	±9	±5	±3
2	Oct. 15, 1962	3285 .401	.799 13	239	1 .986 179	−1 .858 849	0.5506	−0 .721	0 .1116	0 .0180
			±15	±3	±12	±4	±35	±21	±9	±3
3	Apr. 17, 1963	3285 .424	.800 85	319	1 .986 074	−1 .858 983	0.5697	−0 .697	0 .1124	0 .0179
			±9	±3	±7	±3	±39	±11	±9	±3

Table 14.—(O–C) *for 1962 Alpha Epsilon*

	$\dot{\omega}\times10^5$	$\dot{\Omega}\times10^6$	$A_e\times10^6$	$A_i\times10^5$	$A_\omega\times10^4$	$A_\Omega\times10^4$
1	47°.3 ± 1°.0	−60° ± 5°	38 ± 2	8° ± 9°	−22° ± 5°	31° ± 3°
2	44 .0 ± 2 .2	−51 ± 7	32 ± 4	49 ± 21	−24 ± 9	35 ± 3
3	33 .4 ± 1 .0	−57 ± 8	52 ± 4	73 ± 11	−15 ± 9	35 ± 3
Mean	42 ± 6	−56 ± 5	37 ± 20	43 ± 33	−20 ± 5	34 ± 3

Table 15.—*Orbital Data for 1962 Beta Mu 1*

	Epoch	n	i_0	e_0	$\dot{\omega}$	Ω	A_e	A_i	A_Ω
1	Jan. 5, 1963	4804°.149	50°.141 05	0.007 060	2°.964 39	−3°.609 041	0.7822 × 10⁻³	−0°.73 × 10⁻³	0°.99 × 10⁻³
			±15	±2	±61	±10	±20	±25	±34
2	May 5, 1963	4804 .152	.142 46	055	2 .960 06	−3 .609 023	0.7745	−0 .53	1 .95
			±18	±2	±55	±8	±22	±23	±48
3	Mar. 6, 1963	4804 .150	.141 79	060	2 .963 41	−3 .608 983	0.7757	−1 .18	1 .62
			±13	±2	±33	±5	±17	±17	±37

Table 16.—*(O–C) for 1962 Beta Mu 1*

	$\dot{\omega}\times10^5$	$\dot{\Omega}\times10^6$	$A_e\times10^6$	$A_i\times10^5$	$A_\Omega\times10^4$
1	271° ± 61°	16° ± 14°	27 ± 2	−47° ± 25°	1° ± 3°
2	−128 ± 55	−69 ± 18	19 ± 2	−27 ± 23	11 ± 5
3	191 ± 33	18 ± 15	20 ± 2	−92 ± 17	8 ± 4
Mean	131 ± 150	−12 ± 30	22 ± 4	−55 ± 30	7 ± 5

Table 17.—*Orbital Data and (O–C) for 1962 Beta Upsilon*

Epoch	n	i_0	e_0	$\dot{\omega}$	$\dot{\Omega}$	A_e	A_i	A_ω	A_Ω
Apr. 1, 1963	2801°.146	47°.510 10 ± 18	0.284 224 ± 2	1°.212 096 ± 12	−1°.279 119 ± 4	0.521×10^{-3} ± 4	$-0°.867\times10^{-2}$ ± 27	0°.0966 ± 20	0°.0246 ± 6

Epoch	$\dot{\omega}\times10^5$	$\dot{\Omega}\times10^6$	$A_e\times10^6$	$A_i\times10^5$	$A_\omega\times10^4$	$A_\Omega\times10^4$
Apr. 1, 1963	30° ± 7°	−156° ± 7°	18 ± 4	−51° ± 27°	4° ± 20°	88° ± 6°

(g) 1962 Alpha Epsilon—For this satellite three sets of data are given in table 13. However, observations in sets 1 and 2 are overlapped widely. Since ω and $-\Omega$ have nearly the same value, $2(\omega+\Omega)$ and $2(n_{\odot}-2\omega-\dot{\Omega})$ take small values, as for 1962 Beta Mu 1. Therefore we must be careful to compute luni-solar perturbation terms with such arguments.

All values of (O–C) in table 14 are significant.

(h) 1962 Beta Mu 1—This is a geodetic satellite, and although the inclination is not very much different from that of 1956 $\alpha\epsilon$, the eccentricity and the mean motion take quite different values.

The mean height of this satellite is not high enough for the Baker-Nunn cameras to track the object over a long arc. Therefore the accuracy of determination of the orbital elements is not high.

(i) 1962 Beta Upsilon—Unfortunately, precisely reduced Baker-Nunn observations are available for this satellite only for 200 days, during which the argument of perigee moves by 240°. Therefore I will increase by a factor of five the standard deviations given in table 17 in the determination of J_n.

4. DETERMINATION OF J_n

Table 18 gives for the nine satellites the semimajor axes in units of earth equatorial radii, the inclinations, the eccentricity, and the area-to-mass ratio in cgs units. The same table also gives J_2^2 terms and luni-solar secular terms in $\dot{\omega}$ and $\dot{\Omega}$ (Kozai, 1962; Kozai, 1959).

A previous paper (Kozai, 1962) gives the formulas used to compute secular perturbations and amplitudes of long-periodic terms with argument ω by including up to 8th-order harmonics. However, I include up to 14th-order harmonics in the present determination, and the additional formulas are given in the following:

$$\begin{aligned}
\delta\dot{\Omega}= & -\frac{3465J_{10}}{4{,}194{,}304p^{10}}\,\theta n(63-1092\theta^2+4914\theta^4-7956\theta^6+4199\theta^8)\\
& \times(128+2304e^2+6048e^4+3360e^6+315e^8)\\
& -\frac{9009J_{12}}{67{,}108{,}864p^{12}}\,\theta n(231-5775\theta^2+39270\theta^4-106{,}590\theta^6\\
& +124{,}355\theta^8-52{,}003\theta^{10})\cdot(256+7040e^2+31{,}680e^4+36{,}960e^6 \qquad (10)\\
& +11{,}550e^8+693e^{10})\\
& -\frac{45{,}045J_{14}}{2{,}147{,}483{,}648p^{14}}\,n\theta(429-14{,}586\theta^2+138{,}567\theta^4-554{,}268\theta^6\\
& +1{,}062{,}347\theta^8-965{,}770\theta^{10}+334{,}305\theta^{12})\cdot(1024+39{,}936e^2\\
& +274{,}560e^4+549{,}120e^6+360{,}360e^8+72{,}072e^{10}+3003e^{12}),
\end{aligned}$$

Table 18.—*Summary of Parameters*

	a	i	e	J_2^2 in $\dot{\omega}$	$\odot+☾$ in $\dot{\omega}$	J_2^2 in $\dot{\Omega}$	$\odot+☾$ in $\dot{\Omega}$	A/M
(a) 59 α1	1.30	32°.8	0.16	$2°.04\times10^{-3}$	$0°.55\times10^{-3}$	$0°.305\times10^{-3}$	$-0°.378\times10^{-3}$	0.21
(b) 59 η1	1.33	33 .4	0.19	1 .91	0 .57	0 .223	−0 .395	0.27
(c) 60 ι2	1.25	47 .2	0.01	2 .02	0 .26	−0 .705	−0 .272	0.21
(d) 61 ν	1.18	28 .8	0.09	2 .77	0 .52	1 .092	−0 .327	0.15
(e) 61 o	1.15	66 .8	0.01	−0 .87	−0 .04	−1 .875	−0 .139	0.08
(f) 61 $\alpha\delta$1	1.57	95 .9	0.01	−0 .77	−0 .27	0 .114	0 .058	0.06
(g) 62 $\alpha\epsilon$	1.52	44 .8	0.24	1 .01	0 .44	−0 .286	−0 .427	0.08
(h) 62 $\beta\mu$1	1.18	50 .1	0.01	2 .48	0 .19	−1 .209	−0 .235	0.07
(i) 62 $\beta\upsilon$	1.69	47 .5	0.28	0 .58	0 .45	−0 .227	−0 .497	0.08

$$\delta\dot{\omega} = -\theta\delta\dot{\Omega}$$

$$-\frac{3465J_{10}}{8,388,608p^{10}}n(63-3465\theta^2+30,030\theta^4-90,090\theta^6+109,395\theta^8$$

$$-46,189\theta^{10})\cdot(128+1152e^2+2016e^4+840e^6+63e^8)$$

$$-\frac{9009J_{12}}{268,435,456p^{12}}n(231-18,018\theta^2+225,225\theta^4-1,021,020\theta^6$$

$$+2,078,505\theta^8-1,939,938\theta^{10}+676,039\theta^{12})\cdot(1024+39,936e^2$$

$$+274,560e^4+549,120e^6+360,360e^8+72,072e^{10}+3003e^{12}) \qquad (11)$$

$$-\frac{45,045J_{14}}{4,294,967,296p^{14}}n(429-45,045\theta^2+765,765\theta^4-4,849,845\theta^6$$

$$+14,549,535\theta^8-22,309,287\theta^{10}+16,900,975\theta^{12}-5,014,575\theta^{14})$$

$$\times(1024+19,968e^2+91,520e^4+137,280e^6+72,072e^8$$

$$+12,012e^{10}+429e^{12}),$$

$$\delta e = -\sin i\,(1-5\theta^2)^{-1}(1-e^2)\sum_{j=4}^{6} C_jA_jB_j \sin\omega, \qquad (12)$$

$$\delta i = -e\theta\,\delta e/\{\sin i\,(1-e^2)\}, \qquad (13)$$

$$\delta\Omega = e\theta \sin^{-1} i\,(1-5\theta^2)^{-1}\sum_{j=4}^{6} C_j\{-\sin^2 i\cdot D_j$$

$$+(9-5\theta^2)(1-5\theta^2)^{-1}A_j\}B_j\cos\omega, \qquad (14)$$

$$\delta\omega = -\theta\delta\Omega - \sin i\cdot e^{-1}\cdot(1-5\theta^2)^{-1}\sum_{j=4}^{6} C_jA_jE_j\cos\omega, \qquad (15)$$

where

$$\theta = \cos i$$

$$C_4 = \frac{105J_9}{65,536J_2p^7}$$

$$C_5 = \frac{1155J_{11}}{4,194,304J_2p^9}$$

$$C_6 = \frac{3003J_{13}}{67,108,864J_2p^{11}}$$

$$A_4 = 7-308\theta^2+2002\theta^4-4004\theta^6+2431\theta^8$$

$$A_5 = 21-1365\theta^2+13,650\theta^4-46,410\theta^6+62,985\theta^8-29,393\theta^{10}$$

$$A_6 = 33-2970\theta^2+42,075\theta^4-213,180\theta^6+479,655\theta^8-490,314\theta^{10}+185,725\theta^{12}$$

$$B_4 = 64 + 336e^2 + 280e^4 + 35e^6$$

$$B_5 = 128 + 1152e^2 + 2016e^4 + 840e^6 + 63e^8$$

$$B_6 = 512 + 7040e^2 + 21{,}120e^4 + 18{,}480e^6 + 4620e^8 + 231e^{10}$$

$$D_4 = 88(7 - 91\theta^2 + 273\theta^4 - 221\theta^6)$$

$$D_5 = 130(21 - 420\theta^2 + 2142\theta^4 - 3876\theta^6 + 2261\theta^8)$$

$$D_6 = 60(99 - 2805\theta^2 + 21{,}318\theta^4 - 63{,}954\theta^6 + 81{,}719\theta^8 - 37{,}145\theta^{10})$$

$$E_4 = 64 + 1776e^2 + 4760e^4 + 2485e^6 + 210e^8$$

$$E_5 = 128 + 5504e^2 + 26{,}208e^4 + 30{,}072e^6 + 8{,}967e^8 + 504e^{10}$$

$$E_6 = 512 + 31{,}360e^2 + 232{,}320e^4 + 467{,}280e^6 + 300{,}300e^8 + 57{,}982e^{10} + 2310e^{12} \tag{16}$$

(a) Even harmonics—Table 18 gives equations of condition to determine values of J_2 through J_{14}. There are 18 equations with 7 unknowns.

The equations can be solved by assigning to each a weight reciprocally proportional to the standard deviation. Actually, each equation is divided by its standard deviation, and then normal equations are constructed. Before solving the equations, note that $\Sigma(\mathrm{O{-}C})^2$ is 3882 ($=18\times14.7^2$); that is (O–C) is bigger than the standard deviation by factor of 14.7. This value comes down to $23=(18-6)\times1.4^2$ after solving J_{12}, and to $13.4=(18-7)\times1.1^2$ after solving J_{14}, whereas it is $93.5=(18-5)\times2.7^2$ after J_{10} is solved. Therefore we can stop either at J_{12} or at J_{14}, although the solution including J_{14} is, of course, better.

In table 19 residuals based on the solutions up to J_{14} and J_{12} are given under headings I and II, respectively, in units of 10^{-6} degrees. Under the heading KH, residuals based on King-Hele and Cook's values (1964) are given; that is,

$$\begin{aligned} J_2 &= 1802.70\times10^{-6}, & J_4 &= -1.40\times10^{-6},\\ J_6 &= 0.37\times10^{-6}, & J_8 &= 0.07\times10^{-6},\\ J_{10} &= -0.50\times10^{-6}, & J_{12} &= 0.31\times10^{-6}. \end{aligned} \tag{17}$$

In the node equations the residuals based on my new determinations for 1962 $\beta\nu$ are larger than the standard deviations. However, since this datum is not entirely reliable, being based on a single determination covering an incomplete period of time, this may not be a weak point in this determination.

In the perigee equations of 1961 ν and 1962 $\alpha\epsilon$, the residuals are larger than their standard deviations. This may suggest that we must still include higher-order terms to express these data.

Table 19.—*Equations of Condition for Even Harmonics*

	J_2	J_4	J_6	J_8	J_{10}	J_{12}	J_{14}	(O–C)$\times 10^6$	I	II	KH
Perigee:											
(a)	4875	−1563	−2718	2481	410	−1916	934	40° ± 20°	5°	−2°	160°
(b)	4508	−1271	−2546	2124	530	−1744	711	70 ± 30	18	12	190
(c)	2753	2686	−1224	−2302	316	1425	37	910 ± 300	230	370	540
(d)	7476	−5168	−2589	6275	−3121	−2232	4333	−480 ± 200	−290	−360	−1610
(e)	−640	1895	4419	4324	1624	−1623	−1623	−200 ± 400	10	−660	340
(f)	−903	−637	−331	−144	−53	−15	−2	−200 ± 500	100	100	260
(g)	1835	1038	−821	−643	398	340	−202	420 ± 60	160	180	−310
(h)	2740	4130	−333	−4065	−1360	2596	1846	1310 ± 1500	−300	160	−2190
(i)	1120	775	−267	−384	52	167	0	300 ± 350	10	40	−280
Node:											
(a)	−3241	2545	−201	−1099	790	107	−525	−26 ± 6	0	−2	60
(b)	−3026	2274	−96	−1040	680	167	−512	−40 ± 9	1	−7	30
(c)	−2864	261	1168	−16	−480	−37	194	−52 ± 15	−4	−1	260
(d)	−4615	5068	−1992	−1173	2162	−1137	−355	131 ± 40	−33	52	470
(e)	−2240	−2037	−808	331	811	657	219	−1262 ± 25	4	12	260
(f)	194	145	82	42	20	9	4	65 ± 2	0	1	−35
(g)	−1716	300	511	−126	−207	60	96	−56 ± 5	4	6	90
(h)	−3334	−188	1667	489	−747	−441	278	−12 ± 30	20	4	560
(i)	−1181	67	288	3	−97	−11	36	−156 ± 40	−62	−69	35

Table 20.—*Equations of Condition for Odd Harmonics*

	J_3	J_5	J_7	J_9	J_{11}	J_{13}	(O–C)	I	II
Eccentricity:							10^{-6}		
(a)	−192.5	94.0	47.6	−76.3	21.9	25.2	4 ± 2	−2	0
(b)	−190.6	86.0	50.8	−71.5	16.1	26.6	2 ± 2	0	−1
(c)	−271.7	−165.1	138.6	89.6	−53.1	−43.7	8.6 ± 1.3	−0.1	0.1
(d)	−189.0	161.1	−10.2	−93.1	85.3	−16.1	−9 ± 14	−21	−19
(e)	−369.1	1036.4	1457.3	907.1	67.1	−481.1	−42 ± 6	0	−1
(f)	−293.0	−134.6	−51.0	−17.1	−4.9	−1.0	8 ± 4	3	−1
(g)	−214.6	−65.7	83.0	20.9	−30.2	−7.4	37 ± 20	34	33
(h)	−301.9	−312.1	136.1	220.5	−20.3	−125.9	22 ± 4	−4	−4
(i)	−202.0	−88.3	51.3	28.0	−12.2	9.5	18 ± 20	12	10
Inclination:							10^{-4}		
(a)	2890	−1420	−720	1140	−330	−380	−0.2 ± 0.8	0.1	0.4
(b)	3250	−1460	−870	1220	−280	−450	−0.4 ± 0.9	−0.1	0.1
(c)	160	100	−80	−50	30	30	−0.9 ± 0.8	−0.8	−0.8
(d)	1710	−1460	90	840	−770	150	−11 ± 7	−10	−10
(e)	70	−200	−290	−180	−10	90	−0.6 ± 1.3	−0.7	−0.7
(f)	−20	−10	0	0	0	0	1 ± 1	1	1
(g)	3190	980	−1230	−310	450	110	4 ± 3	4	5
(h)	100	110	−50	−70	10	40	−5 ± 3	−5	−5
(i)	3280	1430	−830	−450	200	150	−5 ± 9	−4	−4

Perigee:									
(a)	−64400	47200	11300	−42000	22510	13210	42 ± 8	−7	−5
(b)	−54900	41800	10900	−39100	19630	14600	50 ± 5	6	7
(d)	−123400	115950	−17320	−66120	73910	−22580	−14 ± 50	−141	−116
(g)	−50720	−7880	36420	3680	−21310	−1940	−20 ± 5	3	6
(i)	−41290	−13530	25230	10490	−10980	−6370	4 ± 100	6	8
Node:							10^{-4}		
(a)	−5300	−9700	13700	−1200	−9580	7330	−5 ± 5	−1	−2
(b)	−5900	−11150	14650	−300	−10800	7230	−7 ± 2	−1	−2
(c)	−220	−1490	−410	1000	480	−510	2 ± 4	0	0
(d)	−3550	−4240	11220	−7370	−3080	9310	14 ± 10	1	2
(e)	−80	−12390	−12630	−3900	4730	7500	4 ± 8	−9	−16
(f)	20	210	210	150	80	40	7 ± 7	7	7
(g)	−4520	−19460	−860	10990	1170	−5710	34 ± 6	16	16
(h)	−130	−1340	−760	820	980	−230	7 ± 5	4	4
(i)	−4440	−20940	−4580	7940	3450	−2720	88 ± 30	64	63

The two sets of solutions derived are the following:

Solution I (in units of 10^{-7})

$$\begin{array}{llll} dJ_2 = 1.65, & dJ_4 = 1.81, & dJ_6 = 2.56, & dJ_8 = -2.50, \\ \pm 6 & \pm 16 & \pm 30 & \pm 50 \\ & J_{10} = -0.54, & J_{12} = -3.57, & J_{14} = 1.79, \\ & \pm 50 & \pm 44 & \pm 63 \end{array} \tag{18}$$

Solution II (in units of 10^{-7})

$$\begin{array}{lll} dJ_2 = 1.50, & dJ_4 = 2.03, & dJ_6 = 2.03, \\ \pm 5 & \pm 18 & \pm 31 \\ dJ_8 = -1.29, & J_{10} = -1.55, & J_{12} = -2.94. \\ \pm 34 & \pm 45 & \pm 49 \end{array} \tag{19}$$

(b) Odd harmonics—As shown in table 20, we have 32 equations to determine 6 unknown coefficients of odd harmonics. At first $\Sigma(O-C)^2$ is $349(=32\times3.3^2)$. This number comes down to $153(=28\times2.3^2)$ after J_9 is solved, and to $42(=27\times1.25^2)$ and to $39(=26\times1.23^2)$ after J_{11} and J_{13}, respectively, are solved. Therefore, the inclusion of J_{13} does not reduce the residuals too much. Two sets of solutions are derived, one up to J_{11} and one up to J_{13}; that is,

Solution I (in units of 10^{-7})

$$\begin{array}{lll} dJ_3 = 0.31, & dJ_5 = -1.47, & dJ_7 = 1.36, \\ \pm 20 & \pm 25 & \pm 39 \\ J_9 = -1.67, & J_{11} = 3.02, & J_{13} = -1.14, \\ \pm 60 & \pm 35 & \pm 84 \end{array}$$

Solution II (in units of 10^{-7})

$$\begin{array}{lll} dJ_3 = 0.07, & dJ_5 = -1.22, & dJ_7 = 0.93, \\ \pm 11 & \pm 17 & \pm 22 \\ & J_9 = -0.75, & J_{11} = 2.96. \\ & \pm 17 & \pm 35 \end{array} \tag{20}$$

Table 20 gives the residuals based on solutions I and II for each datum. Residuals in the eccentricities of 1961 ν and 1962 $\beta\mu$, in the perigee of 1961 ν, and in the nodes of 1962 $\alpha\epsilon$ and 1962 $\beta\upsilon$ have much larger values than the standard errors. This may show that still higher-order harmonics are significant.

In this analysis parallactic terms are neglected in computing lunar perturbations. However, in the parallactic disturbing function there is a term,

$$\frac{45}{8}\sin i\cdot\sin\epsilon\left(1-\frac{5}{4}\sin^2 i\right)\left(1-\frac{5}{4}\sin^2\epsilon\right)ee'\left(1+\frac{3}{4}e^2\right)\sin\omega\cdot\sin\omega', \quad (21)$$

where ϵ is obliquity, e is lunar eccentricity, and ω' is lunar argument of perigee. Since ω' moves slowly, we must include this term if we treat observations of high-altitude satellites in the future.

5. RESULTS

The two sets of solutions derived in this paper are the following:

Solution I (units of 10^{-6})

$$\begin{array}{ll}
J_2 = 1082.645, & J_3 = -2.546, \\
\pm 6 & \pm 20 \\
J_4 = -1.649, & J_5 = -0.210, \\
\pm 16 & \pm 25 \\
J_6 = 0.646, & J_7 = -0.333, \\
\pm 30 & \pm 39 \\
J_8 = -0.270, & J_9 = -0.353, \\
\pm 50 & \pm 60 \\
J_{10} = -0.054, & J_{11} = 0.302, \\
\pm 50 & \pm 35 \\
J_{12} = -0.357, & J_{13} = -0.114, \\
\pm 44 & \pm 84 \\
J_{14} = 0.179 & \\
\pm 63 &
\end{array} \quad (22)$$

Solution II

$$\begin{array}{ll}
J_2 = 1082.630, & J_3 = -2.559, \\
\pm 5 & \pm 11 \\
J_4 = -1.627, & J_5 = -0.185, \\
\pm 18 & \pm 17 \\
J_6 = 0.593, & J_7 = -0.376, \\
\pm 31 & \pm 22
\end{array}$$

$$
\begin{array}{llll}
J_8 = & -0.149, & J_9 = & 0.039, \\
 & \pm 34 & & \pm 17 \\
J_{10} = & -0.155, & J_{11} = & 0.296, \\
 & \pm 45 & & \pm 35 \\
J_{12} = & -0.294 & & \\
 & \pm 49 & &
\end{array} \tag{23}
$$

A. H. Cook (1964) recently derived values of J_2, J_4 and J_6 by using high satellites only, and his results show remarkable agreement with Solution I.

The flattening of the reference earth ellipsoid based on this value of J_2 is 1/298.252. The theoretical value of J_4 for the reference ellipsoid assumed to be in hydrostatic equilibrium is computed as -2.350×10^{-6}. The deviation of the geoid computed on the geopotential based on solution I is expressed as a function of geometric latitude:

$$
\begin{aligned}
h = & +0.8-18.3 \sin \beta-87.8 \sin^2 \beta-119.1 \sin^3 \beta+1042.5 \sin^4 \beta \\
& +1191.7 \sin^5 \beta-5074.2 \sin^6 \beta-3636.7 \sin^7 \beta+12{,}668.0 \sin^8 \beta \\
& +5230.8 \sin^9 \beta-16{,}676.3 \sin^{10} \beta-3556.4 \sin^{11} \beta+10{,}913.0 \sin^{12} \beta \\
& +926.8 \sin^{13} \beta-2791.3 \sin^{14} \beta \text{ (in meters).}
\end{aligned} \tag{24}
$$

Figure 1 shows the value of h as a function of β based on this equation. The value of geoid height h in the north pole is 13.5 meters, which is the maximum value, and is -24.1 meters in the south pole.

In the solutions (22) and (23), the values of J_n do not tend to converge to zero as n increases. However, if n is large enough, J_n should take a very small value. Otherwise the gravity expression, which is derived by differentiating the potential with respect to the radius, may give a very great difference of gravities between the equator and the poles and between the north and south poles.

To determine how strong or weak the solutions (22) and (23) are, the correlation coefficients in my determinations are shown in tables 21 and 22. The tables indicate that these solutions are derived from rather strongly correlated equations of condition. Therefore, in the future we must use both low and high satellites having the same inclination.

However, to determine the orbital elements of low satellites with high inclinations we need observations from high latitudes. As I mentioned earlier, I could not assign a large weight to the node equation of 1961*o* to determine even-order coefficients, because the inclination could not be determined with sufficient accuracy. Also, I must mention that I did not use satellites with inclinations below 28°, between 50° and 67°, or between 67° and 85° in this determination.

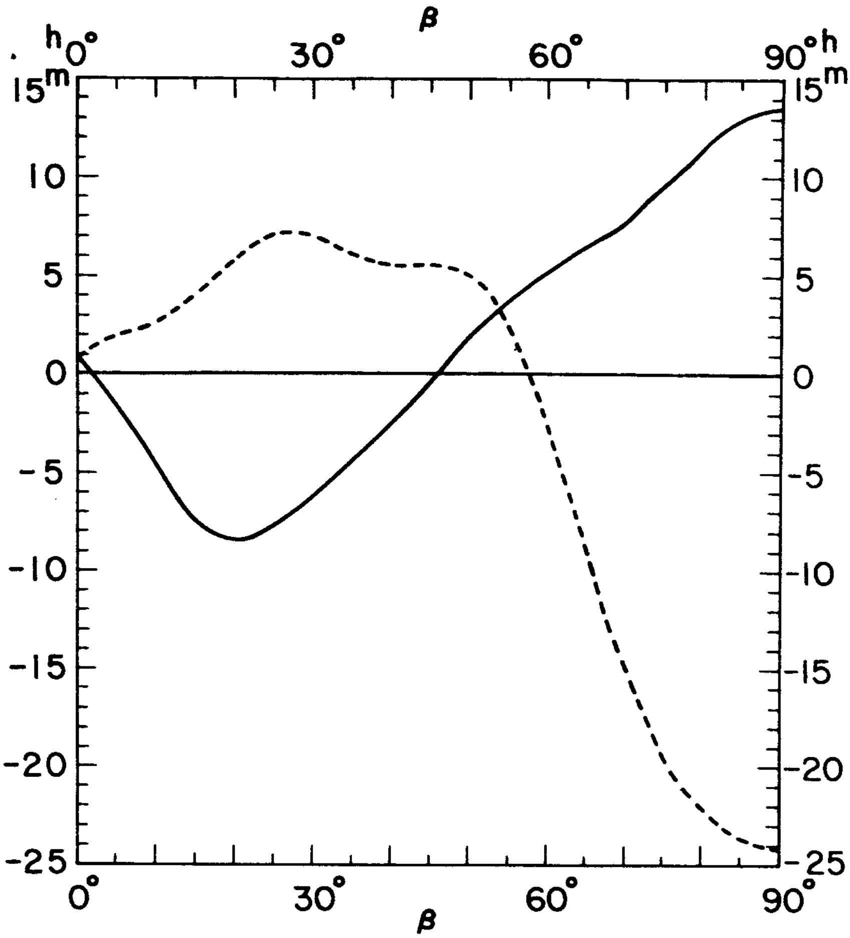

Figure 1.—Geoid height (*h*) as a function of geometric latitude (*p*). Solid line shows geoid height in Northern Hemisphere and broken line shows that in the Southern Hemisphere.

However, I believe that the present determination is much more reliable than the previous one, since the data themselves are more reliable, both because of the number of observations and because I included some satellites that were not used in the previous determination.

ACKNOWLEDGMENTS

This work was supported in part by Asahi Academic Fund. Some of the computations were made on an IBM–7090 computer at the Japan

Table 21.—*Correlation Coefficients for Even Orders*

	J_2	J_4	J_6	J_8	J_{10}	J_{12}	J_{14}
J_2	1.00	−0.60	0.80	−0.89	0.79	−0.71	0.83
J_4		1.00	−0.86	0.80	−0.85	0.91	−0.47
J_6			1.00	−0.79	0.96	−0.88	0.60
J_8				1.00	−0.80	0.84	−0.84
J_{10}					1.00	−0.80	0.70
J_{12}						1.00	−0.50
J_{14}							1.00

	J_2	J_4	J_6	J_8	J_{10}	J_{12}
J_2	1.00	−0.40	0.63	−0.60	0.49	−0.57
J_4		1.00	−0.82	0.84	−0.84	0.88
J_6			1.00	−0.65	0.94	−0.83
J_8				1.00	−0.54	0.90
J_{10}					1.00	−0.73
J_{12}						1.00

Table 22.—*Correlation Coefficients for Odd Orders*

	J_3	J_5	J_7	J_9	J_{11}	J_{13}
J_3	1.00	−0.93	0.98	−0.94	0.48	−0.86
J_5		1.00	−0.96	0.86	−0.69	0.75
J_7			1.00	−0.92	0.57	−0.82
J_9				1.00	−0.27	0.97
J_{11}					1.00	−0.12
J_{13}						1.00

	J_3	J_5	J_7	J_9	J_{11}
J_3	1.00	−0.85	0.93	−0.85	0.75
J_5		1.00	−0.92	0.81	−0.92
J_7			1.00	−0.92	0.84
J_9				1.00	−0.68
J_{11}					1.00

IBM Co., which kindly provided machine time without charge through the Computing Center of the University of Tokyo. I am grateful to Miss Phyllis Stern for her help in the computations.

REFERENCES

Cook, A. H.:
1964. Paper presented at IAU Commission 7 Meeting, Hamburg, August.

King-Hele, D. G., and Cook, G. E.:
1964. A paper presented at meeting of COSPAR Working Group 1, Florence, Italy.

Kozai, Y.:
1959. Smithsonian Astrophysical Observatory, Special Report No. 22, 7.
1962. Astron. J., *67*, 446-461.
1963. The Use of Artificial Satellites for Geodesy, ed. G. Veis, 305-316.

Part 3

Derivation of the Earth's Gravity Field by Nonoptical Tracking

Although precision optical tracking has yielded the most extensive geodetic information to date, electronic tracking methods are rapidly becoming competitive. Of the latter methods, the precise measurement of the frequencies received from stable oscillators in the satellite has been particularly fruitful.

A section of a recent report by Dr. Robert R. Newton of the Applied Physics Laboratory, one of the group which has exploited this technique most successfully, provides an explanation of the basic technique. This is followed by a report of the analysis of some of the Doppler data and data from Syncom 2.

The following is excerpted from a paper presented by Robert R. Newton at the European Symposium on Satellite Geodesy, Paris, December 1964.

Measurements of the Doppler Shift in Satellite Transmissions and Their Use in Geometrical Geodesy

ROBERT R. NEWTON
Applied Physics Laboratory
Johns Hopkins University

1. CHARACTERISTICS OF EXISTING DOPPLER MEASURING EQUIPMENT

THE APPLIED PHYSICS LABORATORY exercises technical direction on behalf of the Department of the Navy of a network of doppler tracking stations that is called the TRANET System. This system has been in operation for approximately five years and currently contains twelve stations with another expected to be added in 1965. Many other sites have been occupied at various times. The Department of the Navy maintains this tracking system and supports geodetic analysis of the data obtained from it as a part of the national geodetic satellite program.*

Up to the present, the data from this system have been used almost entirely in studying dynamics of satellites and in deriving models of the earth's gravity field from these dynamic studies.

The method of operation of the existing doppler stations is described in Ref. 1. Briefly summarized, a station makes a measurement of doppler frequency every 2 or 4 seconds and thus typically obtains several hundred data points during each pass of a satellite.

In these measurements the effects of radio noise and of instrumental contributions to error are virtually negligible. The dominant errors in the raw data arise from refraction both in the ionosphere and in the troposphere.

Of these two sources of refraction ionospheric refraction is by far the

*The station in Antarctica, if it is established, will be supported by the National Science Foundation, and therefore is not strictly speaking a part of the TRANET System. However, data from it will be available for analysis so that it can be considered together with the other stations for the purposes of this paper.

biggest problem. If no correction were made for refraction in the ionosphere at a transmitted frequency of 162 mh, for example, satellite positions derived from the doppler measurements could easily be in error by as much as a kilometer. Fortunately, the refractivity in the ionosphere depends upon the frequency and to first approximation varies inversely with the square of the frequency. This fact is the reason for using two or more transmitted frequencies (see Refs. 1 and 2) which are both controlled from the same oscillator and which are hence always coherent. By measuring the apparent doppler shift at each of two coherent frequencies, it is possible to calculate the effects of ionospheric refraction and therefore to eliminate refraction, on the assumption that the refractivity does indeed vary with the square of the frequency. Since this law does not hold exactly, there is some residual refraction arising from neglected effects. At middle and high latitudes we believe that the residual effects amount to the equivalent of a few meters or less in satellite position. However, there is some indication that at low latitudes and under some circumstances the residual effect may amount to 100 meters or more. Fortunately, position errors from residual refraction have a tendency to average out when many satellite passes are used.

Depending upon the level of accuracy desired, the uncorrected ionospheric refraction may still be unacceptable. There are three ways of reducing the effect of refraction still further. One is by the use of a third frequency which will be provided on GEOS A (Ref. 3). A second method which shows promise involves a calculation of the higher order refraction effects based upon a model of the ionosphere, combined with the measured refraction effect obtained from two frequencies. There is considerable hope that the higher order refraction can be calculated in this way to an accuracy of about 10% of the high order effects. The third way is to use higher frequencies such as the 972 mh beacon provided on GEOS A.

Tropospheric refraction effects can produce the equivalent of about 50 meters in satellite position if no correction is made. Tropospheric refraction does not depend appreciably upon frequency and therefore cannot be removed by the techniques that are successful with the ionosphere. Up to the present time the only way that we have found to correct for tropospheric refraction (Ref. 4) is to calculate this refraction using a model of the troposphere combined with suitable meteorological observations made at the time of each pass. This correction has been quite successful except when a weather front is near a station at the time of a pass. If high accuracy is desired it is necessary to eliminate any data obtained when a weather front is within about 30 km of a station.

As we have already said, the stations that make up the TRANET System supply several hundred data points during each pass. This volume of data is necessary for many research purposes such as research into the effects of tropospheric refraction which were just discussed. However, if the presently used methods for eliminating refraction are considered by an observer to be sufficiently accurate, and if his principal interest is in using the doppler data for geometric purposes, he can work with much simpler receiving equipment which provides a much smaller volume of data.

This simplified equipment is now under development at the Applied Physics Laboratory.

REFERENCES

1. WEIFFENBACH, G. C.: Measurement of the Doppler Shift of Radio Transmissions From Satellites. Proc. of the IRE, v. 48, no. 4, pp. 750–754, April 1960.
2. GUIER, W. H.; AND G. C. WEIFFENBACH: A Satellite Doppler Navigation System. Proc. of the IRE, v. 48, no. 4, pp. 507–516, April 1960.
3. NEWTON, R. R.: Characteristics of the GEOS A Spacecraft. Presented at the Symposium on the Establishment of a European Geodetic Network by Artificial Satellites, Paris, France, 14–16 December 1964.
4. HOPFIELD, H. S.: The Effect of Tropospheric Refraction on the Doppler Shift of a Satellite Signal. J. Geophys. Res., v. 68, no. 18, September 15, 1963.

The following paper was originally published in Nature, *vol. 200, No. 4902, October 12, 1963, pp. 124–125.*

Determination of the Non-Zonal Harmonics of the Geopotential From Satellite Doppler Data

W. H. Guier
Applied Physics Laboratory
Johns Hopkins University

A least squares determination of values for the coefficients, C_n^m, S_n^m, of the non-zonal harmonics of the geopotential:

$$U(r,\varphi,\lambda)=\frac{K}{r}\left\{1+\sum_{n=2}^{\infty}\sum_{m=0}^{n}\frac{P_n^m(\sin\varphi)}{r^n}[C_n^m\cos m\lambda+S_n^m\sin m\lambda]\right\} \quad (1)$$

has been made through $n=m=4$ using Doppler data from the three Satellites 1961 o1, 1961 $\alpha\eta$1, and 1962 $\beta\mu$1. In equation (1):

r = geocentric radius from the Earth's centre of gravity; φ = geocentric latitude; λ = geocentric longitude from Greenwich meridian,

and $P_n^m(z)$ are the associated Legendre polynomials:

$$P_n^m(z)=(1-z^2)^{\frac{m}{2}}\frac{d^m}{dz^m}P_n(z) \quad (2)$$

The values of C_2^1 and S_2^1 were constrained to be identically zero in the determination.

Table 1 presents a brief summary of the Doppler data which were chosen for the determination. The data were chosen as being the best available from the point of view of: (1) quality with respect to noise-level, timing errors, presence of ionospheric refraction errors, and stability of the satellites' transmitted frequencies; (2) uniform distribution of station locations over the Earth's surface with particular care taken to avoid an overweight of data from stations located within the continental United States; (3) uniform coverage of the satellite orbit by the data with respect to the angle between the ascending node and the Greenwich meridian.

The principal ionospheric refraction contribution was removed by coherently combining two frequencies received simultaneously from the satellite in the Doppler receiving equipment[1,2]. To ensure further minimum refraction errors, data were considered only if the maximum elevation of the pass was less than 83° and greater than 20°. Finally, data points which corresponded to instantaneous elevations below 13° were deleted, and the remaining data points corrected for tropospheric refraction[3]. A typical noise-level for that data finally chosen was roughly 5 parts in 10^{10} of the transmitted frequency. Timing errors were judged to be below 0·003 sec (3-sigma value).

The data which survived the foregoing criteria were then grouped by days, one group containing all passes for a given satellite which occurred between two successive midnights (G.M.T.). After grouping, only those were selected which contained ten or more high-quality sets of data from at least five separate stations with at least three being outside the continental United States. From Table 1 it can be seen that the fewest groups of data for any one satellite occurred for Satellite 1961 $\alpha\eta$1. This is due to the low inclination of the satellite precluding reception of data from high-latitude stations. While considerably more groups of data satisfying the foregoing criteria were available for the other two satellites, the total number of groups chosen for each satellite was limited to being roughly equal to avoid overweighting the data corresponding to a particular inclination. In the final choice of groups care was taken to ensure a reasonably even distribution of angles between the ascending node and the Greenwich meridian at the time of the first pass in each group. In addition, groups for two different satellites occurring on the same day were avoided to increase the *a priori* probability that the effects of undetected station instrumentation errors and refraction errors were random.

Having made the final choice of groups, a least-squares determination of a satellite orbit for each group was made, resulting in no computed arc of the satellite motion lasting more than 24 h. Orbit parameters spanning data over such short time-intervals were chosen because: (1) the satellite trajectory could be integrated numerically with negligible error and made unnecessary the very tedious task of solving the perturbed equations of motion to high orders; (2) unknown fluctuations in atmospheric drag and errors in the values for the zonal harmonic coefficients introduce negligible errors.

The computer programme used to determine the orbits[4] includes the Sun and Moon forces, although they should introduce negligible errors for these short data spans. The resulting differences between the Doppler data points and the corresponding computed values for the Doppler shift (based on fixed initial values for the harmonic coefficients of the geopotential) were used as the final data for the least-squares determination of the differential changes in the values of the non-zonal harmonic coefficients.

Table 1.—*Summary of Doppler Data Used*

Satellite designation	Inclination (deg)	Semi-major axis (km)	Eccentricity	No. individual satellite passes	No. distinct station loc.	No data groups (satellite orbits)	Average No. passes per group	Average time span per group (h)
1961 $\alpha\eta 1$	32·4	7,410	0·010	87	9	8	11	15·9
1962 $\beta\mu 1$	50·1	7,510	0·007	199	15	9	22	22·7
1961 $o 1$	66·8	7·320	0·008	155	13	10	16	23·3
			Totals..	441	37	27		

Table 2.—*Values of the Non-Zonal Harmonic Coefficients*

n	m	C_n^m	S_n^m
2	2	$1 \cdot 68 \times 10^{-6}$	$-0 \cdot 64 \times 10^{-6}$
3	1	$1 \cdot 77 \times 10^{-6}$	$0 \cdot 19 \times 10^{-6}$
3	2	$2 \cdot 86 \times 10^{-7}$	$-0 \cdot 25 \times 10^{-7}$
3	3	$1 \cdot 48 \times 10^{-7}$	$1 \cdot 41 \times 10^{-7}$
4	1	$-5 \cdot 69 \times 10^{-7}$	$-4 \cdot 60 \times 10^{-7}$
4	2	$0 \cdot 60 \times 10^{-7}$	$2 \cdot 66 \times 10^{-7}$
4	3	$7 \cdot 90 \times 10^{-8}$	$-0 \cdot 28 \times 10^{-8}$
4	4	$-7 \cdot 85 \times 10^{-9}$	$6 \cdot 56 \times 10^{-9}$

Very briefly, the least-squares procedure used for determining the non-zonal harmonic coefficients was the following. The differences between the theoretical and experimental values for the Doppler shift were assumed to arise wholly from errors in the locations of the tracking stations and values for the non-zonal harmonic coefficients. It was further assumed that because of these errors there existed errors in the orbit parameters associated with each group of data. Perturbation equations were then derived to express these residuals as a function of differential changes in the three co-ordinates of each tracking station represented in the totality of data, differential changes in each of the six orbit parameters for each group of data, and differential changes in the values of the C_n^m and S_n^m of equation (1). A special IBM 7094 computer programme was designed and coded in which the differential values of the station positions and orbit parameters are continually adjusted to yield an extremum of the mean-square data residuals with respect to these parameters (irrespective of whether the resulting values are reasonable) for any given values for the differential harmonic coefficients. Consequently, at any point in the computing process, changes in the values of the differential station and orbit parameters can produce negligible reduction in the mean-square data residuals. In this way the station co-ordinates and orbit parameters are effectively eliminated from the least-squares determination of the harmonic coefficients. The programme is then iterated until stable values for the differential non-zonal harmonic coefficients are obtained.

Table 2 presents the results of the determination using the data summarized in Table 1. Without new data at a different inclination, it is very difficult to estimate the true error in these values; and no attempt has been made to ascribe a realistic error to each coefficient. The fact that the station parameters were effectively eliminated from the determination ensures that the principal error in the resulting values for the coefficients arises from correlated errors in the experimental data and not from erroneous values for the station locations. Consequently, the efficacy of this method depends principally on there being sufficient experimental data of sufficient accuracy that the build-up of computer error combined with experimental errors does not destroy the sensitivity of the data residuals to the harmonic coefficients once the station and orbit differential parameters are eliminated. Several numerical experiments were performed with the amount of data intentionally reduced to the point where a realistic solution would not be expected. The objective of the experiments was to obtain criteria for the number of harmonic coefficients which could be evaluated with the data available. As expected, these experiments indicated that if stable values for the coefficients were produced with successive iterations, and if their resulting values did not change markedly with changes in the relative weighting of the data residuals, the final values should be trustworthy.

Recognizing that the Tesseral harmonic, $n=2$, $m=1$, should have negligibly small coefficients, a final check on the validity of the values in Table 2 was made by performing a new determination with C_2^1 and S_2^1 added to those coefficients listed in Table 2. The resulting values for those coefficients in Table 2 were not materially altered and the values for the new coefficients were found to be:

$$C_2^1 = 1{\cdot}78 \times 10^{-8}$$

$$S_2^1 = -3{\cdot}48 \times 10^{-8} \tag{3}$$

The fact that they are negligibly small (compared with the values in Table 2 for $m=1$) lends considerable credence to the values given in Table 2.

A comparison between the values given in Table 2 and the present literature[5-8] indicates agreement of roughly the same character as the agreement between any two previously published sets of values. Consequently, such comparisons add little additional information on the accuracy of the values presented in Table 2.

Clearly the overall effort involved in obtaining these results was very large, and it is impossible to acknowledge all the people who made valuable contributions. However, I wish to acknowledge especially the contributions of R. R. Newton and S. Yionoulis for their aid in developing the satellite perturbation equations; G. Worsley, G. C. Weiffenbach, P. E. P. White, and their colleagues in connexion with obtaining the experimental Doppler data; and H. D. Black, C. Weisert, R. Henderson, and their colleagues for their help in coding and running the complex computer programmes involved.

This work was supported by the Department of the Navy, Bureau of Weapons, under contract NOw 62–0604–c.

[1] Guier, W. H.; and Weiffenbach, G. C.: Proc. Inst. Rad. Eng., 48, No. 4507 (1960).

[2] Guier, W. H.: (L), Proc. Inst. Rad. Eng., 49, No. 11, 1680 (1961).

[3] Hopfield, H. S.: J. Geophys. Res. (in the press).

[4] Applied Physics Laboratory, The Johns Hopkins University, Rep. TG–401.

[5] Kozai, Y.: Smithsonian Astrophysical Obs., Res. Space Sci., Spec. Rep. No. 72, August, 1961.

[6] Newton, R. R.: Proc. Third Intern. Space Sci. Symp., Washington, D.C., April, 1962 (in the press).

[7] Kaula, W. M.: J. Geophys. Res., 68, 473 (1963).

[8] Izsak, I.: Nature, 199, 137 (1963) and private communication.

Most geodetic data have been derived from comparatively near-Earth satellites. However, some of the terms in the Earth's gravity field are masked for these satellites by various diurnal effects. Conversely, a satellite in a 24-hour orbit is particularly sensitive to these terms because it is constantly affected by the same perturbations. Because of its high altitudes, a 24-hour satellite is difficult to track optically and the Minitrack interferometer does not have the angular accuracy needed. To overcome this problem, an electronic transponder has been developed which provides a measure of both the distance to the satellite and its radial velocity. This range and range-rate system was used on the Syncom satellite. The geodetic analysis of the tracking results is reported in the following paper which was originally published in the Journal of Geophysical Research, *vol. 70, no. 6, 1965, pp. 1566–1568.*

A Determination of Earth Equatorial Ellipticity From Seven Months of Syncom 2 Longitude Drift

C. A. Wagner
Goddard Space Flight Center, NASA

The 24-hour Syncom 2 satellite has been under periodic observation by range and range rate radar and Minitrack Radio Interferometer stations since mid-1963 (Wagner, 1964b). Seven months of longitude drift in the vicinity of two momentarily stationary configurations were analyzed for sensitivity to hypothetical longitude components of the earth's gravity field which would be in "resonance" on such a satellite (Blitzer et al., 1962; Wagner, 1964a). This drift, in the region 54 to 64° W (over Brazil), was derived from orbits calculated at the Goddard Space Flight Center.

From mid-August 1963 to late November 1963, the figure-eight ground track of Syncom 2 drifted from 55° W to 59° W, with a mean acceleration of

$$-(1.27 \pm .02) \times 10^{-3} \text{ degrees/day}^2 \quad (1)$$

The average growth of the semimajor axis for this period was estimated as $(0.0993 \pm .0042)$ km/day. The figure-eight configuration was momentarily stationary at about 54.76° on September 6, 1963, at which time the semi-major axis was ($42166.0 \pm .2$) km. On November 28, 1963, the westward drift of Syncom 2 was stopped by ground command firing of tangentially oriented cold gas jets on-board the satellite.

From early December 1963 to mid-February 1964, the figure-eight ground track of Syncom 2 drifted from a momentarily stationary position at about 59.15° W (semimajor axis: $42165.9 \pm .4$ km) to 63.5° W. The estimated mean geographic longitude acceleration of the ground track for this period was

$$-(1.32 \pm .02) \times 10^{-3} \text{ degrees/day}^2 \tag{2}$$

The average growth of the semimajor axis for this period was ($0.0994 \pm .0080$) km/day. Simulated Syncom 2 trajectories for these drift periods, starting with the initial orbital elements, show good agreement with the observed trajectories if an earth gravity field with longitude dependence is used in the particle program of the simulation. Sun and moon influence, as well as earth zonal gravity influence, on drift acceleration (as assessed by this simulation) for the full seven months of Syncom 2 data analyzed appears to be negligible compared with hypothetical earth gravity with longitude dependence. Other possible causes of this observed long-term accelerated longitude drift, such as (1) selective outgassing or leaking of on-board gas jets, (2) micrometeorite collisions, (3) solar wind or radiation interactions, or (4) geomagnetic field interactions in the environment of Syncom 2 all appear to be extremely unlikely.

Wagner (1946b) showed that any ellipticity of the earth's equator will cause the otherwise stationary figure-eight ground track of a 24-hour near-circular-orbit satellite to drift in longitude with an acceleration given by

$$\ddot{\lambda} = -A_{22} \sin 2\gamma \tag{3}$$

where

$$A_{22} = -72\pi^2 J_{22} \, (R_0/a)^2 \, \frac{(\cos^2 i + 1)}{2}, \text{ rad./sid. day}^2 \tag{4}$$

Relations 3 and 4, without the inclination factor, can be derived from equation 14 in Allan (1963) and equation 57b in Wagner 1964a.

γ is the nodal longitude of the 24-hour configuration east of the minor axis of the elliptical equator. J_{22} is the amplitude of the first significant longitude-dependent term in the spherical harmonic expansion of the earth's gravity potential. It is related to the difference between major and minor earth equatorial radii by (Izsak, 1961; Wagner, 1962; Kaula, 1965)

$$a_0 - b_0 = -6R_0 J_{22}$$

R_0 is the mean equatorial radius of the earth. Small a is the semimajor axis of the 24-hour satellite. Small i is its inclination. For Syncom

2, the inclination during both drift periods analyzed was close to 33.0°.

Under the assumption that the above observed drift acceleration is sensing only the lowest order of longitude-dependent earth gravity (that associated with the ellipticity of the earth's equator), the two drift accelerations of Syncom 2 (equations 1 and 2), satisfy (3) and (4) uniquely with the following values of the magnitude (J_{22}) and phase angle (λ_{22}) of equatorial ellipticity:

$$J_{22}\begin{pmatrix}\text{unadjusted for higher order}\\ \text{earth gravity effects}\end{pmatrix} = -(1.70 \pm .05) \times 10^{-6} \tag{5}$$

corresponding to a difference in major and minor equatorial radii of

$$a_0 - b_0 = 65 \pm 2 \text{ meters}$$

and,

$$\lambda_{22} = (19 \pm 6) \text{ degrees west of Greenwich} \tag{6}$$

(locating the major axis of the earth's elliptical equator).

From Table 1 it is seen that these values for the second-order tesseral harmonic of earth gravity are in reasonable agreement with recent determinations of longitude gravity from lower-altitude satellite observations and surface gravimeter data. From a consensus of recent and older geoids, which give tesseral field coefficients to higher order than the second, it appears that at the high altitude of the 24-hour satellite the second-order longitude effect accounts for about 85% of the full field effect at 54° to 64° W. The full longitude field is consistently depressed below the J_{22} field at these longitudes for all the recent geoids of Table 1. On the basis of the recent measures of higher-order tesseral gravity, calculations show the Syncom 2 estimates 5 and 6 should be:

$$J_{22}\begin{pmatrix}\text{adjusted for probable higher-order}\\ \text{earth gravity effects}\end{pmatrix} = -(1.92 \pm .2) \times 10^{-6} \tag{7}$$

or,

$$a_0 - b_0 = 73 \pm 8 \text{ meters}$$

and

$$\lambda_{22} = (21 \pm 7)^\circ \text{ west of Greenwich} \tag{8}$$

That longitude-dependent earth gravity exists seems well established from a large number of recent gravity reductions on different bases (Table 1). This 24-hour satellite reduction (because the altitude is so high) appears to separate out the second-order effect almost entirely from the sum of all higher-order earth gravity effects. Unless the earth is far more inhomogeneous in longitude than is thought to date, (7) and (8) are to be considered absolute estimates of the bounds on the ellipticity of the equator.

Table 1.—*Tesseral Coefficients in the Earth's Gravity Potential,*[1] *as Reported 1942–1964*[2]

$$\left\{V_E=\frac{\mu}{r}\sum_{n=2}^{\infty}\sum_{m=0}^{n}\left[1-(R_0/r)^nP_n^m\ (\sin\phi)J_{nm}\cos m(\lambda-\lambda_{nm})\right]\right\}$$

Tesseral geoid reference	J_{22}	λ_{22}	J_{31}	λ_{31}	J_{32}	λ_{32}	J_{33}	λ_{33}	J_{41}	λ_{41}	J_{42}	λ_{42}	J_{43}	λ_{43}	J_{44}	λ_{44}
Wagner (1964b)[3]	-1.7×10^{-6}	$-19.0°$														
Izsak (1964)[4]	-1.00	-17.0	$-.934\times10^{-6}$	$-15.5°$	$-.116\times10^{-6}$	19.0°	$-.173\times10^{-6}$	38.0°	$-.949\times10^{-6}$	$-146.0°$	$-.074\times10^{-6}$	47.5°	$-.024\times10^{-6}$	$-3.9°$	$-.0206\times10^{-6}$	25.3°
Kaula (1964)[4]	-1.77	-18.2	-2.12	-5.4	$-.379$	10.5	$-.105$	23.1	$-.263$	-239.0	$-.117$	42.3	$-.0473$	15.0	$-.0104$	14.5
Guier and Newton (1963)[3]	-1.80	-10.4	-1.77	6.3	$-.286$	-2.6	$-.204$	24.1	$-.73$	-141.0	$-.273$	38.6	$-.0791$	$-.7$	$-.0102$	35.0
Kaula (1963)[4]	-1.51	-18.1	-1.65	5.3	$-.144$	46.4	$-.145$	15.8	$-.471$	-228.0	$-.078$	44.2	$-.0265$	22.6	$-.0038$	23.3
Izsak (1963)[4]	-1.05	-11.2	-1.1	3.2	$-.20$	-21.8	$-.14$	20.0	$-.43$	-132.1	$-.13$	37.0	$-.026$	11.5	$-.019$	14.8
Kaula (May 1963)[4]	-1.4	-21.5	-1.6	-1.9	$-.15$	35.8	$-.156$	18.5	$-.53$	-233.7	$-.12$	44.5	$-.019$	10.7	$-.0038$	23.3
Uotila (1964)[5]	-1.52	-36.5	$-.685$	-81.0	$-.409$	-5.2	$-.398$	19.5	$-.238$	-127.0	$-.211$	14.6	$-.082$	-9.3	$-.0142$	-2.6
Kozai (1962)[4]	-1.2	-26.4	-1.9	4.6	$-.14$	-16.8	$-.10$	42.6	$-.52$	-122.5	$-.062$	65.2	$-.035$	0.5	$-.031$	14.9
Zhongolovitch (1961)[5]	-5.95	-7.7	-2.21	-25.7	$-.628$	-26.4	$-.54$	13.0	$-.78$	-149.2	$-.080$	45.0	$-.051$	-3.8	$-.0224$	15.9
Jeffreys (1942)[5]	-4.1	0.0	-2.1	0.0	$-.66$	0.0	$-.24$	33.3								

[1] r is the radial distance of the field point to the center of mass of the earth, μ the earth's Gaussian gravity constant $\doteq 3.9860\times10^{20}$ cm^3/sec^2, R_0 the mean equatorial radius of the earth $\doteq 6378.2$ km. ϕ is the geocentric latitude of the field point. λ is the geographic longitude of the field point. $J_{21}\doteq 0$, since the polar axis is very nearly a principal axis of inertia for the earth. P_n^m (sin ϕ) $=\cos^m\phi$ $\sum_{t=0}^{K} T_{nmt}\sin^{n-m-2t}\phi$, where K is the integer part of $(n-m)/2$ and $T_{nmt}=(-1)^t$ $(2n-2t)!/2^nt!\ (n-t)!\ (n-m-2t)!$ (See Kaula, 1965). The Tesseral coefficients are those for which $m\neq 0$.

[2] J_{nm} and λ_{nm}, except in one or two instances, have been converted from the original author's set of gravity coefficients. The blanks indicate the author did not consider that particular harmonic in fitting an earth potential to the observed data.

[3] Satellite-doppler geoid.

[4] Satellite-camera geoid.

[5] Surface-gravimetric geoid.

Table 1 illustrates the present state of fluidity with respect to *individual* tesseral coefficients. The adjusted bounds on the Syncom 2 determination of equatorial ellipticity encompass "reality" (and not just the random errors of the experiment) as far as can be judged by a number of recent geoids based on different kinds of gravity data. A recent reduction of Syncom 2 drift over the Central Pacific between 120° and 170° west longitude appears to confirm this conjecture. Preliminary results from the accelerated drift in this region yield:

$$J_{22} = -(1.75) \times 10^{-6}$$

$$\lambda_{22} = (18)^{\circ} \text{ west}$$

The experiment-standard deviation on the J_{22} number, however, is a number of times larger than that on the J_{22} value derived in the Syncom 2-Brazil experiment (eq. 5).

REFERENCES

ALLAN, R. R.: Perturbations of a Geostationary Satellite by the Longitude-Dependent Terms in the Earth's Gravitational Field. Planetary Space Sci. 2, 1963, 1325–1344.

BLITZER, L.; BOUGHTON, E. M.; KANG, G.; PAGE, R. M.: Effect of Ellipticity of the Equator on 24-Hour Nearly Circular Satellite Orbits. J. Geophys. Res., 67(1), 1962, 329–335.

GUIER, W. H.; AND NEWTON, R. R.: *In:* Nonzonal Harmonic Coefficients of the Geopotential From Satellite Doppler Data. Johns Hopkins Univ. Applied Physics Lab, Document APL–TG–520, Nov. 1963.

IZSAK, I. G.: Cited in a Private Communication From W. M. Kaula, July 1964.

IZSAK, I. G.: Tesseral Harmonics in the Geopotential. Nature, July 13, 1963, pp. 137–139.

IZSAK, I. G.: A Determination of the Ellipticity of the Earth's Equator From the Motion of Two Satellites. Astron J., 66(5), 1961, 226–229.

JEFFREYS, H.: *In:* Monthly Notices Royal Astronom. Soc. Geophys. Suppl., 5(55), 1942.

KAULA, W. M.: Cited in a Private Communication From W. M. Kaula, July 1964.

KAULA, W. M.: Improved Geodetic Results From Camera Observations of Satellites. J. Geophys. Res., 68(18), Sept. 1963.

KAULA, W. M.: Theory of Satellite Geodesy. Blaisdell Publishing Company (New York), 1965.

KOZAI, Y.: Cited in a Private Communication From Y. Kozai, Oct. 1962.

UOTILA, U.: Cited in a Private Communication From W. M. Kaula, July 1964.

WAGNER, C. A.: The Gravitational Potential of a Triaxial Earth. NASA, Goddard Space Flight Center Document X–623–62–206, October 1962.

WAGNER, C. A.: The Drift of a 24-Hour Equatorial Satellite Due to an Earth Gravity Field Through 4th Order. NASA TN D–2103, Feb. 1964a.

WAGNER, C. A.: Determination of a Triaxiality of the Earth From Observations on the Drift of the Syncom 2 Satellite. NASA, Goddard Space Flight Center Document X–621–64–90, April 1964b.

ZHONGOLOVITCH, D.: *In:* Tesseral Harmonics of the Gravitational Potential of the Earth as Derived From Satellite Motions by Y. Kozai. Astron. J., 66(7), Sept. 1961.

Part 4

Astronomical Constants

Astronomers are very conservative about changing the basic constants which they use in their various ephemerides and in many of their analyses. It is not that they do not recognize the improvements which take place from time to time, but they feel that the confusion resulting from the use of frequently changed values would more than offset the advantages of using improved values. Nevertheless, the rapid improvement in our knowledge of the size, shape, and mass of the Earth, and of the mass of and distance to the Moon and Venus, which has been derived from satellites and probes, as well as from modern radar observations, has been so significant that the following report was approved by the International Astronomical Union in 1964.

Report of the Working Group on the System of Astronomical Constants: Agenda and Draft Reports

International Astronomical Union, Twelfth General Assembly
25 August–3 September 1964

INTRODUCTION

THE PRINCIPAL RECOMMENDATIONS of this report on the system of astronomical constants are in accordance with the resolutions passed at IAU Symposium No. 21 (Paris, May 1963). We first of all give a reference list of the constants of the system and a set of explanatory notes. (See Appendix B.) We have used the term "primary constant," rather than "fundamental constant," since the latter has a connotation in astronomical usage that is inappropriate to the manner of selection of the primary constants. In choosing the values for the primary constants we have, perhaps, adopted a conservative view of the likely errors of their determinations, but even so the new system should be of adequate accuracy for astronomical studies for many years. Limits within which the true values are believed to lie are indicated in a later section, in which we also give expressions for differential corrections to the derived constants. Finally we discuss the manner in which this system should be introduced into the national and international ephemerides.

We regret that owing to severe illness Professor A. Danjon has been unable to share in the preparation of this report; Dr. J. Kovalevsky has, however, been co-opted to the Group in his stead.

NOTES ON THE CONSTANTS

1. The value given for the number of ephemeris seconds in the tropical year at 1900 is taken from the definition of the ephemeris second that was adopted by the Comité International des Poids et Mesures (*Procès Verbaux des Séances*, deuxième série, 25, 77, 1957). It is, in fact, derived from the coefficient of T, measured in Julian centuries of 36525 days, in Newcomb's expression for the geometric mean longitude of the Sun referred to the mean equinox of date. In the list "1900" refers to the

fundamental epoch of ephemeris time, namely 1900 January 0 at 12^h E.T., or to 1900.0, as appropriate; the values for constants 20–23 also refer to the fundamental epoch. Throughout the list and this report the term "second" must be understood to mean the "ephemeris second."

2. The value of the Gaussian gravitational constant (k) is that adopted by the IAU in 1938, and serves to define the astronomical unit of length (a.u.) since the corresponding (astronomical) units of mass and time are already defined. (The unit of mass is that of the Sun and the unit of time is the ephemeris day of 86400 ephemeris seconds. The units of k are: $(\text{a.u.})^{\frac{3}{2}}$ $(\text{ephemeris day})^{-1}$ $(\text{Sun's mass})^{-\frac{1}{2}}$). To simplify the later equations an auxiliary constant k', defined as $k/86400$, is introduced and a rounded value is given in the list.

3. The value for the measure of the a.u. in metres is a rounded value of recent radar determinations.

4. The value for the velocity of light is that recommended by the International Union of Pure and Applied Physics in September 1963.

5. The term "equatorial radius for Earth" refers to the equatorial radius of an ellipsoid of revolution that approximates to the geoid. (See also note 16.)

6. The term "dynamical form-factor for Earth" refers to the coefficient of the second harmonic in the expression for the Earth's gravitational potential as adopted by IAU Commission 7 in 1961. (See also note 16.)

7. The geocentric gravitational constant (GE) is appropriate for use for geocentric orbits when the units of length and time are the metre and the second; E denotes the mass of the Earth including its atmosphere. Kepler's third law for a body of mass M moving in an unperturbed elliptic orbit around the Earth may be written

$$GE(1+M/E)=n^2a^3$$

where n is the sidereal mean motion in radians per second and a is the mean distance in metres. The value of GE is based on gravity measurements and observations of satellites.

8. Again the mass of Earth includes the mass of the atmosphere. The reciprocal of 81·30 is 0·0123001.

9. The value for the sidereal mean motion of the Moon is consistent with the value of the tropical mean motion used in the improved lunar ephemeris, less the general precession in longitude.

10–12. The values of the principal constants defining the relative positions and motions of the equator and ecliptic are those in current use. Secular terms and derived quantities are already tabulated elsewhere.

13. The rounded value $8''\!\cdot\!794$ for the solar parallax should be used except where extra figures are required to ensure numerical consistency.

14. The value of the light-time for unit distance is numerically equal to the number of light-seconds in 1 a.u. Its reciprocal is equal to the velocity of light in a.u. per second.

15. Apart from the factor F_1 the constant of aberration is equal to the ratio of the speed of a hypothetical planet of negligible mass moving in a circular orbit of unit radius to the velocity of light; it is conventionally expressed in seconds of arc by multiplying by the number of seconds of arc in one radian. The factor F_1 is the ratio of the mean speed of the Earth to the speed of the hypothetical planet and is given by

$$F_1 = \frac{n_\odot}{k'} \frac{a_\odot}{(1-e^2)^{\frac{1}{2}}}$$

where $n_\odot$ is the sidereal mean motion of the Sun in radians per second, $a_\odot$ is the perturbed mean distance of the Sun in a.u., and e is the mean eccentricity of the Earth's orbit. Newcomb's values for $n_\odot$, $a_\odot$ and e are of ample accuracy for this purpose. The factor F_1 and the constant of aberration take the following values

	F_1	κ''
1800	1.0001427	20.49583
1900	1.0001420	20.49582
2000	1.0001413	20.49581

The rounded value 20″·496 should be used except where the extra figures are required to ensure numerical consistency.

16. The condition that the reference ellipsoid of revolution for the Earth shall be an equipotential surface implies that three parameters are sufficient to define its geometrical form and external gravitational field, provided that the angular velocity (ω) of the Earth and the relative mass of the atmosphere (μ_a) are assumed to be known. The variability of the rate of rotation of the Earth can be ignored, and the mass of the atmosphere is only just significant; the required values are:

$$\omega = 0{\cdot}000072\,921 \text{ radians per second; } \mu_a = 0{\cdot}000001$$

The expressions for the flattening (f) and the apparent gravity at the equator (g_e) in terms of the primary constants are, to second order:

$$f = \tfrac{3}{2} J_2 + \tfrac{1}{2} m + \tfrac{9}{8} J_2^2 + \tfrac{15}{28} J_2 \, m - \tfrac{39}{56} m^2$$

$$g_e = (GE/a_e^2) \, (1 - \mu_a + \tfrac{3}{2} J_2 - m + \tfrac{27}{8} J_2^2 - \tfrac{6}{7} J_2 m + \tfrac{47}{56} m^2)$$

where $m = a_e\omega^2/g_e$, is obtained by successive approximations. The new values of these constants are not intended for geodetic use.

17. The heliocentric gravitational constant corresponds to GE, but is

appropriate for heliocentric orbits when the units are the metre and the second.

18–19. The derived values of the masses of the Earth and of the Earth +Moon differ from those currently in use, but will not supersede them completely until the system of planetary masses is revised as a whole. (See note 24.)

20. The perturbed mean distance of the Moon is the semi-major axis of Hill's variational orbit, and differs from that calculated from Kepler's law by the factor F_2, which depends on the well-determined ratio of the mean motions of the Sun and Moon. (E. W. Brown, Mem. R.A.S., 53, 89, 1897.)

21. The constant of sine parallax for the Moon is conventionally expressed in seconds of arc by multiplying by the number of seconds of arc in one radian. The corresponding value of $\pi_{\text{☾}}$ itself is 3422″·608.

22. The constant of the lunar inequality is defined by the expression given and is conventionally expressed in seconds of arc.

23. The constant of the parallactic inequality is defined by the expression given; the coefficient F_3 is consistent with the corresponding quantities in Brown's Tables.

24. The system of planetary masses is that adopted in the current ephemerides and the values given for the reciprocals of the masses include the contributions from atmospheres and satellites. The value for Neptune is that adopted in the numerical integration of the motions of the outer planets; the value used in Newcomb's theories of the inner planets is 19700. In planetary theory the adopted ratio of the mass of the Earth to the mass of the Moon is 81·45 (compared with 81·53 in the lunar theory), and the ratio of the mass of the Sun to the mass of the Earth alone is 333432. This system of masses should be revised within the next few years when improved values for the inner planets are available from determinations based on space-probes.

CORRECTION FACTORS AND LIMITS

To first order, relative errors of the derived constants are given by:

$$\frac{\Delta\pi_{\odot}}{\pi_{\odot}}=\frac{\Delta a_e}{a_e}-\frac{\Delta A}{A} \qquad \frac{\Delta\tau_A}{\tau_A}=\frac{\Delta A}{A}-\frac{\Delta c}{c}$$

$$\frac{\Delta\kappa}{\kappa}=\frac{\Delta A}{A}-\frac{\Delta c}{c}=\frac{\Delta\tau_A}{\tau_A} \qquad \frac{\Delta f}{f}=\frac{\Delta J_2}{J_2}$$

$$\frac{\Delta(GS)}{GS}=\frac{3\Delta A}{A} \qquad \frac{\Delta(S/E)}{S/E}=-\frac{\Delta(GE)}{GE}+\frac{3\Delta A}{A}$$

$$\frac{\Delta\{S/E(1+\mu)\}}{S/E(1+\mu)}=\frac{3\Delta A}{A}-\frac{\Delta(GE)}{GE}-\frac{\Delta\mu}{1+\mu}$$

$$\frac{\Delta a_{\mathfrak{C}}}{a_{\mathfrak{C}}}=\frac{1}{3}\frac{\Delta(GE)}{GE}-\frac{2}{3}\frac{\Delta n_{\mathfrak{C}}^*}{n_{\mathfrak{C}}^*}+\frac{1}{3}\frac{\Delta\mu}{(1+\mu)}$$

$$\frac{\Delta \sin \pi_{\mathfrak{C}}}{\sin \pi_{\mathfrak{C}}}=\frac{\Delta a_e}{a_e}-\frac{\Delta a_{\mathfrak{C}}}{a_{\mathfrak{C}}}$$

$$\frac{\Delta L}{L}=\frac{\Delta\mu}{\mu(1+\mu)}+\frac{\Delta a_{\mathfrak{C}}}{a_{\mathfrak{C}}}-\frac{\Delta A}{A}$$

$$\frac{\Delta P_{\mathfrak{C}}}{P_{\mathfrak{C}}}=-\frac{2\Delta\mu}{1-\mu^2}+\frac{\Delta a_{\mathfrak{C}}}{a_{\mathfrak{C}}}-\frac{\Delta A}{A}$$

The true values of the primary constants are believed to lie between the following limits

A: 149597 to 149601×10^6 m

c: 299792 to 299793×10^3 ms^{-1}

a_e: 6378080 to 6378240 m

J_2: 0·0010824 to 0·0010829

GE: 398600 to 398606×10^9 $\text{m}^3\,\text{s}^{-2}$

μ^{-1}: 81·29 to 81·31

$n^*_{\mathfrak{C}}$: correct to number of places given

p: 5026″40 to 5026″90

ϵ: 23°27′08″16 to ... 08″36

N: 9″200 to 9″210

Correspondingly the limits for the derived constants are:

$\pi_{\odot}$: 8″79388 to 8″79434

τ_A: 499ˢ001 to 499ˢ016

κ: 20″4954 to 20″4960

GS: 132710 to 132721 $\times 10^{15}$ $\text{m}^3\,\text{s}^{-2}$

S/E: 332935 to 332968

$S/E(1+\mu)$: 328890 to 328922

f^{-1}: 298·33 to 298·20

$a_{\mathfrak{C}}$: 384399 to 384401×10^3 m

$\sin \pi_{\mathfrak{C}}$: 3422″397 to 3422″502

L: 6″4390 to 6″4408

$P_{\mathfrak{C}}$: 124″984 to 124″989

IMPLEMENTATION OF THE REPORT

We regard it as essential that the new system should be introduced into the national and international ephemerides as soon as possible after its adoption. Accordingly we are requesting the directors of the principal ephemeris offices to study the consequences of the introduction of the new system so that a firm timetable can be drawn up at the meetings of Commission 4 in Hamburg. We provisionally suggest that the new system be introduced into the almanacs for the year 1968; for the Sun, Moon and planets we suggest that differential corrections to the ephemerides based on the current system be tabulated until such time as new or revised theories have been completed.

We intend to meet again at the beginning of the 1964 Assembly so that we may consider any fresh observational evidence or theoretical arguments that may have been brought to our attention since our meeting in January 1964. We will then confirm or amend as necessary the list of constants given above, and this final list will be our recommendation for the "IAU System of Astronomical Constants." We therefore request that the Executive Committee submit the following draft resolution for consideration by Commissions 4, 7, 8, 19, 20 and 31, with a view to its adoption by the General Assembly:

The International Astronomical Union endorses the final list of constants prepared by the Working Group on the System of Astronomical Constants and recommends that it be used in the national and international astronomical ephemerides at the earliest practicable date.

ACKNOWLEDGMENTS

The Working Group wishes to acknowledge the assistance given to the group by those persons who have responded to our request in a circular letter dated 30th August 1963 for comments and results relevant to the system of astronomical constants proposed by the Paris Symposium.

The Group is also grateful to the Astronomer Royal for his hospitality and for providing facilities for the meeting of the Group at the Royal Greenwich Observatory, Herstmonceux Castle, on 8–10 January 1964.

W. Fricke (*Chairman*)
D. Brouwer
J. Kovalevsky
A. A. Mikhailov
G. A. Wilkins (*Secretary*)

Part 5

Determination of Relative Locations of Various Areas of the Earth

Traditionally, geodesy has been concerned primarily with mapping. An understanding of the terrestrial gravity field has also been of interest, but largely because of the necessity of understanding the gravity field in order to interpret observations of astronomic or geodetic positioning. That satellite geodesy has reversed this emphasis is due primarily to the relative ease of interpreting satellite orbits in terms of the terrestrial gravity field.

Satellites also provide excellent targets for geodetic triangulation either through simultaneous observations or through the use of predicted orbits to connect observations separated by short periods of time. Both methods require accurate timing, good coordination between observing sites and, to avoid systematic errors, comparable or identical equipment at each site to be connected. Good calibration procedures are also important and for orbit interpolation an accurate knowledge of the satellite motion between observation times is needed. For these reasons, work in this area is just starting.

The use of Baker-Nunn observations to improve station locations is reported in the paper by Izsak included earlier. The Echo satellites have been very easy to observe because of their brightness. The U.S. Coast and Geodetic Survey has used observations of these satellites for triangulation on the North American continent and as a planning tool for a worldwide network. For the latter, a much higher satellite will be needed, however. The following papers include a report on the use of preliminary observations of Echo I by French geodesists to tie France and North Africa to the same reference system, a report on the observation of a flashing light satellite for geodetic triangulation, and the results of a test of the SECOR electronic ranging system for such interconnections. The SECOR system has the added advantage of providing scale as well.

The following paper is excerpted from a translation of La Jonction Géodésique France Afrique du Nord par Photographies Synchrones du Satellite Echo I. *Symposium de Géodésie par Satellites. Institut Géographique National, 2° Direction—Géodésie, Group d'Etudes Spatiales, December 1964.*

N66 37353

Geodetic Junction of France and North Africa by Synchronized Photographs Taken From Echo I Satellite

H. M. DUFOUR
Institut Géographique National

I. GENERAL PRINCIPLES OF TRIANGULATION BY SATELLITE

THE BASIC PRINCIPLE is quite simple: a luminous object is seen against a different background of stars from different points on the Earth. Photography of this luminous object, together with photography of the stars which surround it, gives information which permits determining the position of points on the Earth's surface, other points presumably being known.

To refine this idea: the solid Earth, considered nondeformable, to which we attach a trihedron TXYZ, has a known motion on the stellar sphere as a function of time, a motion given by positional astronomy; knowing the time means fixing the trihedron in the stellar field; each star thus constitutes an absolute direction in the trihedron TXYZ; a direction given by the stellar ephemerides.

In a similar fashion, we must fix the luminous object, which, practically speaking, requires making synchronous (or quasi-synchronous) observations from the different points on the globe which we want to tie together.

The luminous object can emit flashes of light, thus automatically assuring simultaneity, or it may be continuously luminous, making it necessary to create "artificial flashes" by using synchronously revolving shutters at the various observation stations.

Anna was such a flashing satellite: it has been useful for geodetic experiments. It was more costly than a continuously luminous satellite, it worked only on command, and it is no longer working.

Echo I and Echo II are continuously luminous satellites and Echo I was chosen for the France-North Africa junction.

Practically speaking, photography involves:

—A certain number of star photographs to calculate the orientation of the camera.

—A certain number of light flashes. In the case of the French observations, the shutters turned at the rate of 60 revolutions per minute, producing 60 luminous points per minute, which we call "flashes."

Essentially the problem is to interpolate the position of the flashes among the known star positions; let us mention immediately that the 60 flashes are reduced to 1 central flash, and that the direction for this central flash is obtained in the trihedron TXYZ.

Thus each photograph gives a known direction SF, S being the station and F the fixed point. We shall see how the geodetic problem is treated for the France-North Africa junction, starting from this fundamental principle.

Several results are necessary for precision:

If an angular precision of 1 second of arc (that is, 1/200 000 of a radian) is desired for SF, we must have

—A 1-millisecond precision tolerance for the revolving shutter;

—Accuracy of sidereal time to one-twentieth of a second;

—Accuracy within 2 or 3 microns for the determination of the positions of the stars and of the flashes on the photographic plate (for a focal length of 30 centimeters).

II. INSTRUMENTS

The apparatus includes, essentially

—A camera of 30-centimeter focal length, furnished with a revolving shutter and with a leaf shutter.

—A quartz chronometer, to regulate the shutter at the rate of one rps, for photography of the satellite; and to release the leaf shutter for the star photographs.

The entire apparatus is extremely simple and highly portable.

Notation of time is done

—For the satellite, by direct reading on the revolving shutter scale: each second blip of the time signal illuminates the frame of the shutter, always at the same point, which permits the observer to take a correct reading (to almost 1 millisecond).

—For the stars: according to the same principle—on a revolving graduated disk incorporated into the quartz chronometer.

III. THE FRANCE-NORTH AFRICA GEODETIC TIE (MAY 1964)

Under the auspices of the National Center for Space Studies (CNES), the National Geographic Institute was charged with effecting the France-

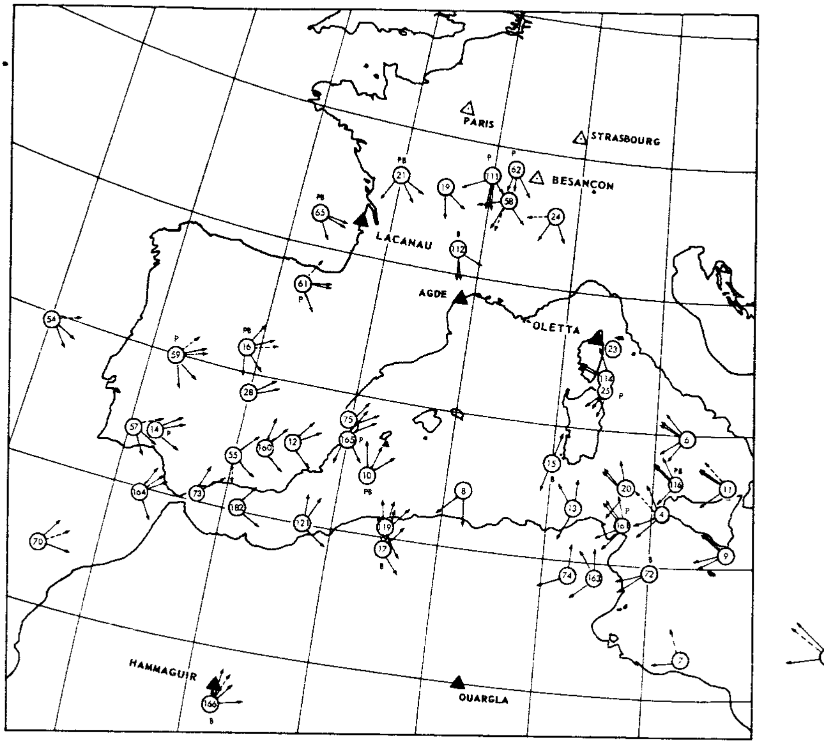

Figure 1.—Geodetic junction, France–North Africa, by Echo I, May 1964. Points of the sky photographed, with an indication of successful stations. ——→ successful photograph. - - - → possibly usable photograph. The direction of the arrow identifies the station. P: Paris Observatory; B: Besancon Observatory.

North Africa tie by means of synchronous photographic observations of the Echo I satellite. (See fig. 1.)

Known points:
- Lacanau (near Bordeaux, on the Atlantic)
- Agde (near Sète, on the Mediterranean)
- Oletta (Corsica)

Points to be determined:
- Hammaguir (West Sahara)
- Ouargla (East Sahara)

Actually, the five points are already known in the European Compensation system (called European Compensation 1950), and the work consists of comparing classical geodetic transfer with transfer by space geodesy.

Satellites Used

The only observations retained are those made of Echo I, which, by reason of its culmination at around 47.5°, is well suited to observation from the Mediterranean area.

The observations took place from the 4th to the 26th of May 1964. It was sometimes possible to obtain four useful passes in one evening.

Echo II was similarly observed beginning May 20, but no observations have been retained. Echo II could have at most only one useful passage.

Geodetic Configuration

In the final calculations, all the observations of absolute directions will be replaced by observational relations, which will permit definition of the unknown points (with their table of errors); but for the observations themselves, it is necessary to define a general line of work which assures *a priori* a satisfactory overall configuration.

One may reason as follows:

First Point of View

The central meridian of the observation zone has a longitude of about 2° East; the central parallel is at 38° latitude. The most important points for the tie are the points of the satellite's trajectory, on the mean parallel, to the West and to the East of the central meridian, respectively (the eastern point is in the zenith in the south of Italy, the western points are in the zenith in Spain). These points are determined by intersection from the three French bases. Their intersection determines the African points. Considering the diagram, it becomes apparent that this latter intersection is a good one, the first one not being as desirable, since the French points constitute a rather narrow base.

Second Point of View

The set of directions defined with reference to the stars determine a certain number of planes: these planes, combined, define the lines joining the points on the ground.

Examining the diagram, one realizes that all the lines are thus well defined, except the line Ouargla-Hammaguir, as it was difficult to have African points outside the shadow cone. Here again, one notes that the African points are defined by an intersection starting from a French base which is rather narrow.

Forecast of the Passages

For each passage of the satellite, the aiming point on the satellite's trajectory is, in practice, imposed; the coordinator of the work chooses this point on the basis of various elements.

—First of all, is the necessity for a generally well formed geometric figure, as we have noted.
—Observation time suitable for star photography: from this point of view, the stations at high latitudes are very unsuitable in summer.
—It is also necessary that the satellite leave the shadow cone soon enough that the observers are not surprised (in practice, the time of the satellite's arrival often cannot be predicted to better than about 5 minutes).

Theoretically, it should be possible to take into account previous successful evenings of observation, but practically, this is hardly possible; in fact, the general coordinator establishes a plan and follows it more or less rigidly.

For the predictions, the Echo I ephemerides furnished by the Smithsonian Astrophysical Observatory in Massachusetts are used.

Upon reception of an ephemeris, the passages are numbered, the ephemeris is extrapolated for about 15 days, and the points of passage are chosen (that is, the points in the sky at which the ballistic cameras will have to be aimed). An electronic program then furnishes a statement indicating for each station all the elements of the observations.

In practice, between the elements of the extrapolated ephemeris and the values from the following ephemeris, we currently encounter differences on the order of 10 minutes in time and 2° to 3° in longitude. These differences, although disagreeable, are acceptable for the observations. They underscore the fact that Echo I, being very light, is extremely sensitive to radiation pressure.

Field Operations

The task of taking the pictures requires only two operators, but in practice it is a good idea to provide a team of three, since, during the usable time period, photographs are taken every 2 hours during the night, every night. It is desirable under these conditions to provide one night's rest every three nights for each operator.

The picture-taking operation includes the following phases:
—Placement of the camera in the station 2 hours before the observation, and starting the chronometer
—Loading a plate in the camera
—Setting the chronometer, by time signals
—Photography of the stars (first exposure)
—Starting the shutter disk; regulation by time signals
—Photography of the satellite, at the rate of one exposure per second, except for the 60th-second blip of each minute, which is eliminated by a disk manipulated by an operator[1]

[1]The operator hears the time signals and places the disk in front of the objective when he hears the long signal of the full minute.

—Stopping the disk: photography of the stars (second exposure)
—Photography of the synchronizing marks at the base of the camera
—Replacing the plate
—Setting up the camera for the next observation

Operations also include:
—Development of the plate
—Recording the following information: direction of the satellite's passage, notation of the minutes . . . direction of diurnal movement.

The important elements of field operations are essentially
—The stability of the apparatus during the interval of time which separates the two photographs of the stars; this interval is presently 15 minutes, and will be reduced to less than 10 minutes.
—Recording the time on the revolving shutter, which must be done with an accuracy within 1 millisecond.

Success of the Observations

About 60 positions of the satellite were selected in advance to be photographed (each comprising 60 points). Here is the tabulation of successful photographs:

Hammaguir: 15	Ouargla: 40
Oletta: 40	Agde: 35
Lacanau: 25	

Naturally, every point photographed simultaneously by at least two stations is usable. Theoretically, the probability of one position in five successful negatives is:

$$\frac{15}{60}\times\frac{40}{60}\times\frac{40}{60}\times\frac{35}{60}\times\frac{25}{60}\cong\frac{1}{37}$$

(In fact, there were only two entirely successful points out of 60.)

IV. PROCESSING THE PLATES—CALCULATIONS

We cannot go into the complete details of this last phase of the work here. We only indicate the fundamental subdivisions, which involve the following operations:

(A) Calculations of the theoretical coordinates of the stars on the plates
(B) Measurement of the plates with a comparator
(C) Calculations of the formulas giving the direction cosines of the flashes in the terrestrial Cartesian system
(D) Intersection of the flashes from the approximate coordinates of the stations
(E) Calculations of the unknown coordinates of the stations from the known coordinates.

The characteristics of these various operations are given in the following pages. All the calculations were made on the CAB 500 of the Geographic Institute.

Other Calculations

In addition, the coordinates of the tie points in the terrestrial Cartesian system were carefully established by means of classical geodesy.

Planar coordinates, the geographic coordinates ($\lambda\phi$) for North Africa in the European Compensation system, are available; their accuracy is close to 10 meters.

Altitudes, the altitudes H of the different points above the International Ellipsoid, are calculated by integration of the deviations of the vertical at the astronomic points.

First calculation: French network

Second calculation: Southern France, Italy, Spain, North Africa

The French network is dense enough to make the results worthy of confidence. The second network is made up of points rather distant from each other. After cross-checking, it may be estimated that 1-decameter precision is preserved here as well.

The calculation is carried out by astronomic leveling, establishing the relations by observations between each point and its nearest neighboring points. We assume that each difference of level has an error independent of the others and proportional to the distance; these hypotheses are not absolutely rigorous. It is proposed to include calculations statistically more valuable, which are presently being undertaken.

The approximate coordinates of the stations (calculations D and E) are furnished by the terrestrial Cartesian coordinates, derived from the coordinates ($\lambda\phi H$), calculated on the International Ellipsoid.

(A) *Calculation of theoretical coordinates of the stars on the plates*

Ecliptic coordinates 1950; $X_E Y_E Z_E$

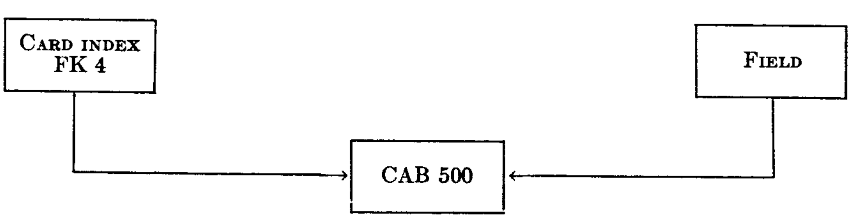

Selection of stars:

Calculation of XYZ ecliptic coordinates of the camera for 1950

Rejection of stars by studying the scalar product:

$$XX_E+YY_E+ZZ_E$$

Reduction of the selected stars to (p, q, r) direction cosines in the terrestrial Cartesian system

Transformation into the local horizontal system:

$$\begin{pmatrix} x_h \\ y_h \\ z_h \end{pmatrix} = R_1 \begin{pmatrix} p \\ q \\ r \end{pmatrix}$$

Refraction

Transformation into the plate system:

$$\begin{pmatrix} x_c \\ y_c \\ -f \end{pmatrix} = R_2 \begin{pmatrix} x_h \\ y_h \\ z_h \end{pmatrix}$$

(f = focal distance)

OUTPUT

TAPE → OPERATION C

PRINTED FORM → OPERATION B

DZ:	zenith distance
AZ:	azimuth
UT:	universal time for the stars
UT:	universal time for the flashes
P:	pressure } Refraction
T:	temperature } Refraction

(B) *Measurement of the plates with the comparator*

The measurement of a plate requires, in practice, a day's work for two operators. It must be done very carefully.

The operators use the approximate coordinates $(x_c y_c)$, given by calculation A, to position the plate under the comparator.

Then they note the elements of the plate in the following order:

—Synchronizing marks at the bottom of the camera —Stars —Flashes	Operator 1, operator 2 acting as secretary
—Flashes —Stars —Synchronizing marks at the bottom of the camera	Operator 2, operator 1 acting as secretary

The use of two operators has the following advantages:

- —Systematic observational errors show up in the course of the work itself; sometimes it is possible to correct these on the spot
- —The secretary figures the averages in the course of the work; therefore, any error is immediately corrected
- —The operators keep each other company (a rather boring task) and they can rest their eyes 50 percent of the time

Following the comparator measurements, the flashes are *smoothed;* instead of 60 flashes in the minute chosen, only 5 flashes are kept, corresponding to seconds 10, 20, 30, 40, and 50. The smoothing is based on the hypothesis that the x and y coordinates on the plate are represented by polynomials of the fourth degree as a function of time.

(C) *Processing the plates*

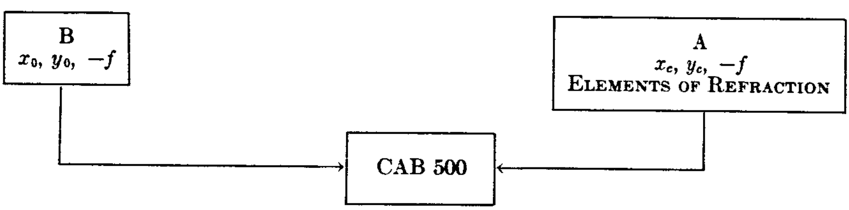

Use of the stars: $x_0 y_0 \ -f$:

Correction of radial distortion

Examination of the homographic formula, in least squares

$$\begin{pmatrix} x_0 \\ y_0 \\ -f \end{pmatrix} \longrightarrow \begin{pmatrix} x_c \\ y_c \\ -f \end{pmatrix}$$

Application to the flashes:

Correction of distortion

Application of the homographic formula

$$\longrightarrow (x_c y_c - f)$$

Return to terrestrial Cartesian system:

$$\begin{pmatrix} p \\ q \\ r \end{pmatrix} = R_1{}^* R_2{}^* \begin{pmatrix} x_c \\ y_c \\ -f \end{pmatrix}$$

Complementary corrections:

Time of propagation of the radio signals

Correction to reduce the position to the even second

Correction of position on the plate

Printing of a tape:

p
q of the flashes and elements P, T
r for refraction

(D) *Intersection.* Several simultaneous plates give a series:

Plate 1 — $C_1 \begin{pmatrix} p \\ q \\ r \end{pmatrix} \begin{matrix} P \\ T \end{matrix}$ → CAB 500

Plate 2 — C_2 → CAB 500

Plate 3 — C_3 → CAB 500

First least squares calculation, without weighting, and without correction for refraction
⟶Approximate coordinates of the flashes.
Second calculation, with weighting, and with correction for refraction
⟶Coordinates $X_F Y_F Z_F$, the most coherent as a function of the coordinates of the stations.

Printing of a tape
↓
Operation E

(E) *Geodetic calculation*

Regrouping of the series: each plate itself gives two observational relations in a general system of least squares.

For these relations, the smoothed values of the central flash is used.*

For each plate:

Approximate coordinates of the central flash orientation (p q r) of the central flash P and T for calculation of refraction Direction of the sun	Approximate coordinates of the stations Connections between the stations

→ CAB 500 ←

*In a more elaborate program, 10 relations will be written corresponding to the 5 smoothed directions (seconds 10, 20, 30, 40, 50) with their table of variances.

For each flash:

Refraction correction
Phase correction
Establishment of the observational relation
Normalization
Elimination of the flash coordinates

Summation of the equations:

(1) resulting from a priori connections between the station points (known points, known distances, etc.)
(2) resulting from the normal equations, after elimination of the flashes
Table N of weights of the coordinates
Table N^{-1} of the variance. Calculation of mean quadratic error of a direction

Coordinates of the stations

V. RESULTS OBTAINED AND PLANNED IMPROVEMENTS

In a general way, the Geographic Institute has been occupied with the production of highly transportable equipment, and with effective experience; we hope in the future to perfect the various operations progressively, according to the successive problems which increased precision poses.

At present, we expect from the France-North Africa experience a theoretical angular precision of 1/100 000 of a degree (that is, two arc-seconds) which corresponds, in gross fashion, to a precision of 20 m between the extreme geodetic points. It is not yet possible to say anything definitive about the practical results, the first of which are just beginning to appear (operation D).[2]

We hope in the future to increase the precision of the measurements as follows:

—Regulation of the entire picture-taking operation by a quartz chronometer; currently, this clock assures regular rotation of the shutter disk, but not its time setting, which is done directly from the time signals. In the future, the chronometer will also set this time, being regulated itself, by different time signals, before and after photography of the satellite and of the stars. This latter operation may thus be cut down to *less than 10 minutes*.

[2] The sightings of series 6 (longitude 13° E, latitude 40°) intersect with a radial uncertainty of 10 m, an excellent result if one considers that the mean distances are 2000 km.

—To use thick photographic plates (6 mm), rigorously flattened.

—To use fast emulsions, in order to increase the number of stars recorded in one session.

—To take two exposures of the stars before and two exposures afterward.

—To place two cameras in parallel in each station systematically: this procedure improves the precision of the directions in the ratio $\sqrt{2}$ and permits the easy disclosure of any discrepancy.

—To air-condition, at least partially, the picture-taking apparatus and the quartz clock.

N66 37354

The following paper is excerpted from Measurements of the Doppler Shift in Satellite Transmissions and Their Use in Geometrical Geodesy. *Presented at the European Symposium on Satellite Geodesy, Paris, December 1964.*

Geometric Geodesy by Use of Doppler Data

ROBERT R. NEWTON
Applied Physics Laboratory
Johns Hopkins University

IT SHOULD NOW BE POINTED OUT that only two of the coordinates of a station can be obtained accurately from the data obtained during one pass. In order to obtain all three coordinates, it is necessary to use data from at least two passes.

By far the dominant error made in a set of station coordinates derived in this way, with our present state of knowledge of the earth's gravity field, is in the position of the satellite. This satellite position error shows up one-for-one in station coordinates. Typical errors in satellite position currently run about 75 meters, which is an unacceptable level for geometrical geodesy.

However, suppose that two stations observe the satellite at about the same time and that each one derives a set of station coordinates. Since the satellite is nearly in the same position as used by both observers, the errors in satellite position almost cancel out and the differences in the station coordinates derived in this way should be quite accurate. The most accurate case of this use of station coordinates to obtain geometric information is that in which both stations are exactly in the same location. This was the case with the information that we showed in the preceding section where we found that relative position could be found from a single pass with an accuracy of a few meters.

As the distance between the stations increases, the accuracy of the geometrical position decreases for at least two reasons. First, neglected refraction effects, which cancelled exactly when the stations were together, will no longer exactly cancel. This error is probably small compared with the fact that the two observers do not use the satellite at the same times and hence the errors in satellite position are not exactly the same for the two observers. Analysis indicates that the error in relative position obtained this way should increase about as the square root of the distance between the stations.

The method of simply extracting station coordinates is equivalent to using data from one station to correct the position of the satellite and using this corrected satellite position to give the position of the other station. The computed satellite orbit, of course, will contain velocity errors as well as position errors and it is these velocity errors which cause the relative station position error to increase with the distance between the stations. The accuracy of relative information can therefore be increased if data from three or more stations at about the same time are used. In effect, what we can do then is to use information from two of the stations to correct both position and velocity errors in the satellite orbit and thus improve the accuracy of the third station relative to the other two. In practice, of course, one would probably treat the data from all three stations simultaneously, varying the orbit and the station coordinates until the best fit to all the data is found. The differences in station coordinates would then represent accurately the lengths of the chords joining the three stations.

Analysis of doppler data by this method has been carried out by Anderle and Oesterwinter (Ref. 5) using data from six TRANET stations within the continental United States. The comparison of the set of chord lengths derived in this way and that derived from ground survey is shown in figure 1, based upon data from about thirty passes. The

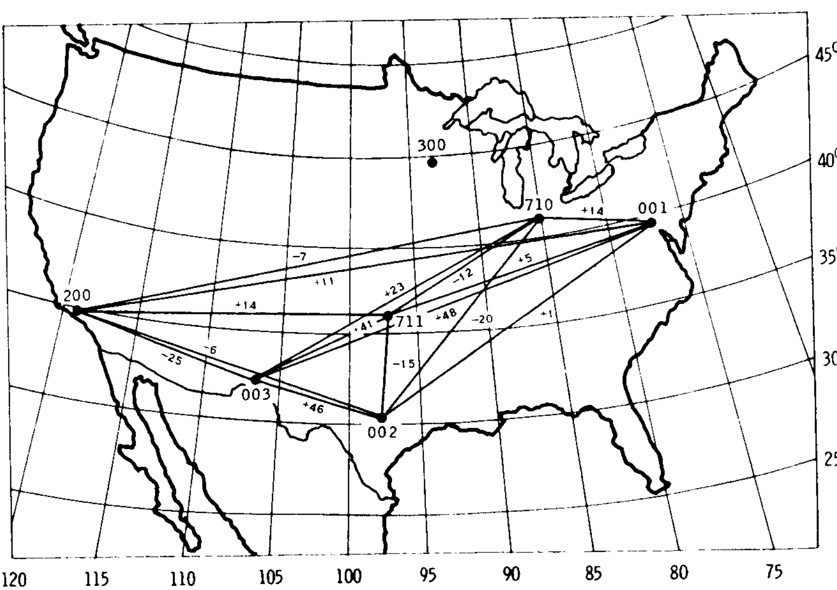

Figure 1.—Comparison of chord lengths derived from ground survey and from doppler observations.

number accompanying each chord in this figure is the discrepancy in meters between the two values of chord length. Figure 1 is copied from reference 1 with the permission of the authors.

Results of at least equivalent accuracy should be obtained using the integral doppler receiver, since studies of the TRANET stations show that they have about the same instrumental errors.

Except for the chords that terminate at Station 003 in New Mexico, no discrepancy exceeds 20 meters, and most are considerably less. The comparatively large errors involving Station 003 caused the location of that station to be investigated again. It has been found that the station antenna was moved several times, in order to improve signal reception, without notification being sent to the analysis center. At the present time, we are trying to trace the time history of the antenna location to see if Station 003 results can be made consistent with other results.

We have considerable confidence in the accuracy of the satellite results because of an incident connected with Station 710. The original results for this station showed an east-west discrepancy of about 30 meters. This discrepancy was traced to a card-punch error of exactly 1″ in the longitude of the station. The results shown in figure 1 were obtained after correcting this card-punch error.

In summary, the relative horizontal position of two stations within a few hundred kilometers of each other can be obtained, using the doppler data from a single pass, with a standard deviation of about 10 or 15 meters. By the use of more passes, all three coordinates of the relative position can be determined, and with a higher accuracy. Across the dimensions of a continent, using four or more observing stations, relative positions can be obtained in all three dimensions with a confidence level of about 10 meters, using a modest number of passes.

REFERENCE

1. Anderle, R. J.; and C. Oesterwinter: "A Preliminary Potential for the Earth From Doppler Observations on Satellites," U.S. Naval Weapons Laboratory, May 1963.

On October 31, 1962, the Department of Defense launched the first satellite designed primarily for geodesy. This permitted the testing of several optical and electronic techniques for precise geodetic satellite tracking. The following papers describe the satellite design and describe the results ofobservations of the flashing light which this satellite carried. Observations of the doppler frequency measurements are included in the results of doppler tracking reported earlier.

N66 37355

The following paper is a chapter from The Use of Artificial Satellites for Geodesy, *G. Veis, ed., North-Holland Publishing Co. (Amsterdam), 1963, pp. 255–260.*

Project ANNA

MARK M. MACOMBER
Bureau of Naval Weapons, Department of the Navy
Department of Defense, Washington, D.C., U.S.A.

PROJECT ANNA IS A UNITED STATES geodetic satellite program. The name ANNA is an acronym for Army, Navy, NASA (the National Aeronautics and Space Administration), and Air Force, the agencies that originally collaborated on formulating the program or that were expected to participate actively in the observation program. When the geodetic satellite program was first proposed, the Department of Defense feared that the output of the program, in addition to being of a scientific nature, might be of critical military significance. The program was therefore temporarily classified, and as a result, NASA participation did not materialize. Recently a review of the program and its expected results has been made, and the classification has been removed, opening the program to participation by NASA and, through them, by the world-wide scientific community.

The belief that the scientific community should participate in ANNA was so firm to the people who formulated the program that in mid-1960 a provision was made to allocate 50% of the available light-flashes from the optical beacon to a scientific program administered by NASA.

The first ANNA satellite is scheduled to be launched into a near-circular orbit inclined 50° to the equator, with an altitude of one megameter. At present, only two launches are authorized, the second being scheduled as a backup to the first in order to ensure a successful orbit and to provide a sufficiently extended period of observation to produce significant data.

The satellite contains three basic types of instrumentation that will be used for obtaining positioning information. For range determination, a transponder in the satellite is coupled with ground instrumentation that makes a phase comparison between a modulating frequency as transmitted to and as returned from the satellite. Three frequencies in the vhf-uhf bands are used: one for transmission to the satellite, and two coherent frequencies for transmission from the satellite to ground. Analysis of the difference in phase shift on the two returning frequencies permits a correction to be made for refraction effects. To resolve any ambiguities in distance measurements, four different modulating frequencies are employed. The satellite transponder receiver is energized at all times, but the transmitters are turned off except when the satellite is being interrogated. Power limitations within the satellite restrict interrogation to six or seven passes per 24 hours; the satellite is thus adequate for use by only one complex of ground stations. In an attempt to keep the satellite instrumentation as simple as possible, the ground stations are tied together by a VLF timing net, and transmit in bursts such that the signals from the various ground stations are received at the satellite sequentially. The highly complex ground instrumentation necessary to accomplish the interrogation and measurement functions, coupled with the limitation on power available for the transponder, make this system unavailable to the scientific community.

For optical determination of satellite topocentric direction, a high-intensity optical beacon is used; when activated, it produces a series of five light-flashes spaced 5.6 seconds apart. The main advantage of the optical beacon is that when it is flashed, an infinite number of observers within the circle of visibility can observe the light with relatively simple equipment, making this system of maximum benefit to the scientific community. One drawback of the optical system is that the power consumption of the beacon is very large, limiting the number of flash sequences per day to about 20 or less, depending on the exposure of the satellite to sunlight to recharge the battery. Because of this power limitation, light flashes cannot be programmed for everyone who might desire to participate in the program, but must be programmed to provide the maximum return in geodetic knowledge. The result is that certain observers will not be able to use the light when most convenient for them, although they will be able to observe it at other times even though the geometry of position solutions will not be optimum.

Range rate information is obtained by observing the doppler shift of ultra-stable transmissions of the satellite. Four frequencies will be broadcast continuously for this purpose. The pair of frequencies designed for geodetic measurements will be 162 and 324 Mc, with another pair, 54 and 216 Mc, reserved for refraction studies and for a possible backup in case of failure of the prime tracking frequencies. All four of the frequencies are coherent, so tracking could be accomplished using any two. Since transmitters are of low power drain, they can be left on continuously, and thus be available to observers throughout the world. The ground instrumentation for receiving the signals and counting the doppler shift imparted to the signal is complex and may be a deterrent to observations by the scientific community.

The temperature-controlled crystals that drive the ultra-stable transmitters are also used to run a satellite-borne clock. Approximately every 90 seconds, time signals are broadcast from the satellite as phase modulation on two of the doppler signals. By keeping track of the frequency drift of the crystals, as obtained by the doppler tracking stations, it is possible to correct the time of transmission of these signals to better than 0.5 millisecond. Since the same clock that provides these timing signals also initiates the flash sequences for the optical beacon, the doppler and optical observations are tied together in time.

The small satellite memory consists of 22 sixteen-bit words. Injected into it are the two's complement of the identification of the 5.6-second timing pulse that should initiate each light-flash sequence. Every 5.6-second timing pulse generated by the satellite clock is added to each of the first 21 words, and when each word overflows a light-flash sequence is initiated.

The satellite is oriented with the earth's magnetic field so that the pole of the satellite visible from earth is a function of the geomagnetic latitude of the satellite. Two beacons face the north pole of the satellite, and two face the south pole. Only 15 bits of the 16 in each word in the memory are used for light-flash timing. The 16th bit has injected into it an indication of whether the north or south lights should be flashed. The 22nd word of the memory will not initiate flash sequences, but is used for telemetry purposes to indicate whether or not the lights did flash as planned.

In addition to the geodetic systems instrumentation, the satellite contains various minor experiments that test the environment and the attitude of the satellite.

During the first three months after launch, an intensive calibration program will be undertaken, wherein the three types of measurements will be compared among themselves, and with terrestrial survey results. This calibration program is considered of prime importance to prove that no biases exist in any of the instrumentation used or in the methods of data handling that are utilized. If any biases do exist, they must be eliminated or corrected before any geodetic program can be undertaken on a world-wide scale. Upon successful completion of the calibration phase, a world-wide geodetic observation program will be undertaken with the intent of refining our knowledge of the earth's gravitational field and of providing the location of tracking stations relative to the earth's center of mass.

Now that the entire program has been declassified, NASA can participate in the observation program, and can coordinate the participation of foreign and domestic scientific interests. Neither details of observation equipment to be used, nor a modus operandi has yet been crystallized, but the following plans for participation are under active consideration:

1. use of the Smithsonian Astrophysical Observatory optical network;
2. use of the MOTS (Minitrack Optical Tracking System) cameras located at most of the NASA minitrack stations;
3. use of minitrack interferometry information;
4. use of the NASA-Jet Propulsion Laboratory radar systems for space probes;
5. voluntary participation of interested observatories.

Because of the power limitation for the optical beacon, only selected observatories that would add strength to the present planned deployment of tracking equipment can be considered for use in this program as far as special programming of the light is concerned. This does not in any way limit participation by all observatories within the area of visibility of each flash sequence, but it does mean that certain observatories will not derive the benefit of optimum geometry. All contact with civilian observers will be through the NASA. Details of this observation program will be promulgated to all interested persons as soon as they are made firm.

At the present time, two satellites have been fabricated. They have completed comprehensive tests, performing perfectly all the while. These two satellites are currently undergoing extensive checkout after the shipment and are being fitted out to the launch vehicle.

The activity collecting data will reduce and preprocess the data to eliminate any spurious data points, if the facilities are available. Since many independent observers will be unable to carry out this function, provisions must be made to handle reduction of data and elimination of spurious points at some central activity. Data will then be processed to produce a unique reference frame within the earth, to determine the earth's gravitational field, and to provide geocentric locations of tracking stations.

The two planned launches, which together assure essentially one orbit of sufficient lifetime, are of course insufficient to meet the needs of any geodetic program. Some planning has taken place on the variety of orbits that would be of value to any program of this sort, and that are feasible from existing launch sites with existing boosters in the moderate price field.

The following paper is excerpted from The Use of a Flashing Light Satellite for Datum Interconnection. *Presented at the DIA Conference, Washington, D.C., October 28–30, 1964.*

Results From Satellite (ANNA) Geodesy Experiments

OWEN W. WILLIAMS, PAUL H. DISHONG, AND GEORGE HADGIGEORGE
Terrestrial Sciences Laboratory
Air Force Cambridge Research Laboratories

INTRODUCTION

ON 31 OCTOBER 1962 with the launch of the Satellite ANNA 1–B into a nearly circular orbit of approximately 600 nautical miles, a new era in the sciences of photogrammetry and geodesy was started (ref. 1). This geodetic satellite (designed for six months' operation) continues to be reproductive some 24 months later. The name ANNA reflects its four United States sponsors, the Air Force, Navy, NASA and the Army. The Army was responsible for the electronic ranging system known as SECOR; the Navy was responsible for the electronic doppler system and integration of the satellite payload; the Air Force was to develop the flashing light system; and NASA was to assist in the optical observational program. This paper will cover only those aspects contributing to the optical phases of the active ANNA program.

In January 1963, after more than two months of excellent performance, a defective capacitor bank caused a malfunction in the optical system. The output of the light system was reduced to about 25% to 30% of its original value and this condition remained in effect into July. Therefore, between January and July only a limited program of flash transmissions transpired and while usable camera data was still received it was for the most part not up to original expectations.

Prior to the capacitor problem in the satellite, geodetic stellar cameras obtained an excellent series of photographs. The image diameter of the flash recorded on 103–F emulsion averaged 70 microns on the PC–1000's and approximately 50 microns on the BC–4–300 plates. In mid-July 1963, the light output returned to normal and good data were again obtained. Because of normal solar cell deterioration, only 7 flash sequences a day can currently be programmed as opposed to the original 30 sequences.

Due to the condition of the main battery controlling the command system and the lack of doppler tracking data, the Applied Physics Laboratory, Johns Hopkins University, suggested to Air Force Cambridge Research Laboratories in October 1963 that we operate the flashing light by employing our alternate optical logic. The emergency over-ride system (EMOS) was developed to provide the necessary redundancy for the optical operations and this bit of foresight continues to pay dividends. The EMOS system consists of a World timing system accurate to one millisecond, a transmitter, a linear amplifier, and an antenna system.

DESCRIPTION OF BEACON

The ANNA optical beacon, developed for AFCRL by Edgerton, Germeshausen and Grier (EG&G), consists of two pairs of xenon filled stroboscopic lamps with reflectors, one pair on the north face of the solar cell panel and one pair on the south face (Figure 1). When either set

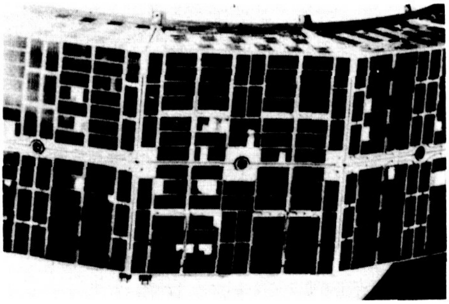

Figure 1.—A close view of one of the four strobe lights located on the ANNA geodetic satellite.

of lights is triggered by the satellite memory (no longer possible) or by EMOS, a series of 5 flashes is produced. An enlargement of a part of one of the first photographs of ANNA clearly demonstrates the above mentioned spacing (Fig. 2).

LIGHT INTENSITY

The light intensity of the ANNA beacons is not constant over the light angle but varies as shown by a dotted line in Figure 3 while the solid line shows the intensity used to predict the image sizes for ANNA.

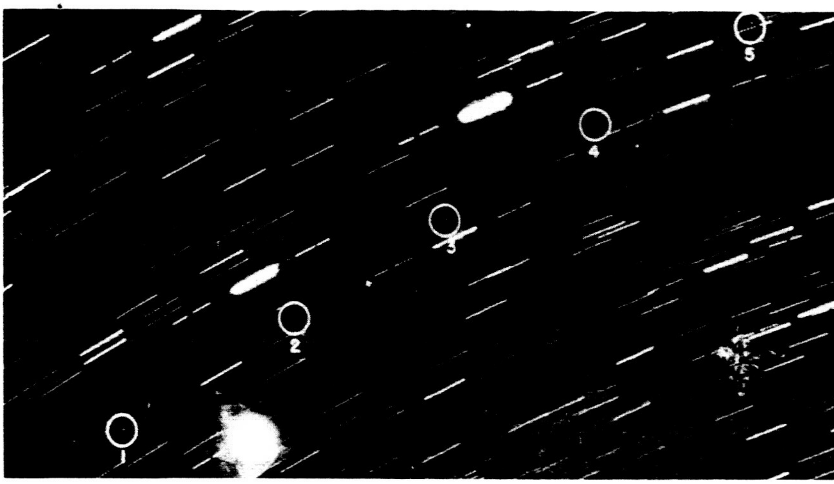

Figure 2.—ANNA 1–B strobe light images. Copy of photograph taken during test to check optical system developed by Air Force Cambridge Research Laboratories. Satellite photographed at 0350 hr e.s.t. as it crossed Boston area with BC–4, 300-mm FL camera. Images on plate.

VALIDITY OF EQUATIONS

During the development phase of ANNA, the image sizes on Air Force PC–1000 geodetic stellar camera plates were predicted for conditions of moderate haze. Currently, two groups, EG&G and Duane Brown Associates, Inc., have examined some of the ANNA PC–1000 plates to determine the validity of the equations.

Duane Brown Associates analyzed 88 images on 20 different plates taken from six different PC–1000 cameras (ref. 2). The plates were selected to be representative of different cameras, different locations, and a wide range of image diameters. The key results of the study are summarized in Table 1. Both groups obtained good agreement between computed and measured image sizes. There were four cases in which cameras 104 and 121 were employed in side-by-side operations. The mean image diameters from 104 turn out to be consistently and significantly larger than those from 121. This convincingly demonstrates that significant differences may exist in the capabilities of cameras of the same type.

On the whole, agreement between theory and observation is considered to be sufficiently good (13.4 micron mean error) for the theory to be used for purposes of general planning.

INTERVISIBLE OBSERVATIONS

Simultaneous photographic observations were made by ten Air Force PC–1000 cameras during the period September 1963 to January 1964.

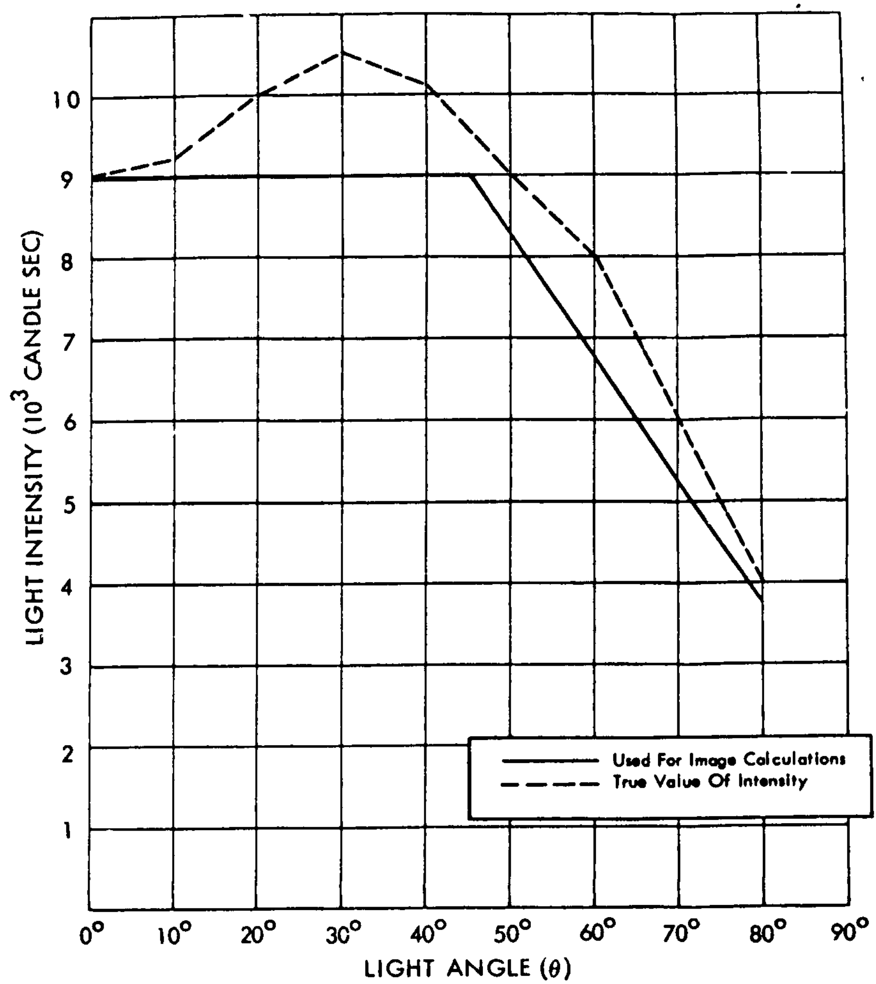

Figure 3.—**Light beam pattern.**

Geodetic position determinations using these ANNA 1–B observations indicate that the PC–1000 camera system used with the intervisible technique is capable of extending geodetic control to a proportional accuracy of better than 1/100,000.

Sixty observation nets were obtained in the Gulf Test. A net is defined as a flash sequence which was successfully photographed from three or more camera stations. Six nets were used to test the capabilities of the PC–1000 cameras. (See Table 2.)

The 1381st Geodetic Survey Squadron of APCS provided the coordinates of the camera sites which were tied to first order control of the North

Table 1.—*Summary of Key Results of Image Diameter*

[RMS difference = 13.4]

Plate No./(No. flashes)	Camera No.	Av. slant range (miles)	Av. zenith distance (degrees)	Slant range normalized to zenith (miles)	Computed image diameter (microns)	Average image diameter (microns)	Standard error of individual image diameter (microns)	Difference between observed and computed diameters (microns)
1 (4)	121	934	50.8	1006	55.8	43.2	6.6	12.6
2 (5)	104	934	50.8	1006	55.8	71.8	13.4	−16.0
3 (5)	121	921	49.1	986	56.7	62.9	11.8	−6.2
4 (5)	104	921	49.1	986	56.7	72.6	6.2	−15.9
5 (5)	110	873	46.0	925	60.0	47.8	6.2	+12.8
6 (5)	104	846	45.7	986	61.6	60.6	12.2	+1.0
7 (5)	104	831	42.7	876	63.0	77.4	11.8	−14.4
8 (4)	110	804	42.3	844	64.9	65.6	10.4	−0.7
9 (5)	121	802	38.8	836	65.4	58.0	8.4	+7.4
10 (5)	104	802	38.8	836	65.4	76.1	12.2	−10.7
11 (4)	121	776	35.8	804	67.6	51.7	10.6	+15.9
12 (3)	104	760	33.5	785	69.1	81.6	9.7	−12.5
13 (3)	108	759	31.3	781	69.3	58.0	10.8	+4.1
14 (4)		752	34.2	777	70.0	44.7	7.9	+25.3
15 (5)	101	720	25.6	736	72.9	67.3	6.3	+5.6
16 (5)	104	702	25.7	718	74.4	63.2	7.2	+11.2
17 (4)	107	690	21.5	703	75.7	56.8	6.3	+18.9
18 (4)	121	680	15.8	690	76.8	58.9	8.0	+17.9
19 (4)	104	680	15.8	690	76.8	95.0	16.0	−18.3
20 (4)	112	638	10.3	646	81.0	81.6	14.3	−0.6

Table 2.—*Station Observations (ANNA Satellite Altitude Approximately 1100 Km)*

Net No.	Date	Time GMT	Subsat Lat N°	Subsat Long W°	Flash mode	640	641	643	647	648	649	650M
8	1 Oct 63	0955	33	85	Memory	-------	x	x	x	x	-------	-------
19	22 Oct 63	0347	31	87	EMOS	x	-------	x	x	x	-------	-------
22	26 Oct 63	0306	26	88	EMOS	-------	x	x	x	x	-------	-------
28	19 Dec 63	0228	33	90	EMOS	x	-------	x	x	x	x	x
30	20 Dec 63	0149	31	88	EMOS	x	-------	-------	x	x	x	x
34	3 Jan 63	0601	28	92	EMOS	x	x	x	x	x	x	x

American Datum (NAD 1927). ACIC supplied the geoid-spheroid separations necessary to convert heights above mean sea level to heights above the reference spheroid.

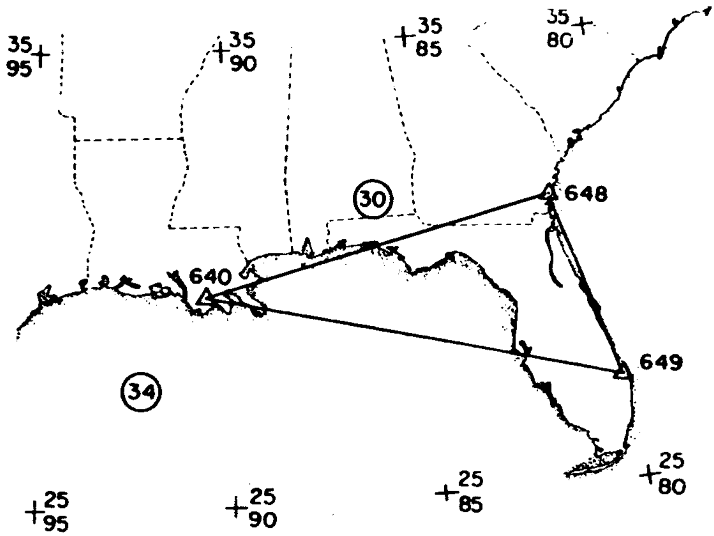

Figure 4.—The coordinates of station 640 are determined from those of stations 648 and 649 by nets 30 and 34.

Table 3.—*Geodetic Position Determination of Station 640 From Stations 648 and 649*

Reference stations 648 and 649 $\sigma_{N-S}=\sigma_{E-W}=\sigma_H=0$

Input standard deviations station 640 $\sigma_{N-S}=100$ m, $\sigma_{E-W}=100$ m, $\sigma_H=5$ m

Input error station 640 $\phi=+3''$; $\lambda=-4''$

Observations: All stations observed 5 flashes each on nets 30 and 34

Average observation σ used: 648, .″85; 649, 1.″08; 640, 1.″56

	ϕ	λ	H(meters)	R(meters)
North American Datum 27	29°33′44.″80	90°40′44.″19	7.0	
ANNA Data Reduction	44.″78	43.″93	7.6	
Δ	.″02	.″26	−.6	7.1
σ	.″11	.″25	4.8	8.7
$R=[(\Delta x)^2+(\Delta y)^2+(\Delta z)^2]^{1/2}$	Distance: 987 km			
$R_\sigma=[\sigma_x^2+\sigma_y^2+\sigma_z^2]^{1/2}$	Proportional Accuracy (NAD Standard) 1/140,000			

GULF TEST REDUCTION

The coordinates of station 640 (Table 3 and Figure 4) were determined from intervisible observations of 10 flashes in nets 30 and 34, using 648–649 as a baseline. The mean observation standard deviations were 0.″85 for station 648, 1.″08 for station 649, and 1.″56 for station 640.

Stations 648 and 649 were regarded as being perfectly known in location, whereas station 640 was given an input position error of +3″ in latitude and −4″ in longitude and standard deviations of 100 m in the North-South and East-West directions and 5 m in height above the spheroid. The sizeable station 640 position error was removed in the reduction with a resulting R; NAD–ANNA, of 7.1 m which corresponds to a proportional accuracy of 1/140,000.

The overall reduction considered Station 647 as unknown and six surrounding stations (640, 641, 643, 648, 649, and 650M) as references (Table 4 and Figure 5). Again, the reference stations were held fixed and the unknown station had horizontal standard deviations of 100 m

Table 4.—*Geodetic Position Determination of Station 647 From Stations 640, 641, 643, 648, 649 and 650M*

Reference stations 640, 641, 643, 648, 649 and 650M: $\sigma_{N-S}=\sigma_{E-W}=\sigma_H=0$

Input standard deviations stations 647: $\sigma_{N-S}=100$ m, $\sigma_{E-W}=100$ m, $\sigma_H=5$ m

Observations: (1) All stations observed 5 flashes on Net 34, (2) Stations 641, 643, 648 and 647 observed 3 flashes on Net 8 and 5 flashes on Net 22, (3) Stations 640, 643, 648 and 647 observed 4 flashes on Net 19, (4) Stations 640, 643, 648, 649 and 647 observed 2 flashes on Net 28, (5) Stations 640, 648, 649, 650M and 647 observed 5 flashes on Net 30.

Average observation σ used: 640, 2.″11; 641, 1.″01;
643, .″78; 648, .″81;
649, .″99; 650M, 1.″07;
647, .″90

	φ	λ	H(meters)	R(meters)
North American Datum 27	30°14′48.″28	88°04′42.″51	5.2	
ANNA Data Reduction	48.″16	42.″38	4.8	
	Δ .″12	.″13	.4	5.2
	σ .″03	.″03	2.8	3.2

$$R=[(\Delta x)^2+(\Delta y)^2+(\Delta z)^2]^{1/2}$$

$$R_\sigma=[\sigma_x^2+\sigma_y^2+\sigma_z^2]^{1/2}$$

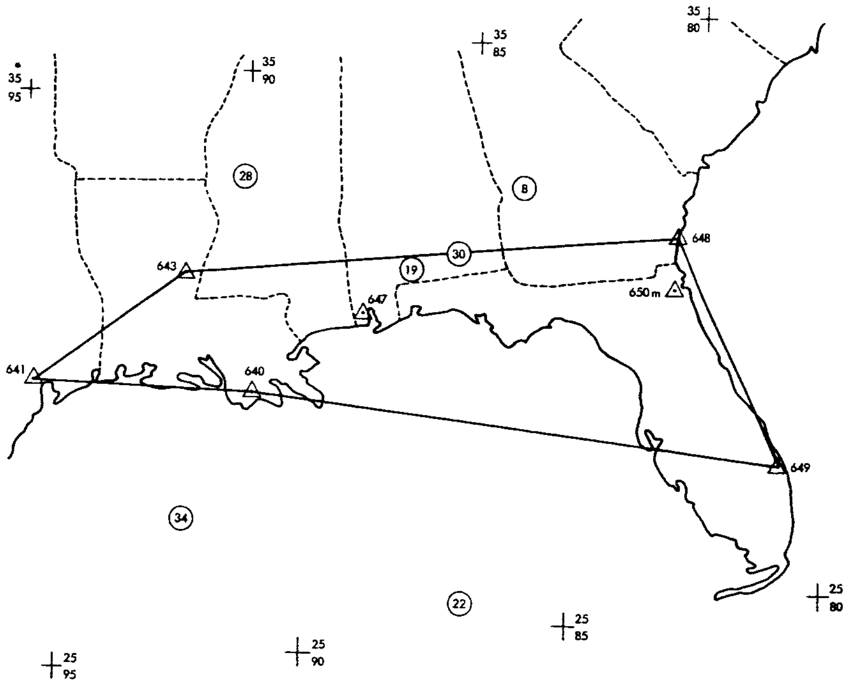

Figure 5.—Coordinates of station 647 are determined from those of stations 640, 641, 643, 648, 649, and 650M by nets 8, 19, 22, 28, 30, and 34.

and a vertical standard deviation of 5 m. The geometry is favorable for a strong determination of the coordinates of the unknown station. Mean observation sigmas were as follows: 2."11 for 640; 1."01 for 641; 0."78 for 643; 0."90 for 647; 0."81 for 648; 0."99 for 649; and 1."07 for 650M. The resulting R of the reduction was 5.2 m and the R_r was 3.2 m. Because of the geometry, proportional accuracy has no meaning in this case.

LONG LINE AZIMUTH TEST

Geodetic azimuths of 4 lines ranging from 264 km to 1365 km have been determined. These lines were from the Gulf Test Nets. The test lines involve first order off-set stations 640, 641, 643 and 648. The azimuths between the stations were computed by ACIC using Rudoe's method for normal section azimuths.

RESULTS

Table 5 shows the good agreements, ±1 second of arc, that can be obtained.

Back azimuths between 648–641, 648–643 and 648–640 compute to essentially the same degree of accuracy.

These results are encouraging considering that:

a. Distribution of observations relative to the baselines is mediocre at best, being nonuniformly distributed about the line between the stations.

b. The number of observations is very small.

PLANS

The remaining nets are now being analyzed. It is anticipated that all possible nets will eventually be combined in one overall reduction and published.

Table 5.—*ANNA-Determined Azimuths Compared to the Normal Section Computed Inverses*

	Forward azimuth	Line	Distance (m)
ANNA	75°11′36.7″		
Normal Section	75°11′37.5″	641–648	1,365,165
ΔA_z	0.8″		
ANNA	71°04′33.6″		
Normal Section	71°04′34.5″	640–648	950,628
ΔA_z	0.9″		
ANNA	83°01′09.1″		
Normal Section	83°01′10.1″	643–648	1,080,640
ΔA_z	1.0″		

CONCLUSION

The ANNA 1–B satellite is part of a research program, and it has proven the feasibility of using multi-angulation space surveying techniques to obtain geodetic data previously not obtainable with a sufficient degree of accuracy. The results of the Long Line Azimuth and the Gulf Test reductions demonstrate that the PC–1000 geodetic stellar camera system is operationally capable of extending geodetic control to a proportional accuracy of better than 1/100,000 when cameras in a network simultaneously observe a flashing satellite beacon.

REFERENCES

1. Williams, O. W.: "Geodetic Research in the Space Age," Conference of Commonwealth Survey Officers, Cambridge, England, July 1963.
2. Brown, D. C.: "An Investigation of Theoretical Vs. Observed Diameters of ANNA Images on PC–1000 Plates," AFCRL Rpt., 31 March 1964.

The following paper is excerpted from a report presented at the 10th International Congress of Photogrammetry, Lisbon, Portugal, September 1964.

SECOR for Satellite Geodesy

T. J. Hayes

Topography and Military Engineering Office
Chief of Engineers

THE SECOR CONCEPT

SECOR is an acronym formed from the method by which the system operates: *Se*quential *Co*llation of *R*ange. The system is essentially an electronic distance measuring system designed to make use of the intermediary space positions of artificial satellites for determining geodetic positions on earth. The application of the geodetic data that is collected is based on the trilateration principle whereby three or more ground stations are placed at surveyed geographical locations of known geodetic coordinates. These individual locations can be as much as 2300 miles apart, depending on the altitude of the satellite. A fourth station is placed at some geographic location for which the coordinates are desired. When the satellite appears above the radio horizon of the ground stations, each ground station sequentially ranges to the spaceborne satellite on a time-shared basis in exact synchronism as established by the station selected to be the master timekeeper.

The precise slant range between each of the four stations and the transponder in the satellite is determined from phase comparisons of modulations transmitted to and returned from the transponder on radiofrequency electromagnetic waves. Each station records its range data on magnetic tape simultaneously with signals from an electronic clock (accurately set by means of Bureau of Standards timing signals) which permits fixing the location of the satellite in space. Since several positions (at least three) of the satellite relative to the ground stations are then known, the position of the fourth station relative to the first three stations can be calculated. The recorded data are translated into a format suitable for use by an electronic computer located at the Army Map Service. Using basically a space resection computation from satellite position triangles, the computer calculates the desired geodetic coordinates independent of the satellite's orbital parameters. The accuracy of the calculations for the position location is enhanced by the vast data redundancy provided by the system. For a typical satellite pass of six minutes duration, for example, the total number of ranges measured by four ground stations is approximately 29,000. Because of considerations of geometry it is necessary to collect data during at least two satellite passes to determine the geodetic position of the unknown station. In practice, a larger number of passes are used to afford the best geometry.

The computational procedure is repeated until the required precision criteria are met. When the unknown station's geodetic coordinates are considered acceptable, this fourth station can then be designated as a station of known geographical location. This permits one of the other stations to leapfrog to another location whose position is desired. Thus, control will be extended by this progressive method.

EQUIPMENT COMPRISING THE SECOR SYSTEM

The new SECOR system has been developed by the Cubic Corporation under the guidance of the U.S. Army Engineers. The basic equipment for operation of the SECOR system consists of at least four identical ground stations and an earth-orbiting satellite carrying a SECOR transponder.

SECOR GROUND STATION COMPONENTS

The most complex part of the SECOR system is the ground station element. Each SECOR ground station consists of three air-transportable shelters: The Radio Frequency (RF) Shelter, the Data Handling (DH) Shelter, and a Storage Shelter. Each ground station also carries its own support equipment which includes test equipment, generators, air conditioners, ranging antenna, communications antenna, single side band communication equipment, and wheel adapters for each shelter. All shelters and equipment are ruggedized for extensive and varied field operations.

Major units in the RF Shelter include receivers, transmitters, power supplies, antenna control assembly, and intercommunications equipment. Although the antenna is normally mounted on the RF Shelter, it may be operated from a ground mount if required. After the satellite signal is acquired (usually from prediction data provided to each station ahead of time) the RF operator tracks the satellite by keeping the antenna pointed in the direction of maximum signal as shown by signal strength meters mounted on the antenna control panel.

The digitizing of the ranging and timing data is accomplished in the Data Handling (DH) Shelter. The major units in this shelter include the magnetic tape recorder, quick-look recorders, control console, timing assembly and master intercommunications. The data handling equipment controls the modulation and timing of the pulses transmitted by the RF equipment and converts the transponder replies into a form suitable for recording on magnetic tape. The quick-look recorders, by presenting a continuous visual plot on moving paper tape, provide the operator with a constant check of system operation during a pass.

The Storage Shelter contains radio equipment for communication with the other ground stations and with Field Headquarters. It also accommodates test equipment and working space for servicing electronic equipment.

Since the SECOR system is planned for use in a worldwide, leapfrogging operation to tie continents, geodetic datum, and islands into one geodetic control net, the ground-based components have been designed to be compatible with several modes of transport. SECOR ground stations may be air transported by aircraft and helicopter. The stations also can be carried over water by ship and landed by landing craft. Overland travel is easily effected by towing.

Each ground station and the satellite transponder comprise an electronic distance measuring unit which is largely automatic in operation. Distance measurements are made to the satellite-borne transponder by determining the round-trip phase shift of a series of modulated signals transmitted by the ground station and retransmitted by the transponder. The RF signal carrying the modulation frequencies is transmitted by the ground station to the satellite whose transponder demodulates these frequencies and retransmits the modulations on two offset carrier frequencies to the ground station. The shift in phase between outgoing and returned modulation signals is measured and then recorded on magnetic tape. By measuring the phase delay on several related modulation frequencies and augmenting these data with the time delay of a radar-like pulse, unambiguous measurements are obtained. The two offset carrier frequencies provide correction for ionospheric refraction, a problem common to all techniques using electronic magnetic waves.

SECOR SPACEBORNE COMPONENTS

The spaceborne portion of the SECOR system consists of a SECOR transponder which may be mounted in its own separable satellite or installed as an integral part of a larger satellite.

The SECOR transponder is composed of a receiver, transmitters, and power supply which converts the satellite battery voltage to the voltages required.

In operation, the transponder remains in a standby condition until activated by a select call signal generated by a SECOR ground station. Upon activation, the transponder receives and retransmits the ranging frequencies. This sequence is repeated for each ground station in turn, one complete cycle from the four ground stations occurring every 50 milliseconds. The same ranging and carrier frequencies are used by all four stations.

SECOR SATELLITE

To attain a flexible launch capability required to carry out an operational program, the U.S. Army Engineers developed a self-contained, separable SECOR satellite that could operate in its own orbit and would be of a size, shape and weight that would permit the satellite to ride as a hitchhiker on one of many available boosters. This resulted in the currently orbiting Type II SECOR satellite. It is 10 in. wide, 13 in. long, 9 in. high, and weighs about 40 pounds. In addition to the SECOR transponder, the satellite carries solar cells, batteries, a telemetry system, an antenna system, and a magnetic orientation device.

OPERATING MODES

Figure 1 illustrates the operation of the SECOR system in its two principal modes of operation: simultaneous and orbital. The simultaneous mode will be used except when geography forces the use of the orbital mode.

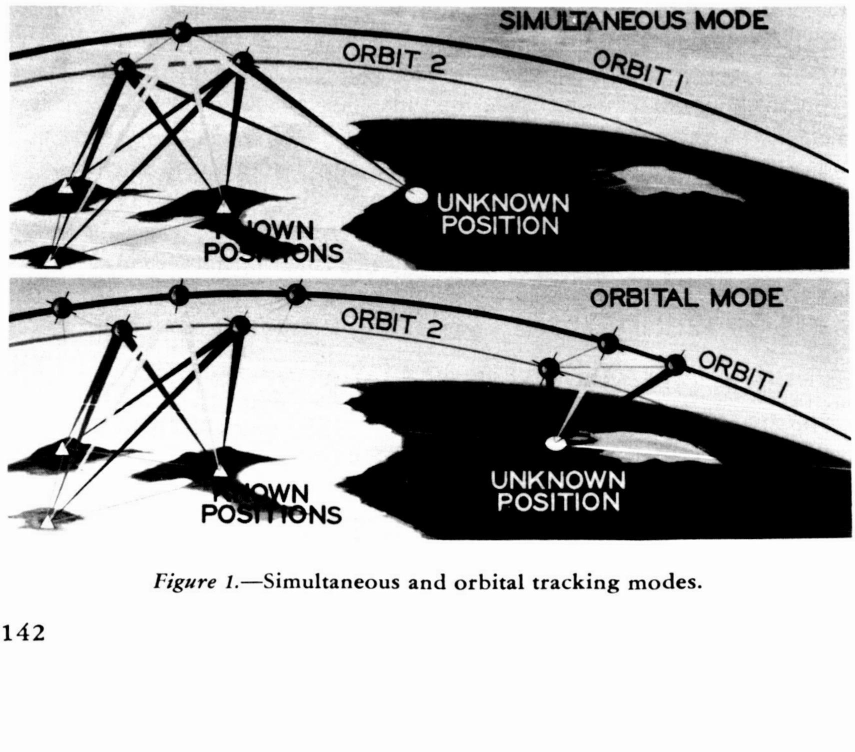

Figure 1.—Simultaneous and orbital tracking modes.

In the simultaneous mode, range measurements are made to the satellite in rapid sequence (essentially simultaneously) from each of four ground stations during the period when the satellite is above the radio horizon of the ground stations. Three of the ground stations are located at known geodetic positions, and the fourth ground station is positioned at a site where geodetic coordinates are desired. Range measurements obtained in the simultaneous mode permit the determination of the desired geodetic coordinates independent of the satellite's orbital parameters.

When the geographic locations are such that the satellite can be viewed simultaneously by the three known stations only, and the unknown station is able to view the satellite shortly before or after on the same pass, the orbital mode will be used. In this case an arc of two or more satellite orbits precisely determined by the three known stations will be extrapolated over the vicinity of the unknown station. Observed ranges from the unknown station to satellite positions on the extrapolated sections permit the desired geodetic coordinates to be established.

The line crossing mode is a special case of the simultaneous mode. Geography may force the spread of the stations in a less-than-optimum ground geometry with associated low-look angles and long distances. The simultaneous solution for the position of the unknown station in the above case may be strengthened by the direct determination of the geodetic length of the lines from the unknown station to the three known stations by incorporating line crossing techniques. The known stations accurately determine the height of the satellite at the time when the sum of the ranges from the unknown station to the satellite and from the satellite to a known station is a minimum. This provides an additional mathematical constraint on the geodetic solution.

TESTING THE SECOR SYSTEM

To insure that the SECOR system as developed would fulfill the requirements of this research and development task, tests were performed on the various units and subsystems which comprise the system, then upon the composite system as a whole. Essentially, these tests may be described as tests of the ground station equipment prior to satellite launch, tests on the satellite prior to launch, and system tests conducted both prior to and after launch.

To insure that the satellite would carry out the mission for which it was designed and developed, it was subjected to a full program of tests covering all the parameters and conditions considered important to system operation. The results indicated that the satellite would perform quite favorably within the anticipated launch and space environments.

The satellite tracking phase of this development was planned to evaluate the test data obtained in the different operating modes to enable a determination of SECOR system capabilities and thus to minimize the training, operating, maintenance, and data processing problems inevitably encountered after a new system goes operational. At the time that the satellite tracking plan was prepared it was envisioned that most of the simultaneous mode test data would be obtained on a small (500-mile) quad, with ground stations based at Stillwater, Oklahoma; Las Cruces, New Mexico; Austin, Texas; and (the unknown site) Fort Carson, Colorado, and that the orbital mode test data would be acquired utilizing the small quad plus the station located at East Grand Forks, Minnesota.

Orbital mode operations were conducted for a period of about three weeks on the small quad with the East Grand Forks station. The tracking data were obtained in such a manner that the data could be evaluated in both the simultaneous and orbital modes of operation. The results of simultaneous data reduction were used to check the results of orbital data reduction, clearly indicating where the orbital data reduction was erroneous. This comparison was necessary due to the unprecedented accuracy required in the projection of the satellite trajectory.

It is believed at this time that reduced accuracy in the orbital mode accrues from three primary sources; namely,

(1) Relatively small orbit fitting spans.
(2) System errors.
(3) Base site survey errors.
(4) Internal timing errors.

Small fitting spans allow any error in the data to upset the vector fitting and give less accuracy in the injection vector determination; the forward prediction then deteriorates rapidly. System and survey biases give a slight misorientation of the injection vectors and, therefore, affect the forward predictions also. Timing error arises from lack of exact synchronization of clocks at the ground stations, and any time offset will mean that the predicted satellite positions and the measured ranges will not be coincident. Time synchronization problems are not encountered when the Geodetic SECOR equipment is used in the simultaneous mode.

The station at Las Cruces, New Mexico, was then moved to Larson Air Force Base, Washington, to complete the large quad shown in Figure 2. The longer ranges and lower elevation angles to the satellite obtained on this quad provide the difficult operating conditions more typical of those likely to be met in operational usage. Data obtained in the simultaneous mode on this quad were also reduced and evaluated in the orbital and line crossing modes to compare the capabilities and limitations of each mode for given satellite/ground station geometries, etc.

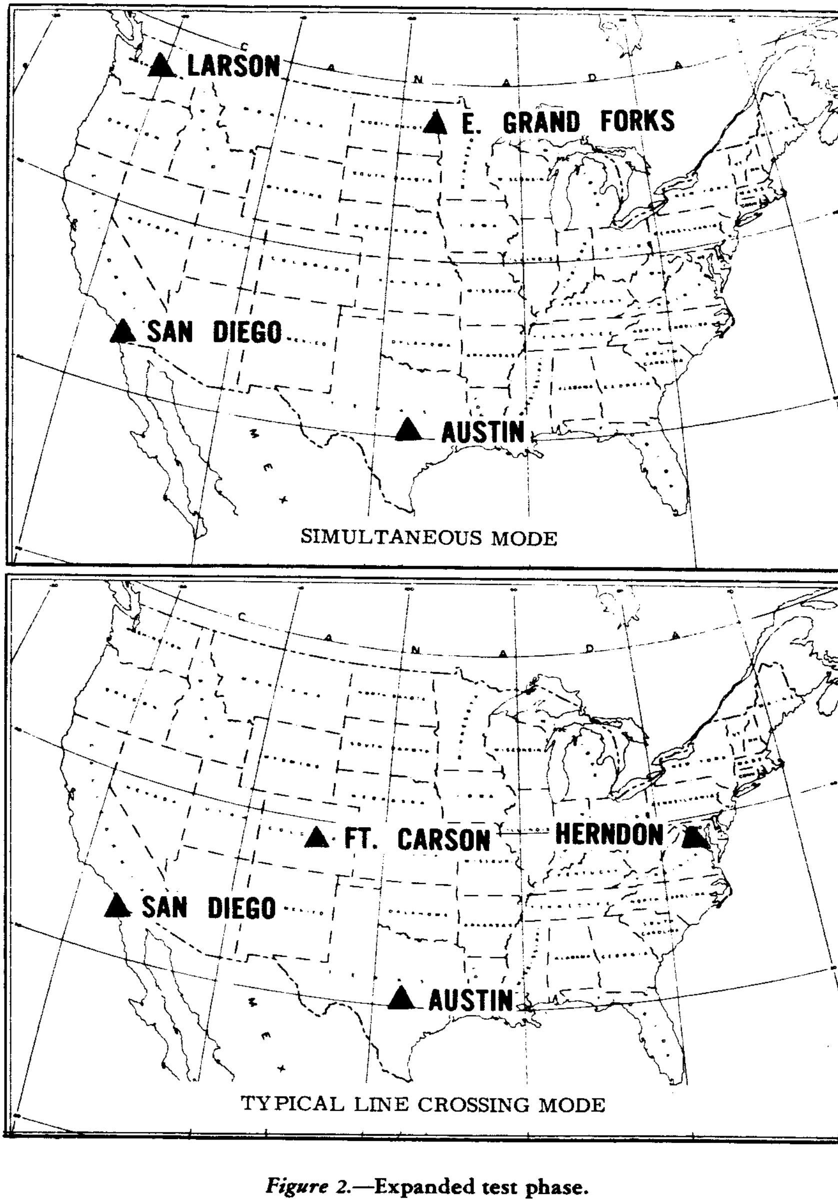

Figure 2.—**Expanded test phase.**

In the large quad data reduction, Larson Air Force Base, Washington, was the unknown station.

[Table 1 lists the majority of the unknown station solutions processed for the large quad. SECOR survey differences result from averaging a sequence of actual Geodetic SECOR solutions and subtracting the U.S. Coast and Geodetic Survey site coordinates from this average solution. The standard deviations shown per solution are computed from the residuals which are the differences between each SECOR-survey offset and the average of the offsets for one particular solution. RSS refers to "root sum square" and indicates composite bias and noise error. The RSS is computed by squaring the mean offset and the standard deviations, adding and taking the square root of the sum.]

Utilizing generally the same line crossing technique currently employed by systems such as HIRAN (but in this case employing the satellite as a super-elevated spaceborne station in place of the HIRAN airborne station), line crossings were initiated on a comparatively short line (1150 miles) between San Diego, California, and Stillwater, Oklahoma, for a period of about one week to resolve operational problems, determine the accuracy obtainable with the line crossing technique, and finalize the computer program. Geometry was selected to allow good satellite altitude determination by data obtained from three of the four stations on the small quad. Data from the line crossings then were used to determine satellite position and geodetic distances between San Diego and Stillwater.

Line crossing operations were then switched to a long line (2300 miles) between San Diego and Herndon, Virginia, for a period of about three weeks to determine the ultimate operational and accuracy limitations of the SECOR system for line crossing operations. Measurement errors from tropospheric refraction, ionospheric refraction, and multipath effects increase as elevation look angles are decreased. The data gathered should determine the accuracy of SECOR measurements at the long ranges obtainable when using satellites for line crossings.

Table 2 contains a summary of the line crossing solutions and comparisons computed from the satellite data. The results of the line crossing mode are commensurate with the theoretical results with the exception that all but 2 of 17 lines measured to the Herndon, Virginia, site are longer than the inverse lengths.

The line crossing solution in this experiment is made possible by the use of ground stations to track the satellite during the crossing. The line crossings processed here represent the longest lines ever measured and clearly demonstrate the potentiality of the technique.

A simulation study was performed by the contractor, Cubic Corporation, to aid in the evaluation of the different operational modes (simultaneous, orbital and line crossing). Effects of base site geometry, errors in site survey, tropospheric and ionospheric refraction, scale factor, and

Table 1.—*Geodetic SECOR Satellite Solutions*

[Larson AFB site solutions; (3-3 simultaneous mode); Large quad]

Solut. No.	Orbits used for solution	No. of indiv. compu.	SECOR-survey				Standard deviations				Comparisons		
			Lat, m	Long, m	Height, m	RSS, m	Lat, m	Long, m	Height, m	RSS, m	Total RSS, m	Theoretical (1) RSS, m	Theoretical (2) RSS, m
1	1305, 1319, 1167	50	−15.6	−19.1	−36.4	44.0	2.2	3.8	5.0	6.7	44.5	91.1	101.5
2	1305, 1333, 1167	55	−11.1	14.5	14.9	23.6	2.2	2.3	2.8	4.2	24.0	61.0	68.3
3	1305, 1305L, 1319L	86	−15.6	9.1	0.5	18.1	3.3	2.3	3.3	5.2	18.8	83.6	94.5
4	1305, 1319L, 1291L	81	−14.5	3.8	−2.2	15.2	3.3	3.0	2.4	5.1	16.0	64.8	73.5
5	1167L, 1291L, 1319L	81	−20.0	5.3	−5.7	21.5	4.4	2.3	4.0	6.4	22.4	64.3	73.1
6	1291L, 1167, 1319	50	−5.6	−9.1	−16.4	19.6	3.3	2.3	6.1	7.3	20.9	95.0	108.1
7	1269, 1269M, 1291L	81	3.3	14.5	40.0	42.7	4.4	3.0	3.8	6.5	43.2	84.7	96.4
8	1269M, 1269, 1305L	91	−11.1	38.1	45.2	60.1	2.2	3.8	4.8	6.5	60.5	84.0	93.8
9	1269, 1291L, 1167L	81	−22.2	22.9	28.1	42.5	4.4	1.5	3.9	6.1	42.9	59.0	67.0
10	1269, 1291L, 1305L	81	−31.1	25.9	23.7	46.9	3.3	2.3	3.4	5.3	47.2	69.0	79.5
	Mean		−14.4	10.6	9.2	33.4	3.3	2.7	4.0	6.0	34.0	75.7	85.6
	Standard deviation		8.9	15.7	24.3								

(1) Error model used: $\sigma_{Sys} = 9'$; $\sigma_{Tropo} = 5\%$; $\sigma_{Scale} = 1$ ppm; $\sigma_{Survey} = 4$ ppm; $\sigma_{Iono} = 5\%$.
(2) Error model used: $\sigma_{Sys} = 15'$; $\sigma_{Tropo} = 5\%$; $\sigma_{Scale} = 1$ ppm; $\sigma_{Survey} = 4$ ppm; $\sigma_{Iono} = 5\%$.

Table 2.—*Geodetic SECOR Satellite Line Crossing Solutions*

[Line crossing results based on international spheroid]

Orbit No.	Stations	SECOR, m	Survey, m	SECOR-survey, m	RMS noise, m	Observed RSS, m	Theoretical (1) RSS, m
463	Austin Ft. Carson	1,137,573.2	1,137,559.8	13.4	5.6	14.5	25.8
532	Austin Ft. Carson	1,137,573.0	1,137,559.8	13.2	65.0	66.3	25.8
648	Austin San Diego	1,860,074.3	1,860,051.9	22.4	9.0	24.1	15.0
648	Stillwater San Diego	1,862,470.1	1,862,456.7	13.4	3.2	13.8	15.0
670	Stillwater San Diego	1,862,473.4	1,762,456.7	16.7	15.4	22.7	15.0
808	Stillwater San Diego	1,862,449.4	1,862,456.7	−7.3	12.3	14.3	15.0
1131	Stillwater San Diego	1,862,457.0	1,862,456.7	0.3	2.0	2.0	15.0
896	San Diego Herndon	3,628,320.3	3,628,265.0	55.3	0.5	55.3	9.6
1401	San Diego Herndon	3,628,315.4	3,628,265.0	50.5	3.5	50.6	9.6

1241	San Diego Herndon	3,628,300.5	3,628,265.0	35.5	13.1	37.8	9.6
1365	San Diego Herndon	3,628,296.3	3,628,265.0	31.3	5.0	31.7	9.6
1365	Larson Herndon	3,494,039.5	3,493,993.6	45.9	3.5	46.0	10.3
1365	Ft. Carson Herndon	2,374,063.3	2,374,034.5	28.8	7.7	29.8	13.8
1305	Austin Larson	2,641,159.4	2,641,164.4	−6.0	2.7	6.6	11.4
1305	G. Forks Larson	1,675,760.3	1,675,745.8	14.5	26.3	30.0	18.6
1305	San Diego G. Forks	2.387,105.5	2,387,098.2	7.3	1.7	7.5	12.0
1269	San Diego G. Forks	2,387,105.0	2,387,098.2	6.8	7.3	10.0	12.0
Mean Standard deviation				20.1 18.0	10.8	27.2	14.3

(1) Error model used: $\sigma_{Sys}=9'$; $\sigma_{Tropo}=5\%$; $\sigma_{Scale}=1$ ppm; $\sigma_{Survey}=4$ ppm; $\sigma_{Iono}=5\%$.

equipment limitations have been considered with respect to their effect on solution accuracy. In the computer simulation, geometries were selected to correspond to the actual site locations used in satellite tracking tests.

LINE CROSSING ERROR ANALYSIS

The method employed to obtain geodetic line crossings from Geodetic SECOR ranging data is not directly analogous in computational technique or operational procedure to that performed with HIRAN or SHIRAN observational data. A distinctly different approach is necessary because the path of the satellite is not essentially concentric with the earth's surface. The occurrence of a minimum range sum derived simultaneously from two tracking sites will, therefore, not be coincident in time with the minimum geodetic line crossing. However, if the range

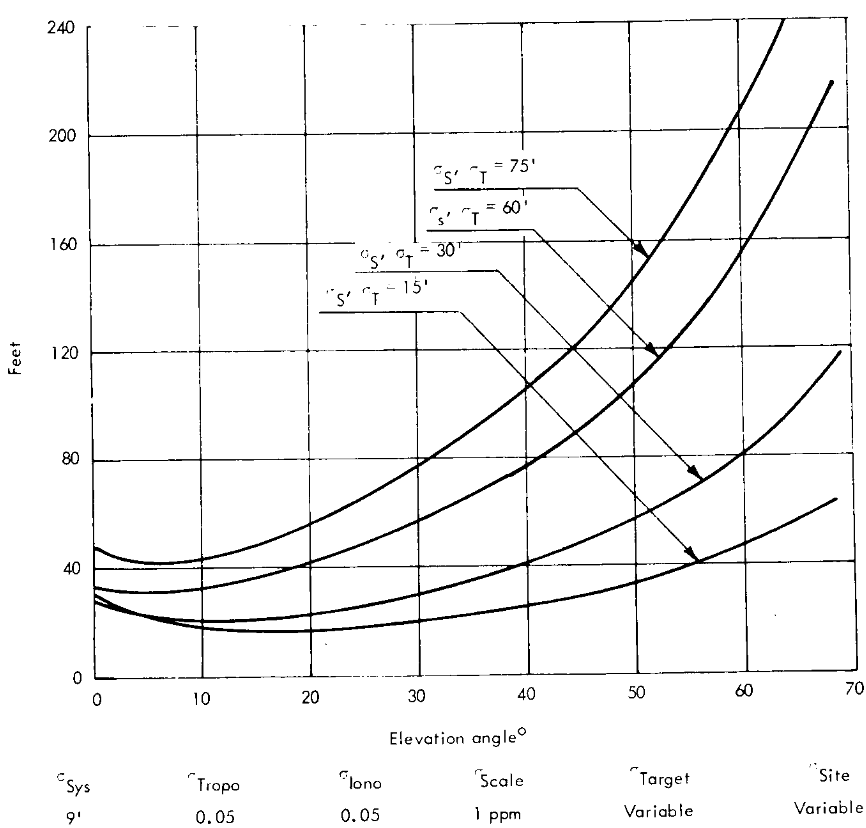

Figure 3.—**Geodetic distance error vs. elevation angle.**

observations are projected onto the earth's surface at each point along the satellite's orbit, then the sum of the geodetic distances from two sites to the subtrace of the satellite will have a minimum coincidently and approximately equal to the minimum distance between the two tracking sites.

In the modified version of the classic HIRAN-SHIRAN line crossing schemes, it is assumed that the heights above mean sea level of the end points of a line are known. It has also been assumed that the geocentric coordinates of the vehicle will be known too, either by direct solution from three simultaneously-tracking known base sites or by orbital predictions. The distance of the satellite from earth center is computed from the geocentric coordinates. With the station heights, satellite to earth center distance, and approximate knowledge of the geodetic coordinates of the end points of a line, the projections onto the reference spheroid of the range measurements to each site can be computed. The minimum geodetic distance is now computed from the composite set of adjacent projections.

In the error analysis for the geodetic satellite line crossing, the effects of three major factors on the geodetic distance computation are evaluated; namely,

(1) Ranging errors due to sources such as refraction, scaling, system, etc.

(2) Station height errors, which are errors in independent height-above-mean-sea-level measurements.

(3) Vehicle height errors, or errors in earth center to satellite distance.

Table 3.—*Relative Contribution of Error Sources to Geodetic Line Crossing Error*

Elevation angle	Total RSS	Vehicle height	Ranging	Station height
10°	18.3′	7.7′	16.3′	2.6′
20°	17.7	9.1	14.2	5.5
30°	19.8	11.3	13.8	8.6
40°	24.0	14.5	14.7	12.5
50°	30.8	19.0	16.6	17.6
60°	44.0	26.0	21.4	25.0
70°	64.0	40.5	29.3	40.0

Error Model

σ_{Sys}	σ_{Tropo}	σ_{Iono}	σ_{Scale}	σ_{Target}	σ_{Site}
9′	0.05	0.05	1 ppm	15′	15′

A set of geodetic distance versus elevation angle error curves were processed using a composite typical error model and different station and vehicle height errors. Figure 3 illustrates these error propagations. Table 3 shows the amount each major error source contributed to the total geodetic distance error for one case shown on Figure 3. A satellite height of approximately 500 NM was used in this propagation.

The line crossing analysis demonstrates that ranging accuracy controls the geodetic distance error propagation at low elevation angles. When elevation angles exceed 30°, station height and vehicle height errors predominate. In all cases, solutions should be constrained to lines with elevation angles less than 45°.

All errors propagated in this evaluation are carried as random and uncorrelated errors. The results are therefore conservative. In actual solutions, and in particular under the scheme used to compute the satellite geodetic line crossing, errors will be correlated and will give either equal or more accurate results.

CONCLUSION

The advent of artificial satellites has opened doors to technological advances that were only dreams less than a decade ago. In January 1964 a United States Army Corps of Engineers artificial satellite carrying a SECOR transponder successfully achieved orbit. This event made possible a series of tests of this new geodetic electronic ranging system. The tests, which were completed on 1 May 1964, clearly established that the SECOR system has the full capability of a first order geodetic tool.

Part 6

Summary and Conclusions

Summary and Conclusions

SATELLITE GEODESY is conveniently considered as divided into gravitational or dynamical geodesy and geometrical geodesy; in practice, of course, there is some overlap.

Dynamical geodesy comprises the study of the Earth's gravitational field through the use of satellites as *in situ* probes. The techniques employed are the traditional techniques of celestial mechanics modified and updated to apply to close-Earth satellites in the presence of a perturbing nonspherical Earth, the Moon, and the Sun, and particularly adapted to rapid calculation with modern high-speed electronic computers.

Starting with the determination of the improved value of the flattening of the Earth in 1958, this field has matured until, in the past 18 months, consistent values have been derived for a number of zonal and tesseral harmonics by several analysis techniques and from several types of data. The lower terms, which are best determined, are summarized in the following table for the zonal harmonics, and in the table of tesseral harmonics (Pt. 3, paper by Wagner). By contrast, only the flattening value was well established before the

Zonal Harmonics

	Kaula	*Kozai*	*Anderle*
J2	1082.20×10^{-6}	1082.63×10^{-6}	1082.65×10^{-6}
J3	−2.57	−2.56	−2.59
J4	−2.01	−1.63	−1.53
J5	−0.066	−0.185	−0.165
J6	+0.324	+0.593	+0.793
J7	−0.465	−0.376	−0.426

satellite era and, as was mentioned above, this proved to be significantly in error. Additional satellites in a variety of orbits will be needed before the dynamical analysis of the Earth's gravity field reaches the point of diminishing returns, and particularly before we understand major differences between terms derived by diverse methods. However, the quality of the data is already good enough to stimulate geophysical interpretations and attempts to correlate the satellite results with surface measurements.

Geometrical satellite geodesy, that is, the use of satellites as reference points for determining precisely the relative locations of various points on the surface of the Earth and particularly for interconnecting datums and placing all observing stations and all individual datums on a common Earth-centered reference system, is in its infancy. Analyses of the Baker-Nunn observations of various satellites by reflected light, simultaneous photographs of the Echo satellite from widely separated portions of the Earth, analyses of Doppler data by various TRANET stations and analyses of the ranging data obtained using the SECOR system have all indicated that we are on the verge of significant progress in the area of geometric geodesy, but it will probably be at least 5 years before such observations contribute in a major way to map-making. Not only will placing the entire world on the same coordinate system be useful to geographers and navigators but it will also aid in space-probe tracking and in geophysics. At present, observations from various stations in NASA's deep space net cannot be combined without introducing an additional error from the uncertainty in the relative coordinates of the various stations. World gravity observations also lose some of their value because of the difficulty in interconnecting observing sites accurately. The geodetic satellite program should signficantly improve this situation.

The launch of Geos in 1965 into an orbit specifically selected for dynamical geodesy should contribute appreciably to both geometrical and dynamical geodesy. Geos will carry a flashing light, a Doppler transmitter, two ranging systems, and corner reflectors for use with laser transmitters. The ranging systems and the laser reflections, if the latter prove to be a satisfactory operational system, should greatly improve the determination of scale—a major problem in geometrical geodesy. The launch of the Pageos satellite, an Echo-type balloon, in a 3000-km orbit will provide an excellent target for triangulation across intercontinental distances and can serve as a basis for a worldwide geodetic network. Finally, for a detailed understanding of the mass distribution in the outer regions of the Earth, the gravitational field derived from satellite observations must be combined with local measurements. An appreciable extension of ground-based gravity surveys will be needed for this purpose, an extension which undoubtedly lies outside of the field of satellite geodesy.

On a broader scale, both satellites and probes have given us better values of the various constants needed to compute ephemerides for astronomical bodies. The newly adopted values are given in appendix B. The selection and use of these values is discussed in Part 4. As the tracking of interplanetary probes improves and as lunar and then planetary orbiters become operational, our knowledge of the shapes, masses, and gravity fields of the Moon, Venus, and Mars should be well established. This will, in addition to providing information on the present structure of these bodies, provide important boundary conditions for theories of the origin of the solar system.

Appendix A

A Review of Geodetic Parameters

WILLIAM M. KAULA

The following paper was presented at the International Astronomical Union Symposium No. 21, "The System of Astronomical Constants," Paris, May 27–31, 1963.

A Review of Geodetic Parameters

WILLIAM M. KAULA
Goddard Space Flight Center, NASA

SUMMARY

IT IS RECOMMENDED that the parametric values which are currently most used in orbital computation be adopted as provisional standards, rather than those which may be the best available, because the "most used" values differ only slightly from the "best" values and further improvements in the values are expected within the next 4 years. Some of these values are:

$$GM_{\oplus} = 3.986032 \times 10^{20} \text{ cm}^3 \text{ sec}^{-2},$$
$$J_2 = 1082.30 \times 10^{-6},$$
$$J_3 = -2.3 \times 10^{-6},$$
$$J_4 = -1.8 \times 10^{-6},$$
$$a_e = 6{,}378{,}165.0 \text{ m}.$$

With parameters such as the foregoing the most serious geodetic errors affecting astronomy are tracking station positions. Standard methods of describing and transforming positions are suggested.

INTRODUCTION

This review recommends which geodetic parameters should be adopted as standard, the manner in which the parameters should be expressed, and the values which should be adopted. In making these recommendations, current practice, available determinations, and anticipated improvements will be considered.

GRAVITATIONAL PARAMETERS

For the notation of the earth potential, recommendations have already been made by Commission 7 on Celestial Mechanics, of the International Astronomical Union (Reference 1):

$$U = \frac{\mu}{r}\left[1 + \sum_{n=1}^{\infty} \sum_{m=0}^{n} \left(\frac{R}{r}\right)^n P_n^m (\sin \beta)\left(C_{n,m} \cos m\lambda + S_{n,m} \sin m\lambda\right)\right] \quad (1)$$

where $\mu = GM_{\oplus}$, r is the distance from the center of the earth, R is the mean equatorial radius of the earth, P_n^m is the associated Legendre polynomial, β is the latitude, and λ is the longitude. Alternative notations recommended for the gravitational coefficients are

$$J_n = -C_{n,0}, \tag{2}$$

and

$$(A_{n,m}, B_{n,m}) = \left[\frac{(n+m)!}{(n-m)!}\right]^{1/2} (C_{n,m}, S_{n,m}). \tag{3}$$

These two additions are suggested:

1. Define

$$\left(\bar{C}_{n,m}, \bar{S}_{n,m}\right) = \left[\frac{(n+m)!}{(n-m)!\,(2n+1)\;(2-\delta_m{}^0)}\right]^{1/2} (C_{n,m}, S_{n,m}), \tag{4}$$

where the Dirac delta $\delta_m{}^0$ is 1 for $m=0$ and 0 for $m \neq 0$. The $\bar{C}_{n,m}$, $\bar{S}_{n,m}$ are coefficients of harmonics which have a mean square amplitude of 1 for all values of n and m.

2. Define the mean equatorial radius more precisely as the equatorial radius of the mean earth ellipsoid, i.e., the ellipsoid of revolution which best fits the geoid. This definition is consistent with geodetic practice and involves the equatorial radius with only two of the set of orthogonal parameters defining the radius vector of the geoid—the zeroth and second degree zonal harmonics. (The more literal definition of the mean equatorial radius as the radius of the circle which best fits an equatorial section through the geoid would connect the radius to the infinite set of even degree zonal harmonics.) An alternative possibility for the equatorial radius in Equation 1 is the mean radius of the entire earth which, since it differs by a factor of 10^{-3}, would affect the value of J_2. The mean radius seems slightly preferable aesthetically, but current practice overwhelmingly favors the equatorial radius; a perusal of some papers on close satellite dynamics and orbit analysis found ten workers using the equatorial radius but none using the mean radius (in addition, five theoreticians did not define their radius).

To be consistent with the connection of equatorial radius to the mean earth ellipsoid, it is recommended that the following be the relationships between the astronomical parameters $\mu = GM_{\oplus}$ and $J_2 = -C_{2,0}$ and the geodetic parameters $R = a_e$, the equatorial radius; γ_e, the equatorial gravity; f, the flattening; and ω, the rate of the earth's rotation with respect to inertial space (References 2, 3, and 4):

$$GM_{\oplus} = a_e{}^2\,\gamma_e\left[1 + \frac{3}{2}m - f - \frac{15}{14}mf - \frac{1}{294}mf^2 - 0(f^4)\right], \tag{5}$$

$$J_2=\frac{2}{3}f\left(1-\frac{1}{2}f\right)-\frac{1}{3}m\left[1-\frac{3}{2}m-\frac{2}{7}f+\frac{9}{4}m^2+\frac{11}{49}f^2+0(f^3)\right], \tag{6}$$

where

$$m=\frac{\omega^2 a_e}{\gamma_e}. \tag{7}$$

The values of $GM_\oplus$ and J_2 which are probably the most extensively used at orbit computation centers in the United States are (References 5, 6, and 7):

$$\left.\begin{aligned} GM_\oplus &= 3.986032 \pm 0.000030 \times 10^{20} \text{ cm}^3 \text{ sec}^{-2}, \\ J_2 &= 1082.30 \times 10^{-6}. \end{aligned}\right\} \tag{8}$$

In the alternative notation of Herrick, Baker, and Hilton (Reference 8) and Makemson, Baker, and Westrom (Reference 9):

$$k_e = (GM_\oplus)^{1/2} = 0.019965049 \text{ megameter}^{3/2} \text{ sec}^{-1}. \tag{9}$$

The values of $GM_\oplus$ and J_2 in Equation 8 are consistent with these values for the geodetic parameters:

$$\left.\begin{aligned} a_e &= 6{,}378{,}165.0 \pm 25.0 \text{ meters}, \\ \gamma_e &= 978.0300 \pm 0.012 \text{ cm sec}^{-2}, \\ f &= 1/298.30, \\ \omega &= 0.729211585 \times 10^{-4} \text{ sec}^{-1}. \end{aligned}\right\} \tag{10}$$

The value for a_e is a compromise between the solutions of Fischer (Reference 10), and Kaula (Reference 11), and other values which are unpublished. The γ_e value differs from that of the International Formula and the Potsdam System (978.0490 cm sec^{-2}) in three ways:

1. Correction to Potsdam System absolute g (Reference 12) $= -0.0128 \pm 0.0003$;
2. Change of flattening from 1/297 to 1/298.3 $= -0.0051$;
3. Change of mean gravity over the earth's surface (Reference 11) $= -0.0005 \pm 0.0012$.

The correction to absolute g is a provisional value and has not been adopted by the International Union of Geodesy and Geophysics; an improved value should be forthcoming within the next few years from several determinations in progress (Reference 13). The correction to mean gravity is negative, mainly because correlation between gravity and topography was used to estimate anomalies for the areas without observations, which are predominantly oceans. Solutions by Uotila which fit observed gravimetry and do not use correlation with topography give positive corrections ranging from $+0.0004$ to $+0.0019$ cm sec^{-2}. (Reference 14). Rather slow improvement is expected; problems in observing gravity at sea are not entirely solved (References 15 and 16). Some improvement may also come from using the better statistical techniques which larger capacity computers permit.

The value of $GM_\oplus$ may also be obtained through the modified Kepler equation by using the radar mean distance of the moon A and the moon's mean motion n:

$$GM_\oplus = \frac{n^2\,(1+\beta)^3}{1+\frac{\mu_M}{\mu_E}} A^3, \tag{11}$$

where β is the solar perturbation of the mean semimajor axis and μ_M/μ_E is the ratio of the moon's mass to the earth's mass, equal to the lunar inequality (Reference 17). The most recently published value for A is $384{,}402.0 \pm 1.2$ km (Reference 18). As pointed out by Fischer, this value should perhaps be corrected because it is dependent on an excessively rounded-off lunar radius of 1740 km (Reference 19). The mean radius of the lunar limb is 1737.85 ± 0.07 km. Geometrical determinations of the radius toward the earth vary considerably; Baldwin's conclusion (Reference 20) leads to 1740.05 km, whereas Schrutka-Rechtenstamm (Reference 21) concludes that the bulge is too small to be determined. However, we are not interested in just the long axis of a best-fitting triaxial ellipsoid, but rather in the mean radius of the area contributing to the leading edge of the radar return pulse, which would fall within the ± 7 degree area of libration. Contour maps of the moon (Reference 22, for example) indicate that the average radius of this ± 7 degree area could differ by as much as 2 km from the best-fitting ellipsoid. If the lunar surface is assumed to be an equipotential surface, then using the moments of inertia obtained from the physical libration yields 1738.57 km as the radius toward the earth. Letting $A = 384{,}400.5 \pm 1.2$ km, $\beta = 0.0090678$, $n = 2.6616997 \times 10^{-6}$ sec^{-1} (Reference 23), and $\mu_M/\mu_E = 1/(81.375 \pm 0.026)$ (Reference 24) gives

$$GM_\oplus = 3.986094 \pm 0.00004 \times 10^{20} \text{ cm}^3 \text{ sec}^{-2}. \tag{12}$$

Using the $\mu_M/\mu_E = 1/81.219$ of Delano (Reference 25) reduces $GM_\oplus$ to 3.986001×10^{20} cm^3 sec^{-2}, so the difference from solutions based on terrestrial data seems largely explicable as an error in the lunar inequality. The larger computers of today permit the application of more elaborate statistical techniques than it was possible to apply in 1950 (the year Delano and Rabe published their work). However, since the stellar positions are a major suspect for systematic error, it seems premature to reanalyze the Eros observations before the revised reference star systems are available (Reference 26). Meanwhile, improved determination of the lunar inequality may be obtained from radio tracking of space probes such as Mariner II (1962 $\alpha\rho 1$). Also, since spacecraft have been launched into high, nearly circular orbits such as those of Midas III (1961 σ) and Midas IV (1961 $\alpha\delta$), it may be worthwhile to try to determine $GM_\oplus$ from close satellite orbits.

In addition to $GM_\oplus$ and J_2, standard orbit computation programs usually incorporate J_3 and J_4. The values which are probably most common at United States computation centers are (Reference 6):

$$\left.\begin{aligned} J_3 &= -2.3\times 10^{-6}, \\ J_4 &= -1.8\times 10^{-6}. \end{aligned}\right\} \tag{13}$$

At present the best values of the zonal harmonics are undoubtedly those of Kozai (Reference 7):

$$\left.\begin{aligned} &J_2 = 1082.48\pm 0.06\times 10^{-6}, && J_3 = -2.562\pm 0.012\times 10^{-6}, \\ &J_4 = -1.84\pm 0.08\times 10^{-6}, && J_5 = -0.064\pm 0.019\times 10^{-6}, \\ &J_6 = 0.39\pm 0.12\times 10^{-6}, && J_7 = -0.470\pm 0.021\times 10^{-6}, \\ &J_8 = -0.02\pm 0.02\times 10^{-6}, && J_9 = 0.117\pm 0.025\times 10^{-6}. \end{aligned}\right\} \tag{14}$$

Note that the J_2, J_3, and J_4 now used, given in Equations 8 and 13, each differ from Kozai's improved values by less than 0.3×10^{-6}; and that the coefficients J_5 and higher are all very small in absolute magnitude. Therefore, it does not seem worthwhile to adopt values, other than those already in general use, before 1966 or 1967, when analysis of geodetic satellite orbits observed during the International Year of the Quiet Sun will be completed.

Most of the current close satellite orbit analyses for geodetic purposes seek tesseral harmonic perturbations. In view of the smallness of these perturbations, it does not seem appropriate to adopt standardized values for the tesseral harmonics $C_{n,m}$, $S_{n,m}$. The one exception might be $C_{2,2}$, $S_{2,2}$, for which an upper limit would be useful because of its effect on supplemental energy requirements for 24 hour orbits. The most recent, unpublished determinations of Izsak, Kaula, Kozai, and Newton range from 0.9×10^{-6} to 1.8×10^{-6} in amplitude $\left(\sqrt{C_{2,2}^2+S_{2,2}^2}\right)$ and from 8° to 25° W in the direction of the principal axis $\left[(1/2)\tan^{-1}(S_{2,2}/C_{2,2})\right]$.

GEOMETRICAL PARAMETERS

As shown by analyses involving large systems of observations (References 10, 11, and 19), the equatorial radius is a derived, rather than a fundamental, quantity: accurate knowledge of the radius is not necessary to obtain other parameters, such as the lunar distance, geoid undulations, or datum positions by fitting of the astro-geodetic to the gravimetric geoid. However, for astronomical purposes, it is desirable to have a reference ellipsoid correct within ±50 meters in order to obtain reasonably correct positions of isolated tracking stations from astronomic latitude and longitude. Also it is convenient to have a unit of length approximating the earth's radius for use in the potential formula (Equation 1) and for use as a base line to compare or combine parallax observations. For these astronomical purposes, the value of 6,378,165.0 meters given in Equation 10 should be entirely adequate. Marked improvement is not expected for about 5 years, by which time satellite observations should contribute significantly to the strengthening of triangulation systems and to the interconnection of geodetic datums.

By far the most annoying problems in the astronomical application of geodetic data pertain to tracking station positions. Errors in the adopted values of station positions, in conjunction with drag and nonuniform distribution of observations, prevent accurate determination of tesseral harmonics and are even believed to be a major cause of discrepancies in space probe trajectories (Reference 27). These station position errors are due to both inadequate data and mistaken treatment of data; in descending order of reprehensibility they include:

1. Weak, erroneous, or nonexistent connection of tracking stations to local geodetic control (this includes the moving of antennas by stations without informing the computing center);
2. Failure to state the datum or ellipsoid to which tracking station positions refer;
3. Use of obsolete or erroneous standard datum and ellipsoid;
4. An incomplete or ambiguous statement about how datum or ellipsoid transformations were made;
5. Failure to provide for geoid-ellipsoid difference in calculating heights;
6. Neglecting systematic error due to incorrect observation (for example, no Laplace stations) or incorrect adjustment (for example, arbitrary scale changes or rotations) of geodetic control connecting tracking stations more than, say, 1000 km apart;
7. Actual observational error of position.

In view of the number of geodetic datums and corrections thereto, they do not seem to be appropriate parameters to be adopted as standard by an international organization, except possibly for the large continental triangulation systems. The corrections to coordinates u, v, w with positive axes directed respectively toward latitude and longitude (0°, 0°), (0°, 90° E), (90° N) obtained in the world geodetic system solution of

Table 1.—*Corrections to* u, v, w *From Reference 11 (Meters)*

Datum shift	Δu	Δv	Δw
WGS–NAD	-23 ± 26	$+142\pm22$	$+196\pm22$
WGS–ED	-57 ± 23	-37 ± 29	-96 ± 23
WGS–TD	-89 ± 40	$+551\pm53$	$+710\pm40$

Kaula (Reference 11) are listed in Table 1, where NAD, ED, and TD refer to the North American, European, and Tokyo datums, respectively. The uncertainties in this table are based on estimates of the errors due to interpolation and representation in the astro-geodetic and gravimetric geoids, and are probably a fair measure of item 7 on the above list, but may neglect significant effects falling under item 6. The relationships of the rectangular coordinates u, v, w to the geodetic latitude ϕ, longitude λ, and elevation h, referred to an ellipsoid of parameters a_e and f, are:

$$\left.\begin{aligned} u&=(\nu+h)\cos\phi\cos\lambda,\\ v&=(\nu+h)\cos\phi\sin\lambda,\\ w&=[(1-e^2)\,\nu+h]\sin\phi,\end{aligned}\right\}\qquad(15)$$

where $\nu=a_e/(1-e^2\sin^2\phi)^{1/2}$ and $e^2=2f-f^2$.

To help minimize the number of unnecessary errors in categories 1 through 5 on the above list, it is suggested that organizations be urged to publish the following information pertaining to each tracking station for which they publish any precise observations of artificial satellites or probes, or orbital data based thereon:

1. The names and coordinates of local geodetic control points, both horizontal and vertical, to which the tracking station is connected;
2. The geodetic datum and ellipsoid to which the horizontal coordinates refer;
3. The organization which established the local geodetic control points;
4. The manner in which the horizontal and vertical survey connections were made from the local control points to the tracking station;
5. The date of the survey connection and a description of the termination point of the survey;
6. The geodetic (ϕ, λ, h) and rectangular (u, v, w) coordinates of the station referred to the local geodetic datum;
7. A statement of the geoid height, if any, estimated for the station and the basis for the estimate;
8. If the tracking station position has been shifted for the purpose of referring observations (direction cosines or altitude and azimuth) or

calculating orbits, the geodetic and rectangular coordinates after the shift and the ellipsoid to which the new coordinates refer.

Every item on this list is an action which must be accomplished for any tracking station, but thus far the Smithsonian Astrophysical Institute Baker-Nunn camera network is the only one for which even part of the list has been published (Reference 28). It is symptomatic of the difficulties which occur that, since this publication, the coordinates for at least four of the twelve Baker-Nunn cameras have been found to be in error by 20 meters or more. These geometrical details of tracking station position are rather uninteresting, but they must be examined carefully and determined correctly if the full potentialities of modern tracking techniques are to be realized.

REFERENCES

1. Hagihara, Y.: Recommendations on Notation of the Earth Potential. Astronom. J. 67(1): 108, February 1962.
2. Lambert, W. D.: The Gravity Field of an Ellipsoid of Revolution as a Level Surface. Annales Academiae Scientiarum Fennicae, Ser. A–III, No. 57, 1961; Reprinted in Ohio State Univ., Inst. of Geodesy, Photogrammetry and Cartography, Publ. No. 14, 1961.
3. Cook, A. H.: The External Gravity Field of a Rotating Spheroid to the Order of e^3. Geophys. J. 2(3): 199–214, September 1959.
4. Hirvonen, R. A.: New Theory of the Gravimetric Geodesy. Annales Academiae Scientiarum Fennicae, Ser. A–III, No. 56, 1960; Reprinted in Ohio State Univ., Inst. of Geodesy, Photogrammetry and Cartography, Publ. No. 9, 1960.
5. Kaula, W. M.: Tesseral Harmonics of the Gravitational Field and Geodetic Datum Shifts Derived from Camera Observations of Satellites. J. Geophys. Res. 68(2): 473–484, January 15, 1963.
6. Clarke, V. C.: Constants and Related Data Used in Trajectory Calculations at the Jet Propulsion Laboratory. Calif. Inst. Tech., Jet Propulsion Lab., Tech. Rept. 32–273, May 1, 1962.
7. Kozai, Y.: Numerical Results from Orbits. Smithsonian Inst., Astrophys. Observ. Spec. Rept. No. 101, July 31, 1962.
8. Herrick, S.; Baker, R. M. L., Jr.; and Hilton, C. G.: Gravitational and Related Constants for Accurate Space Navigation. In: Proc. 8th Internat. Astronaut. Cong., Barcelona, 1957, ed. by F. Hecht, Vienna: Springer-Verlag, 1958, pp. 197–235.
9. Makemson, M. W.; Baker, R. M. L., Jr.; and Westrom, G. B.: Analysis and Standardization of Astrodynamic Constants. J. Astronaut. Sci. 8(1): 1–13, Spring 1961.
10. Fischer, I.: An Astrogeodetic World Datum from Geoidal Heights Based on the Flattening $f = 1/298.3$. J. Geophys. Res. 65(7): 2067–2076, July 1960.
11. Kaula, W. M.: A Geoid and World Geodetic System Based on a Combination of Gravimetric, Astrogeodetic, and Satellite Data. J. Geophys. Res. 66(6): 1799–1811, June 1961.
12. Rice, D. A.: Compte rendu des réunions de la Section IV—Gravimétrie. Bulletin Géodésique No. 60, June 1, 1961, p. 109.
13. Cook, A. H.: Report on Absolute Measurements of Gravity. Bulletin Géodésique No. 60, 131–139, June 1, 1961.

14. Uotila, U. A.: Corrections to Gravity Formula from Direct Observations and Anomalies Expressed in Lower Degree Spherical Harmonics. Ohio State Univ., Inst. of Geodesy, Photogrammetry and Cartography, Publ. No. 23, 1962.
15. Allan, T. D.; Dehlinger, P.; et al.: Comparison of Graf-Askania and LaCoste-Romberg Surface-Ship Gravity Meters. J. Geophys. Res. 67(13): 5157–5162, December 1962.
16. Harrison, J. C.: The Measurement of Gravity. Proc. IRE 50(11): 2302–2312, November 1962.
17. O'Keefe, J. A.; Eckels, A.; and Squires, R. K.: The Gravitational Field of the Earth. Astronom. J. 64(7): 245–253, September 1959.
18. Bruton, R. H.; Craig, K. J.; and Yaplee, B. S.: The Radius of the Earth and the Parallax of the Moon from Radar Range Measurements on the Moon. Astronom. J. 64(8): 325, October 1959 (Abstract).
19. Fischer, I.: Parallax of the Moon in Terms of a World Geodetic System. Astronom. J. 67(6): 373–378, August 1962.
20. Baldwin, R. B.: The Face of the Moon. Chicago: Univ. of Chicago Press, 1949.
21. Schrutka-Rechtenstamm, G.: Neureduktion der 150 Mondpunkte der Breslauer Messungen von J. Franz. Sitzungsberichte der Österreichischen Akademie der Wissenschaften, Mathematisch-Naturwissenschaftliche Klasse, Abt. II 167: 71–123, 1958.
22. Baldwin, R. B.: A Lunar Contour Map. Sky and Telescope 21(2): 84–85, February 1961.
23. Brown, E. W.: Theory of the Motion of the Moon. Part 4. Mem. Roy. Astronom. Soc. 57: 51–145, 1908.
24. Rabe, E.: Derivation of Fundamental Astronomical Constants from the Observations of Eros During 1926–1945. Astronom. J. 55(4): 112–126, May 1950.
25. Delano, E.: The Lunar Equation from Observations of Eros, 1930–1931. Astronom. J. 55(5): 129–132, August 1950.
26. Scott, F. P.: Status of the International Reference-Star Programs. Astronom. J. 67(10): 690–695, December 1962.
27. Hamilton, T. W.: Applications of Celestial Mechanics to Spacecraft Flight. In: Proc. of the NASA-University Conf. on the Sci. and Tech. of Space Exploration, Chicago, November 1962, NASA SP-11, December 1962, Vol. 1, pp. 253–260.
28. Veis, G.: The Positions of the Baker-Nunn Camera Stations. Smithsonian Inst., Astrophys. Observ. Spec. Rept. No. 59, March 3, 1961.

Appendix B

Reference List of Recommended Constants

Reference List of Recommended Constants

Defining Constants

1. Number of ephemeris seconds in 1 tropical year (1900)	s	$=31\ 556\ 925{\cdot}9747$
2. Gaussian gravitational constant, defining the a.u.	k	$=0{\cdot}017\ 202\ 09895$

Primary Constants

3. Measure of 1 a.u. in meters	A	$=149\ 600\times 10^6$
4. Velocity of light in meters per second	c	$=299\ 792{\cdot}5\times 10^3$
5. Equatorial radius for Earth in meters	a_e	$=6\ 378\ 160$
6. Dynamical form-factor for Earth	J_2	$=0{\cdot}001\ 082\ 7$
7. Geocentric gravitational constant (units: $m^3 s^{-2}$)	GE	$=398\ 603\times 10^9$
8. Ratio of the masses of the Moon and Earth	μ	$=1/81{\cdot}30$
9. Sidereal mean motion of Moon in radians per second (1900)	$n_{\text{☾}}^{*}$	$=2{\cdot}661\ 699\ 489\times 10^{-6}$
10. General precession in longitude per tropical century (1900)	p	$=5025''.64$
11. Obliquity of the ecliptic (1900)	ϵ	$=23^\circ 27' 08''.26$
12. Constant of nutation (1900)	N	$=9''.210$

Auxiliary Constants and Factors

$k/86400$, for use when the unit of time is 1 second	$k'=1{\cdot}990\ 983\ 675\times 10^{-7}$
Number of seconds of arc in 1 radian	$=206\ 264{\cdot}806$
Factor for constant of aberration (note 15)	$F_1=1{\cdot}000\ 142$
Factor for mean distance of Moon (note 20)	$F_2=0{\cdot}999\ 093\ 142$
Factor for parallactic inequality (note 23)	$F_3=49853''.2$

Derived Constants

13. Solar parallax................arcsin $(a_e/A)=\pi_{\odot}=8''.79405\ (8''.794)$
14. Light-time for unit distance...........$A/c'=\tau_A=499^s.012$
$=1^s/0\cdot002\ 003\ 96$
15. Constant of aberration...............$F_1k'\tau_A=\kappa=20''.4958(20''.496)$
16. Flattening factor for Earth...................$f=0\cdot003\ 352\ 9$
$=1/298\cdot25$
17. Heliocentric gravitational constant (units: $m^3\,s^{-2}$).............$A^3k'^2=GS=132\ 718\times10^{15}$
18. Ratio of masses of Sun and Earth..................... $(GS)/(GE)=S/E=332\ 958$
19. Ratio of masses of Sun and Earth +Moon.........................$S/E(1+\mu)=328\ 912$
20. Perturbed mean distance of Moon, in meters

$$F_2(GE(1+\mu)/n_{\mathfrak{C}}{}^{*2})^{\frac{1}{3}}=a_{\mathfrak{C}}=384\ 400\times10^3$$

21. Constant of sine parallax for Moon.......................... $a_e/a_{\mathfrak{C}}=\sin\pi_{\mathfrak{C}}=3422''.451$
22. Constant of lunar inequality .... $\frac{\mu}{1+\mu}\frac{a_{\mathfrak{C}}}{A}=L=6''.43987\ (6''.440)$
23. Constant of parallactic inequality .... $F_3\frac{1-\mu}{1+\mu}\frac{a_{\mathfrak{C}}}{A}=P_{\mathfrak{C}}=124''.986$

System of Planetary Masses

		Reciprocal mass		Reciprocal mass
24.	Mercury	6 000 000	Jupiter	1 047·355
	Venus	408 000	Saturn	3 501·6
	Earth+Moon	329 390	Uranus	22 869
	Mars	3 093 500	Neptune	19 314
			Pluto	360 000

★ U.S. GOVERNMENT PRINTING OFFICE: 1966—O 214-249